NON-PROPRIETARY

DOCKET 71–9393

orano

CR3MP

TRANSPORT PACKAGE

Safety Analysis Report

Revision 3

December 2022

Orano Federal Services LLC

TABLE OF CONTENTS

GLOSSARY OF ACRONYMS AND ABBREVIATIONS

This list of acronyms and abbreviations is consistent across all chapters and appendices in this Safety Analysis Report.

Acronym	Description
ACI	American Concrete Institute
ANSI	American National Standards Institute
ASME	American Society of Mechanical Engineers
ASTM	American Society for Testing and Materials
AWS	American Welding Society
BPVC	ASME Boiler and Pressure Vessel Code
BWR	Boiling Water Reactor
CAD	Computer Aided Drafting/Design
CFR	Code of Federal Regulations
CG	Center of Gravity
Ci	Curie
CJP	Complete Joint Penetration
CMTR	Certified Material Test Report
CR3	Crystal River Reactor Unit #3
CR3MP	CR3 Middle Package
CSI	Criticality Safety Index
DOT	Department of Transportation
DWS	Diamond Wire Saw
EOS	Equation of State
EPS	Effective Plastic Strain
FEA	Finite Element Analysis
GISSMO	General Incremental Stress-State Dependent Damage Model
GTCC	Greater Than Class C
HAC	Hypothetical Accident Conditions
HHT	Heavy Haul Trailer
ISFSI	Independent Spent Fuel Storage Installation
ksi	thousand pounds per square inch
lb	pounds
LDCC	Low Density Cellular Concrete
LST	Lowest Service Temperature
LSTC	Livermore Software Technology Corporation
M&TE	Measuring and Test Equipment
MCNP	Monte Carlo N-Particle®
MNOP	Maximum Normal Operating Pressure
MS	Margin of Safety
MT	Magnetic Particle Examination
NAA	Neutron Activation Analysis
NCT	Normal Conditions of Transport

Acronym	Description
NDE	Non-Destructive Examination
NDT	Nil Ductility Transition
NRC	Nuclear Regulatory Commission
OEM	Original Equipment Manufacturer
OFS	Orano Federal Services
pcf	pounds per cubic foot
psi	pounds per square inch
psia	pounds per square inch absolute
psig	pounds per square inch gauge
PT	Liquid Penetrant Examination
QA	Quality Assurance
RCS	Reactor Coolant System
RPV	Reactor Pressure Vessel
RT	Radiographic Examination
RVI	Reactor Pressure Vessel Internals
SAR	Safety Analysis Report
SPA	Special Package Authorization
SPMT	Self-Propelled Modular Transporter
TF	Triaxiality Factor
UT	Ultrasonic Examination
VT	Visual Examination
VTK	Visualization Toolkit
WCS	Waste Control Specialists

LIST OF FIGURES

LIST OF TABLES

1.0 GENERAL INFORMATION

This section presents a general introduction and description of the Crystal River Reactor Unit #3 (CR3) Middle Package (CR3MP). The CR3MP is used to safely and compliantly transport the segmented middle section of the decommissioned CR3 Reactor Pressure Vessel (RPV) and RPV Internals (RVI). This Safety Analysis Report (SAR) supports a license application seeking authorization of the CR3MP as a Type B(U)–96 shipping package in accordance with the provisions of Title 10, Part 71 of the Code of Federal Regulations (CFR) [1]. This SAR follows the general format and content provided in the Nuclear Regulatory Commission (NRC) Regulatory Guide 7.9 [2].

The major components comprising the package are discussed in Section 1.2, *Package Description,* and illustrated in Figure 1.1-1. Detailed packaging SAR drawings are presented in Appendix 1.3.2, *Packaging General Arrangement Drawings*.

1.1 Introduction and Background

The CR3MP has been developed by Orano Federal Services (OFS) to transport the segmented middle section of the decommissioned CR3 RPV and RVI. The middle section is the core portion of the RPV, extending approximately over the active fuel assembly region and containing a high amount of activated metal. The top and bottom RPV sections are planned for shipment in Department of Transportation (DOT) packages. The middle section segment of the consolidated RPV and RVI components will be transported in the CR3MP Type B package described herein. As such, the CR3MP is a one-time, single use, expendable package. The CR3MP will be shipped via exclusive use from CR3 to the licensed low-level waste disposal facility of Waste Control Specialists (WCS) near Andrews, Texas.

In terms of the packaging configuration, an isometric cross section of the CR3MP is shown in Figure 1.1-1. The CR3MP consists of a 3-in. thick steel body assembly shell, 6-in. thick top and bottom covers, a closure joint weld, and other welds necessary for fabrication of the large material cross-sections. In addition, a layer of Low-Density Cellular Concrete (LDCC) grout fills the annulus between the RPV shell exterior and the CR3MP shell. The overall height of the package is 178.1-in. tall while the overall diameter is 200.3-in. The package is designed to be transported by ground or water with its cylindrical axis vertical. The overall package gross weight is a maximum of 860,000 lb.

As defined by 10 CFR 61.55 [3] for Class B and Class C radiological waste materials, the CR3MP authorized contents will contain both waste classes. None of the source contents contain fissile content, therefore the payload is fissile exempt per the provisions of §71.15(b) [1]. Since the RPV and RVI contents transported in the CR3MP are fissile-exempt, the Criticality Safety Index (CSI) described in 10 CFR 71.59 does not apply.

The CR3MP does provide shielding from gamma radiation via the thick steel covers and thick steel walls of the shell. The containment boundary is provided by the shell walls and covers and the circumferential weld joint between the cover and shell wall. The containment boundary will be described in greater detail in Section 1.2.1.1, *Containment Vessel*.

OFS is seeking a Special Package Authorization (SPA) in accordance with 10 CFR 71.41(d) for the one-time shipment of the CR3MP. There is one equivalency determination sought, as follows:

Due to material property limits discussed in Section 2.1.2.1.1, *Brittle Fracture*, a Lowest Service Temperature (LST) of 0°F is established. Therefore, OFS is requesting a condition for the LST to be greater than or equal to 0°F during the entirety of the transport. As outlined in NRC Regulatory Guide 7.12 [8], an equivalent level of safety for the 10 CFR 71.71 and 10 CFR 71.73 Normal Conditions of Transport (NCT) and Hypothetical Accident Conditions (HAC) initial test conditions is offered for brittle fracture criteria of the bounding 6-in. thick CR3MP top and bottom covers at the LST identified. Of note, a buffer zone ranging from 0-5°F is included for operational convenience in Section 7.1.3, *Preparation of the CR3MP for Transport*.

For the LST low ambient temperature, the primarily impacted test conditions (i.e., the NCT and HAC structural drop tests) use the more conservative properties of steel at the high temperature condition of 150°F (see Appendix 2.12.2, *Free Drop Evaluation*). In addition, as recommended by NUREG/CR-3826 [9], in order to preclude a brittle fracture failure initiation mode under any NCT or HAC, a supporting analysis in Section 2.1.2.1.1, *Brittle Fracture*, has been performed showing that the material conforms to the toughness requirements of NUREG/CR-6491 [10] at the LST.

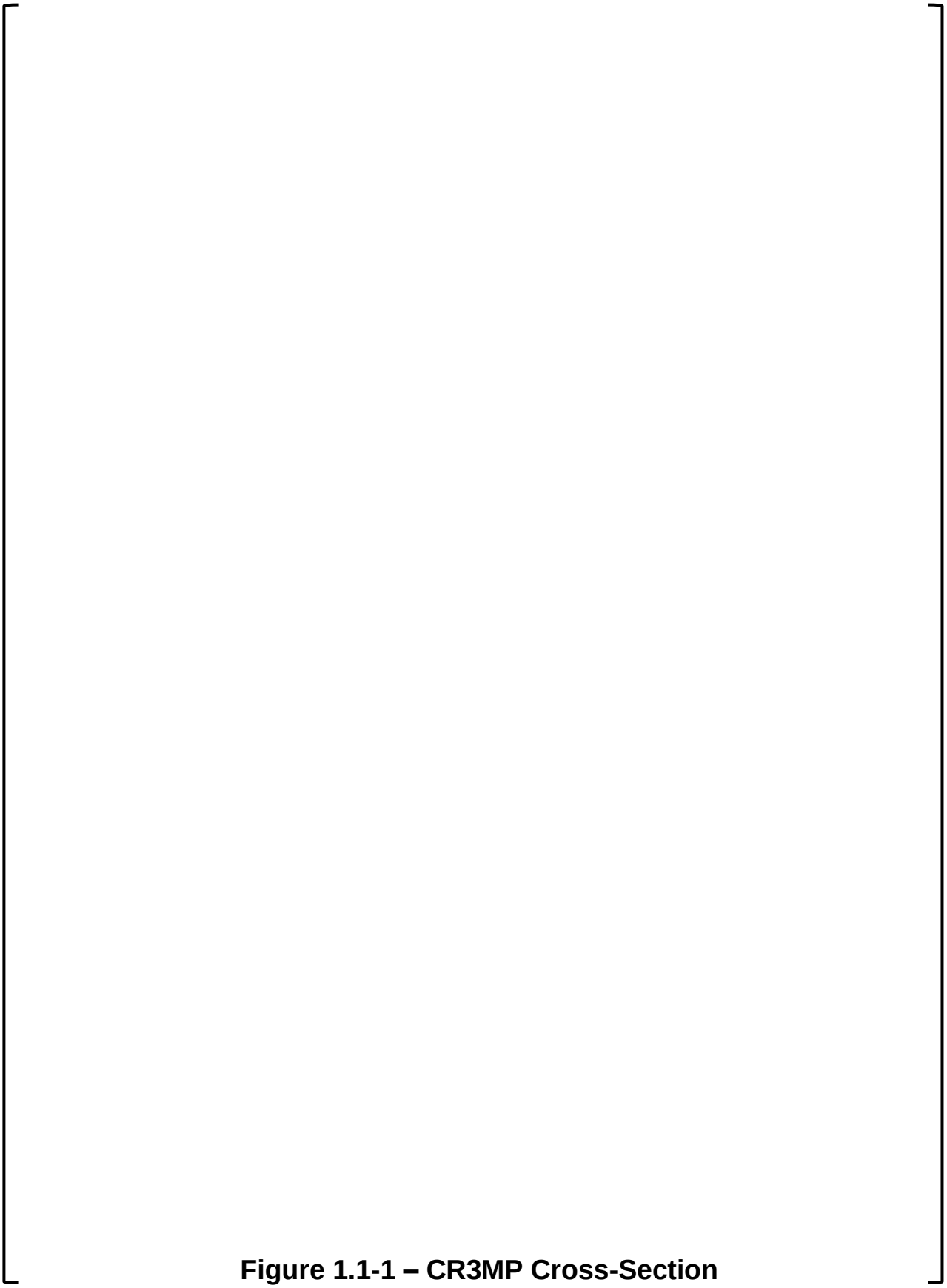

Figure 1.1-1 – CR3MP Cross-Section

1.2 Package Description

This section presents a basic description of the CR3MP components and construction. In the following, drawing references are to the general arrangement drawings provided in Appendix 1.3.2, *Packaging General Arrangement Drawings*.

1.2.1 General CR3MP Description

In terms of the packaging configuration, as shown in Appendix 1.3.2, *Packaging General Arrangement Drawings*, the packaging is a right circular cylinder steel shell made of 3-in. thick steel and two 6-in. thick covers, one top and one bottom. Each top and bottom cover is groove welded to the shell wall along the circumference. A ½-in. square backing ring under the top cover helps to facilitate welding of the top cover in the field. The package cross section is shown in Figure 1.1-1. The overall nominal height of the package is 178.1-in. tall, while the overall diameter is 200.3-in.

There are also a few non-structural components of the package. Four 1.5-in. diameter by 4-in. maximum deep threaded holes reside on the top cover. These holes are used to facilitate lifting the top cover and will be plugged by set screws. One of the holes will be tapped through to facilitate a pressure vent port. Prior to transport, the vent port is plugged by a fully threaded rod installed approximately flush to the package surface and secured with a closure weld (see details in Section 1.2.1.1, *Containment Vessel*). In addition, if used and prior to loading the package, 2-in. thick lugs on the interior of the packaging for lifting the empty packaging will be thermally or mechanically removed, leaving only a remnant of the original lug.

The RPV payload centrally rests on the inside of the bottom cover. **[**

] The nominal 3-in. gap between the top surface of the RPV and the bottom surface of the top cover is unfilled (i.e., nominal air gap). However, the radial 3-in. nominal annular gap between the shell inner wall and the RPV outer diameter is filled with LDCC, or informally identified simply as "*grout.*"

As shown in Figure 1.1-1, RVI components are rigidly constrained within the RPV by built-up layers of LDCC grout into one rigid monolith. The LDCC density is nominally 53 pcf but is considered to have a range from 30 to 60 pcf.

The maximum gross weight of the CR3MP is 860,000 pounds, while the authorized contents weight of the RPV with RVI is conservatively set to 645,000 pounds maximum. A summary of overall component weights is provided in Table 2.1-3.

The CR3MP complies with the requirements of 10 CFR Part 71 [1]. The remaining paragraphs in this section provide reference to the sections of this SAR that are used to specifically address compliance with the requirements of Subparts E and F of 10 CFR Part 71.

The shell and top and bottom covers provide adequate structural load bearing capacity in order to comply with resultant effects on the package from the 10 CFR 71.71 NCT and 10 CFR 71.73 HAC. Structural performance of the package is covered in greater detail in Chapter 2.0, *Structural Evaluation*. The materials of construction of the package are carbon steel plate and cementitious grout. A complete evaluation of the materials and their acceptance criteria under both NCT and HAC conditions is covered in Section 2.2, *Materials*.

The dissipation of heat from the CR3MP is entirely passive and is adequate to comply with the requirements of 10 CFR Part 71 and no coolants are required. A more detailed description of the package thermal design is given in Chapter 3.0, *Thermal Evaluation*.

Containment of the radioactive waste in the package is provided by the main cylindrical shell, top and bottom covers, and weld joints of the CR3MP. A brief description of the package body's containment boundary and performance is included in Section 1.2.1.1, *Containment Vessel* and the containment capabilities of the CR3MP after both the NCT and HAC tests are evaluated in Chapter 4.0, *Containment* and are shown to be adequate.

Biological shielding of gamma radiation is provided by the steel located in walls of both the shell body and top and bottom covers. In addition, the RPV steel shell primarily provides radial shielding on the sidewalls of the package. No other components whose primary purpose is shielding are included in the CR3MP. Gamma shielding is described and evaluated in Chapter 5.0, *Shielding Evaluation* and are shown to be adequate.

As stated in Chapter 6.0, *Criticality Evaluation*, the CR3MP transports fissile exempt material. Therefore, no moderation or neutron absorption is necessary to control criticality.

In addition, a detailed discussion of the materials acceptance tests and weld examinations, along with a description of the maintenance program is covered in Chapter 8.0, *Acceptance Tests and Maintenance Program*.

The CR3MP is of conventional design and is not complex to operate. Operational features are depicted on the drawing provided in Appendix 1.3.2, *Packaging General Arrangement Drawings*. The package is oriented with the cylindrical axis of the package in a vertical orientation during transport. A complete description of the operating controls and procedures for the CR3MP is covered in Chapter 7.0, *Package Operations*. The operational procedures, acceptance tests and maintenance program adequately comply with 10 CFR Part 71 requirements. Finally, the CR3MP will be fabricated and assembled in accordance with an NRC approved Part 71 Quality Assurance (QA) program.

Lifting of the CR3MP is performed via direct external jacking of the package from below or jacking while the package is resting on a skid or beams. All tie-downs for the CR3MP are indirect devices, which are not structurally part of the package. These tie-down devices are hold-down structures placed over the top of package cover, which are then fastened to a shipping skid or directly to the conveyance. Thus, there are no lifting or tie-down devices that are a structural part of the package.

1.2.1.1 Containment Vessel

The CR3MP's containment feature is the container's steel body itself consisting of the shell, both top and bottom covers and the circumferential closure joint welds for each of the covers. Due to material construction and availability considerations, the shell along with both the top and bottom covers are constructed of multiple plate sections joined with Complete Joint Penetration (CJP) welds.

The shell is constructed from one or more longitudinal CJP welds and one circumferential CJP weld, as necessary. Each of the top and bottom covers are constructed with up to three flat segments joined with CJP welds. Since they are located at the containment boundary, these additional welds are also part of the containment boundary. As detailed in Chapter 4.0, *Containment*, the CR3MP demonstrates containment compliance with 10 CFR 71 under the NCT conditions of 10 CFR 71.51(a)(1) and with HAC conditions of 10 CFR 71.51(a)(2) [1].

The packaging containment boundary is of welded construction, using American Society for Testing and Materials (ASTM) A516, Grade 70 [4] or American Society of Mechanical Engineers (ASME) SA-516, Grade 70 [5] carbon steel plate. The CR3MP packaging consists of a 3-in. thick cylindrical shell body with a nominal inner diameter of 194.3-in. and two flat heads (i.e., covers), one top and one bottom, both 6-in. thick. Each of the covers is nominally 193.8-in. (Outside Diameter) OD.

The plate section CJP welds for the top and bottom covers and the shell longitudinal weld seams are full penetration welds classified as Category A welds per Subparagraph ND-3352.1 of the ASME Boiler and Pressure Vessel Code (BPVC) [6]. The shell circumferential weld (if required) is classified as a Category B weld in accordance with Subparagraph ND-3352.2.

In accordance with Subparagraph ND-3352.3, the closure corner joint welds for the shell to top/bottom cover interface are considered as Category C weld joints [6]. These welds are also CJP welds following the likeness of Figure ND-4243-1(j) in the BPVC.

Finally, as mentioned in Section 1.2.1, *General CR3MP Description*, one of the top cover lifting holes will be a fully threaded through hole in order to facilitate a pressure vent port. This pressure vent port is part of the containment boundary. Therefore, prior to transport, the vent port is plugged by a fully threaded, minimum 6-in. long threaded carbon steel rod installed approximately flush to the package surface and secured with a minimum ¼-in. groove closure weld, inspected as described in Section 2.3.2, *Examination*.

1.2.1.2 Grout

The annulus between the RPV shell and the interior body surface of the CR3MP is filled with a layer of cementitious LDCC grout. The grout fills the 3-inch layer within the annulus. The grout is a low-density grout which has a nominal target density of 53 pcf but may range from 30 to 60 pcf, with a minimum compressive strength of 100 psi at a 28-day cure time. The grout used in the CR3MP principally consists of dry cement and water, but also has a small percentage of foam concentrate.

1.2.2 Contents

1.2.2.1 Reactor Vessel and Reactor Vessel Internals

The CR3MP content consists of the sectioned RPV and the RVI. The RPV shell is carbon steel plate. It is a sectioned cylindrical steel tubular structure [

]

The RVI is of solid physical form [

] The RVI is fabricated from Type 304 stainless steel. [

]

1.2.2.2 Grout within the RPV

The voids in the RPV will be filled with grout to prevent any shifting of the contents during transport. After placement of the [ ] RVI into the RPV is complete, the RPV will be drained of water, and grout will be introduced into the RPV. The RVI components are rigidly constrained as one monolith body within the RPV by built up layers of LDCC grout. The LDCC grout is nominally 53 pcf but may range from 30 to 60 pcf, with a minimum compressive strength of 100 psi at a 28-day cure time.

The grout used in the RPV principally consists of dry cement and water with a small percentage of foam concentrate. The physical properties of the grout are detailed in Section 2.2, *Materials*.

1.2.2.3 Radioactive Contents Description

As required by 10 CFR 71.33(b), to be authorized for transport and consistent with the above description of the RPV, RVI and grout, this section describes in greater detail the radioactive material, including radionuclides, their quantities, and as needed, mass. This is covered in greater detail in Chapter 5.0, *Shielding Evaluation*.

The radioactive contents are of normal form. Table 1.2-1 lists the package radionuclide activity levels. The total payload activity due to neutron activation as of June 30, 2021 is [

] A Neutron Activation Analysis (NAA) provides the activated segment specific activity (Ci/g), weight, and material density input for all the components. Of note, GTCC waste is not part of the RVI authorized contents.

[

]

A conservative estimate of surface contamination activity within the CR3MP is based on samples from both primary Reactor Coolant System (RCS) piping coupons and RCS leakage throughout the CR3 plant in conjunction with the calculated wetted surface areas of the packaged RPV and RVI. Once the reactor is opened up for inspection, and prior to shipment, this estimated activity will be verified to be within the bounding application activity based on confirmatory sampling and surveys.

Since the interior of the RPV/RVI is currently inaccessible, surrogate data was used to develop a contamination activity estimate. RCS piping coupons were chosen as surrogates based on sharing a similar operating environment (temperature, pressure, duration) as the RPV/RVI.

[

] The contamination distribution contains a comprehensive variety of radionuclides consistent with plant operating history. Periodic confirmatory sampling of wastes is performed, ensuring the radionuclide distribution is within applicable guidelines such as the NRC's branch technical position papers on waste classification [11].

[

]

The estimated surface contamination activity [ ] was derived by an evaluation of all available RCS systems: [ ] These RCS systems were surveyed for segmentation, packaging and disposal. [

]

[

], or 24.8 Ci. This value is used in the containment evaluation in the SAR Section 4.3, *Containment under Hypothetical Accident Conditions*. As mentioned above, the contamination activity will be empirically verified prior to shipment to be within the bounding 24.8 Ci value.

Summarizing, the total bounding activation activity is set to 30,000 Ci Co-60. A concentration for both fixed and loose surface contamination is conservatively determined to be an average concentration of **[**] (24.8 Ci total). The bounding A_2 quantity is 3,000 A_2. The decay heat for the thermal analysis is set conservatively at 500 watts. For radiolytic gas generation, the decay heat, based on a shipment date of March 31, 2023, is 358.1 watts.

Table 1.2-1 – CR3MP Contents Radionuclide Activity Levels

1.3 Appendices

1.3.1 References

1. Title 10 – Energy, Code of Federal Regulations, Part 71 (10 CFR 71), *Packaging and Transportation of Radioactive Material*, 01–01–20 Edition.
2. U.S. Nuclear Regulatory Commission, Regulatory Guide 7.9, Revision 2, *Standard Format and Content of Part 71 Applications for Approval of Packages for Radioactive Material*, March 2005, NRC Accession Number ML050540321.
3. Title 10 – Energy, Code of Federal Regulations, Part 61 (10 CFR 61), *Licensing Requirements for Land Disposal of Radioactive Waste*, 01–01–20 Edition.
4. ASTM A516 – 2017, *Standard Specification for Pressure Vessel Plates, Carbon Steel, for Moderate- and Lower-Temperature Service*, ASTM International, November 2017.
5. American Society of Mechanical Engineers (ASME) Boiler and Pressure Vessel Code, *Section II, Materials, Part A, Ferrous Material Specifications (SA-451 to End), SA516/SA-516M, Specification for Pressure Vessel Plates, Carbon Steel, for Moderate- and Lower-Temperature Service*, 2017 Edition.
6. American Society of Mechanical Engineers (ASME) Boiler and Pressure Vessel Code, *Section III, Rules for Construction of Nuclear Facility Components, Division 1 – Subsection ND, Class 3 Components*, 2017 Edition.
7. Title 49 – Transportation, Code of Federal Regulations, *Subtitle B – Other Regulations Relating to Transportation (Continued) (Parts 100 - 1699); Chapter I – Pipeline and Hazardous Materials Safety Administration, Department of Transportation (Parts 100 - 199), Subchapter C – Hazardous Materials Regulations*, 10–01–2019 Edition.
8. U.S. Nuclear Regulatory Commission, Regulatory Guide 7.12, Revision 0, *Fracture Toughness Criteria of Base Material for Ferritic Steel Shipping Cask Containment Vessels with a Wall Thickness Greater than 4 Inches (0.1 m) But Not Exceeding 12 Inches (0.3 m)*, June 1991, NRC Accession Number ML003739424.
9. U.S. Nuclear Regulatory Commission, NUREG/CR-3826, UCRL-53538, *Recommendations for Protecting Against Failure by Brittle Fracture in Ferritic Steel Shipping Containers Greater Than Four Inches Thick*, July 1984, NRC Accession Number ML20093N045.
10. U.S. Nuclear Regulatory Commission, NUREG/CR-6491, UCRL-ID-124583, *Recommendations for Protecting Against Failure by Brittle Fracture*, August 1996, NRC Accession Number ML20117F196.
11. U.S. Nuclear Regulatory Commission, *Final Waste Classification and Waste Form Technical Position Papers, May 1983, NRC Accession Number ML103420507.*

1.3.2 Packaging General Arrangement Drawings

The packaging general arrangement SAR drawing is as follows (see attached):

- 3024427, CR3MP Assembly SAR Drawing, 2 sheets

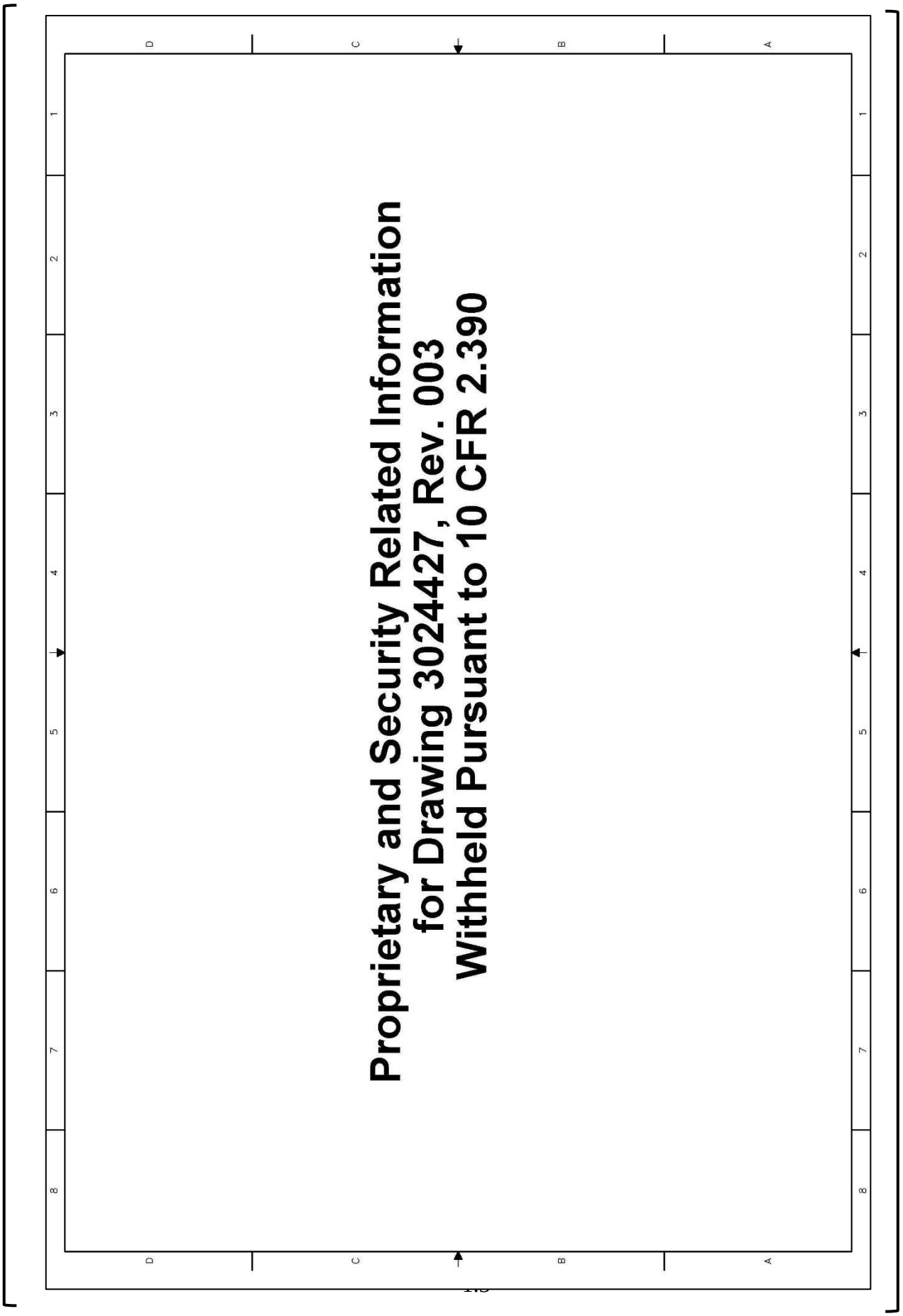
Proprietary and Security Related Information
for Drawing 3024427, Rev. 003
Withheld Pursuant to 10 CFR 2.390

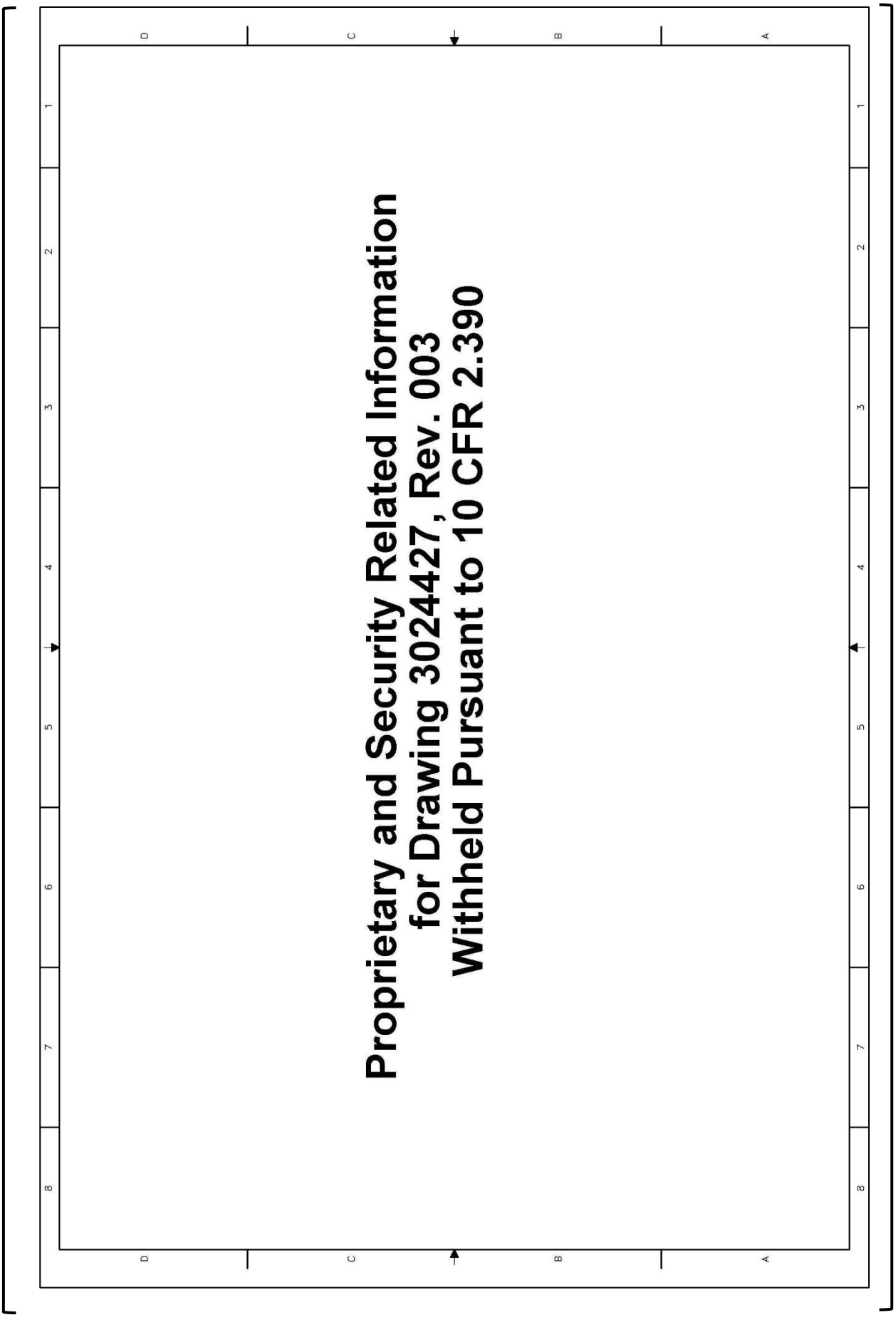
Proprietary and Security Related Information
for Drawing 3024427, Rev. 003
Withheld Pursuant to 10 CFR 2.390

2.0 STRUCTURAL EVALUATION

This section presents evaluations demonstrating that the CR3MP meets all applicable structural criteria of 10 CFR 71 [1], or else provides equivalent safety per the provisions of 10 CFR 71.41(d). The CR3MP is evaluated by analysis. Demonstration techniques comply with the methodology presented in NRC Regulatory Guides 7.6 [2] and 7.8 [3]

2.1 Structural Design

2.1.1 Discussion

As shown in the SAR drawing in Appendix 1.3.2, *Packaging General Arrangement Drawings*, the CR3MP is a thick-walled steel shell that encloses the middle portion of the CR3 RPV. The CR3MP and the RPV payload are described in detail in Sections 1.2.1, *General CR3MP Description*, and 1.2.2, *Contents*, respectively.

The CR3MP packaging consists of a cylindrical 3-in. thick steel shell, and 6-in. thick top and bottom cover plates. These components and their welds make up the containment boundary. The material of construction of the packaging base metal is ASTM A516 Grade 70 [4] or optionally ASME SA516 Grade 70 [5]. The cylindrical shell and each cover may have multiple full penetration welds connecting constituent plates. The cover plates are attached to the shell with full penetration closure welds. The top cover plate closure weld is a field weld, performed after placement of the payload into the packaging. The package is fully welded closed with one of the top cover lifting holes being fully tapped through in order to facilitate a pressure vent port. Prior to transport, the vent port is plugged by a fully threaded rod installed approximately flush to the package surface and secured shut with a closure weld (see details in Section 1.2.1.1, *Containment Vessel*). The package is 200.3-in. in diameter and 178.1-in. tall and has a maximum bounding weight of 860,000 pounds. A cross section of the package and payload is depicted in Figure 2.1-1.

The payload consists of the middle portion of the CR3 RPV. In addition, RVI components, immobilized in grout, are included in the RPV cavity. The RPV payload will rest on the bottom of the package, leaving an approximately three-inch thick annulus around the sides and an approximately three-inch thick space over the top of the payload. The annulus is filled with low density grout, leaving a nominal air space of 3 inches at the top of the payload.

The CR3MP design does not include any impact limiters or any other features that are specifically designed to absorb free drop energy. The package is designed to be resistant to fracture at the LST and provides containment of radioactive material under NCT and HAC.

The package will be transported in exclusive use by barge and by road between the CR3 site and the WCS disposal site.

2.1.2 Design Criteria

The acceptance criteria for analytic assessments are in accordance with NRC Regulatory Guide 7.6. These design criteria meet the following safety requirements of 10 CFR 71.51:

- For NCT, there shall be no loss or dispersal of radioactive contents, as demonstrated to a sensitivity of 10^{-6} A_2 per hour, no significant increase in external radiation levels, and no substantial reduction in the effectiveness of the packaging.
- For HAC, there shall be no escape of krypton-85 exceeding 10 A_2 in 1 week, no escape of other radioactive material exceeding a total amount of one A_2 in one week, and no external radiation dose rate exceeding one rem per hour at 40 inches from the external surface of the package.

The CR3MP contains a bounding value of [ ] of activity. [

] Accordingly, the CR3MP design will follow the guidance of Subsection ND. A summary of allowable stresses used for the containment (outer cylindrical shell and top and bottom closure plates) is presented in Table 2.1-2. The allowable stresses shown in the table are consistent with NRC Regulatory Guide 7.6.

For the NCT free drop event and the HAC free drop and puncture events, the containment shell materials are allowed to deform plastically. Material properties for non-linear analyses are developed in Appendix 2.12.2, *Free Drop Evaluation*.

The packaging has no lifting provisions available for use in the transport configuration. Thus, 10 CFR 71.45(a) does not apply to the CR3MP. In addition, since the CR3MP is not attached to the conveyance using any structural part of the package, tiedown structural criteria are not required.

2.1.2.1 Miscellaneous Structural Failure Modes

2.1.2.1.1 Brittle Fracture

All structural materials of the CR3MP are made from ASTM/ASME A516/SA516, Grade 70 alloy steel [4] [5]. This is a fine grain steel designed for low temperature service. The recommendations of NRC NUREG/CR-6491 [11] for a Category II package are used to establish the LST of the base material, equivalent to the minimum transportation ambient temperature, for transport of the CR3MP.

Entering Figure 1 of NUREG/CR-6491 [11] with a thickness of six inches (equal to the maximum thickness of material in the package) and following that down to the $\beta = 0.6$ curve, the resulting value of K_{ID}/σ_{yd} is 1.9 $in^{1/2}$. The room temperature yield strength of ASTM A516, Grade 70 is 38 ksi. Following down to the ordinate from $\sigma_{ys} = 38$ ksi yields an A-value of 19 °F. (Conservatively, a value of 20 °F will be used.) The SAR drawing states that the Nil Ductility Transition (NDT) temperature of the material in the CR3MP shall be no higher than -20 °F, as determined by the drop weight test of ASTM E208 [8].

The LST of the CR3MP is therefore:

$$LST = T_{NDT} + A = -20 + 20 = 0\ °F$$

Per the recommendation of NRC NUREG/CR-3019, Table 2 [12], the criteria for the welding material for a Category II package shall meet the requirements of ASME BPVC Subarticle ND-2400 [7].

The CR3MP will not commence transport, or will be stopped if in overland transport, if the ambient temperature falls below 0 °F. This will prevent a brittle fracture failure mode under NCT or HAC.

2.1.2.1.2 Fatigue Assessment

Fatigue failure of the CR3MP is not of concern. The package is designed for a single use to transport the payload from CR3 in Florida to WCS, the disposal site in Texas. The design of the package is very simple, having only an outer shell and two end cover plates, welded in place. There are no repetitively used components such as bolts, and no repetitive loading. Fatigue associated with normal vibration over the road is addressed in Section 2.6.5, *Vibration.*

2.1.2.1.3 Buckling Assessment

The CR3MP, when loaded and closed for transport, is a very robust and stout mass, which is not subject to buckling instability. The principal part of the payload is a cylindrical cross-section of RPV steel, [ ] thick and running almost the full length of the package. The interior of the RPV is filled with grout, and the annulus between the RPV and the package is also filled with grout. The packaging body shell and covers are also made of very thick steel. As such, for the conditions specified by 10 CFR 71, buckling behavior is not of concern.

2.1.3 Weights and Centers of Gravity

The maximum gross weight of the CR3MP is 860,000 lb. The CR3MP maximum bounding weights are summarized in Table 2.1-3. The Center of Gravity (CG) of the CR3MP is located essentially at the package geometric center.

2.1.3.1 LDCC Bounding Actual Volumes and Weights

For usage throughout the SAR as required, LDCC actual minimum, maximum and nominal weights are calculated below, given the densities of 30pcf, 60 pcf and 53 pcf, respectively. For reference, the nominal density of 53 pcf is based on the down-selected formulation that will be used during grout pouring.

Volume of LDCC within reactor vessel (central LDCC)

The volume in the central region (confined by the shell walls of the RPV) may be computed as shown below as the volume of a right circular cylinder. Using this volume and subtracting off the volume taken by the RVI will provide the central LDCC volume. As shown in Table 2.1-1, the RVI volume is determined using 3-D CAD models of individual RVI components in SolidWorks.

Then, the sum of the volume of RVI components from Table 2.1-1 is:

[ ]

Table 2.1-1 – Individual RVI Component Volumes Based on Solidworks Models

[ ]

$= 3.045 \times 10^6$ in^3 = 1762 ft^3 = 49.90 m^3

Given this volume, the minimum, maximum and nominal weight of the central LDCC region is as follows:

$W_{LDCC.int}^{max} = V_{LDCC}^{cavity} \times \rho_{LDCC}^{max} = 105.7\ kips$

$W_{LDCC.int}^{min} = V_{LDCC}^{cavity} \times \rho_{LDCC}^{min} = 52.9\ kips$

$W_{LDCC.int}^{nom} = V_{LDCC}^{cavity} \times \rho_{LDCC}^{nom} = 93.4\ kips$

The volume in the annular region (confined by the outside of the RPV shell wall and inside of the CR3MP shell wall for the full height of the RPV shell wall) may be computed as shown below as the volume of a right circular cylinder.

[ ]

[ ]

Therefore, the annular LDCC maximum, minimum, and nominal weights are as follows:

$$W_{LDCC.annular}^{maximum} = \rho_{LDCC}^{max} \times V_{LDCC.annular}^{maximum} = 60pcf \frac{1pci}{1728pcf} \times 3.46 \times 10^5 \text{ in}^3 = 12.0kip$$

$$W_{LDCC.annular}^{minimum} = \rho_{LDCC}^{min} \times V_{LDCC.annular}^{minimum} = 30pcf \frac{1pci}{1728pcf} \times 2.72 \times 10^5 \text{ in}^3 = 4.7kip$$

$$W_{LDCC.annular}^{nominal} = \rho_{LDCC}^{nominal} \times V_{LDCC.annular}^{nominal} = 53pcf \frac{1pci}{1728pcf} \times 2.97 \times 10^5 \text{ in}^3 = 9.1kip$$

2.1.4 Identification of Codes and Standards for Package Design

As discussed in Section 2.1.2, *Design Criteria*, the CR3MP is classified as a Category II package, and per the guidance of NUREG/CR-3854, the appropriate design criteria for the containment is Section III, Division 1, Subsection ND of the ASME BPVC. Consequently, the design of the containment boundary is based on the methodology of NRC Regulatory Guide 7.6, and load cases are applied and combined according to NRC Regulatory Guide 7.8.

Table 2.1-2 – Packaging Allowable Stress Limits

Stress Category	NCT	HAC
General Primary Membrane Stress Intensity	S_m	Lesser of: $2.4S_m$, $0.7S_u$
Primary Membrane + Bending Stress Intensity	$1.5S_m$	Lesser of: $3.6S_m$, S_u
Range of Primary + Secondary Stress Intensity	$3.0S_m$	N/A
Pure Shear Stress	$0.6S_m$	$0.42S_u$

Table 2.1-3 – CR3MP Component Maximum Bounding Weights

Figure 2.1-1 – CR3MP Cross Section

2.2 Materials

The CR3MP consists of ASTM/ASME A516/SA516 Grade 70 steel shell and covers, with the shell nominally 3-in. thick and the covers nominally 6-in. thick. The void space within the RPV segment surrounding the RVI and the annulus between the RPV and the package wall is filled with grout. The package as assembled for transport is depicted in Figure 2.1-1. There are no bolts or other structural components used in the CR3MP and no seals as well. Nonstructural elements of the CR3MP include the following plain carbon steel components: top cover backing bar, top cover set screw plugs, threaded vent port rod and remnants of empty packaging lift lugs on the inside of the shell.

2.2.1 Material Properties and Specifications

Table 2.2-1 presents the material properties for the ASTM/ASME A516/SA516 Grade 70 material. Of note, for purposes of this SAR, the material properties of ASTM A516, Grade 70 are considered identical to those of ASME SA516, Grade 70. As necessary and as noted in Table 2.2-1, material data is interpolated or extrapolated from the tabulated dataset. The density of steel used is 0.280 lb/in^3.

The interior of the RPV is filled with grout, filling the void space and immobilizing the RVI components within. A LDCC grout having a density range of 30 to 60 pcf is used. Outside of the RPV, in the nominal 3-in. wide annulus between the RPV and the interior of the package, LDCC is used. The nominal 3-in. wide space above the RPV and below the top cover is filled with air.

The LDCC consists of Portland cement per ASTM C150 [13]. The LDCC is mixed with foaming agents per ASTM C869 [14] and follows the guidance of American Concrete Institute (ACI) 523.1R [15]. The thermal expansion coefficient for the grout material is similar to that of steel (i.e., ranging between approximately $5 – 7 \times 10^{-6}$ in/in/°F) per [15] and ACI 523.3R-14 [16]. In the free drop evaluations under NCT and HAC, a crush strength of 100 psi is conservatively assumed for both densities of grout material.

Material properties for non-linear analyses are developed in Appendix 2.12.2, *Free Drop Evaluation*.

2.2.2 Chemical, Galvanic, or Other Reactions

The CR3MP steel and concrete materials of construction will not have significant chemical, galvanic or other reactions, neither internally nor externally. The integral contact between carbon steel and concrete is a common practice in structures designed to last many years (e.g., reinforcement rods in concrete structures). The outside (top and sides) of the package is painted. The marine leg of the transport from the CR3 site to the WCS disposal site will be of relatively brief duration, and the package is designed for a single trip. No deleterious corrosion is expected from the brief sea voyage. Therefore, the CR3MP will not be compromised by any chemical, galvanic, or other reactions.

2.2.3 Effects of Radiation on Materials

The radiation associated with the RPV and its RVI contents is essentially all gamma radiation and will have no effect on the material properties of the containment boundary steel or on the integrity of the grout material. Some radiolysis of the moisture hydrated in the grout may occur, releasing hydrogen and oxygen gas. The accumulation of hydrogen within the package air space is further discussed in Section 4.2, *Containment under Normal Conditions of Transport*. Properties related to the interaction of the grout and absorbed radiation and thus hydrogen and total gas production rates of the grout is discussed in greater detail in Section 5.4.4, *Radiolytic Gas Generation*.

Table 2.2-1 – Mechanical Properties of ASTM/ASME A516/SA516 Grade 70 Steel

Material Specification[6]	Temperature (°F)	Yield Strength, S_y (psi)[1]	Ultimate Strength, S_u (psi)[2]	Design Stress Intensity, S_m (psi)[3]	Elastic Modulus, E ($\times 10^6$ psi)[4]	Thermal Expansion Coefficient, α ($\times 10^{-6}$ /ºF)[5]
ASTM A516 Grade 70 or ASME SA516 Grade 70	-100	38,000	70,000	23,300	30.3	5.8
	-40	38,000	70,000	23,300	30.0	6.0
	-20	38,000	70,000	23,300	29.9	6.1
	70	38,000	70,000	23,300	29.4	6.4
	100	38,000	70,000	23,300	29.3	6.5
	150	35,700	70,000	23,300	29.0	6.6
	200	34,800	70,000	23,200	28.8	6.7
	300	33,600	70,000	22,400	28.3	6.9
	400	32,500	70,000	21,600	27.9	7.1
	500	31,000	70,000	20,600	27.3	7.3
	600	29,100	70,000	19,400	26.5	7.4
	700	27,200	70,000	18,100	25.5	7.6

Notes:
[1] - ASME BPVC, Section II, Part D, Table Y-1. Value at -100 ºF – 70 ºF conservatively assumed using the value at 100 ºF.
[2] - ASME BPVC, Section II, Part D, Table U. Value at -100 ºF – 70 ºF extrapolated using the values at 100 ºF and 150 ºF.
[3] - ASME BPVC, Section II, Part D, Table 2A. Value at -100 ºF – 70 ºF extrapolated using the values at 100 ºF and 150 ºF.
[4] - ASME BPVC, Section II, Part D, Table TM-1, Carbon Steels with C ≤ 0.30%. Values for -40 ºF and -20 ºF interpolated from 70 ºF and -100 ºF. Values at 100 ºF and 150 °F interpolated using the values at 70 ºF and 200 ºF.
[5] - ASME BPVC, Section II, Part D, Table TE-1, Material Group 1, Mean Coefficient. Values for -100 ºF, -40 ºF and -20 ºF extrapolated from 70 ºF and 100 ºF.
[6] - All ASME BPVC references from [17].

2.3 Fabrication and Examination

2.3.1 Fabrication

The containment boundary material (cylindrical shell, Item No. 1 on SAR drawing, and top and bottom covers, Item No. 2) must meet the ASTM specifications delineated on the SAR drawing shown in Appendix 1.3.2, *Packaging General Arrangement Drawings*. Containment boundary material requirements are as follows:

- Material shall meet a maximum NDT temperature of -20 °F using the drop weight test method per ASTM E208 [8].
- Material carbon content shall not exceed 0.30%.
- Weld metal tensile strength shall not be greater than 10% above the specified maximum tensile strength of the base metal.
- Category A and B cover and shell welds (i.e., those welds joining separate sections of the shell or covers, as required) shall be full penetration joints.
- Closure joint welds between the top and bottom covers and the outer shell are CJP Category C welds meeting the requirements of ASME BPVC, Section III, Subparagraph ND-4243.1, Figure ND-4243-1(j) [7].

Welding requirements are as follows:

- All welding procedures and welding personnel must be qualified in accordance with Section IX of the ASME BPVC [19].
- Weld Coupons of Each Heat of weld filler metal shall be Charpy V-Notch tested in accordance with ASME BPVC, Section III, Division 1, Subsection ND, Subarticle ND-2400 and Table ND-2331(A)-2 [7]. The lowest service temperature shall be 0°F.
- Weld filler material and welding procedure qualifications shall be in accordance with ASME BPVC, Section III, Division 1, Subsection ND, Paragraph ND-4335 [7].
- Weld procedure qualifications shall be performed using base metal having a carbon content and carbon equivalency greater than or equal to that of the actual containment component materials.

The LDCC shall have a wet-cast density between 30 – 60 pcf. The LDCC grout will be formulated and placed using a written procedure that uses guidance from ACI 523.1R [15]. Of note, the terms “wet-cast” and “as-cast” used herein are considered synonymous and follow the definition in Section 6.1.2.1 of ACI 523.3R-14 [16].

2.3.2 Examination

All welds are subject to visual examination (VT) per ASME BPVC, Section III, Division 1, Subsection ND, Paragraph ND-4123 with acceptance criteria of Paragraph ND-4424 [7]. The Category A and B cover and shell welds shall be radiograph (RT) inspected and liquid penetrant (PT) or magnetic particle (MT) inspected on the inner and outer finished surfaces in accordance with ASME BPVC, Subsection ND, Subarticle ND–5300 [7]. In lieu of the RT requirement of Subsubarticle ND-5230, and in accordance with Paragraph ND-5279, the Category C CJP closure joints (both top and bottom covers) shall receive a full volumetric inspection of the final weld joint via Ultrasonic Examination (UT). The Category C weld joining the bottom cover and the shell shall be UT inspected on the finished weld and either PT or MT inspected on the inside fillet weld and on the outer finished surface in accordance with ASME BPVC, Subsection ND, Subarticle ND-5300. The Category C weld joining the top cover and the shell shall be UT inspected on the finished weld and either PT or MT inspected on the root pass and on the outer finished surface in accordance with ASME BPVC, Subsection ND, Subarticle ND-5300.

The pressure vent port groove weld described in Section 1.2.1.1, *Containment Vessel*, shall be PT or MT inspected on the final surface in accordance with ASME BPVC, Section III, Division 1, Subsection ND, Subarticle ND-5300, and ASME BPVC Section V [28], Article 6 (PT) or Article 7 (MT), as applicable.

The LDCC shall have a minimum compressive strength of 100 psi at 28 days, when tested using guidance from ASTM C495 [21].

2.4 General Standards for All Packages

This section defines the 10 CFR 71.43 compliance standards required to be met by the CR3MP. The CR3MP meets all requirements delineated in this section.

2.4.1 Minimum Package Size

In accordance with 10 CFR 71.43(a), the overall dimensions of the CR3MP must be greater than 4 inches. The minimum dimension of the CR3MP is approximately 178 inches. Thus, the 4-in. minimum requirement of 71.43(a) is satisfied.

2.4.2 Tamper-Indicating Feature

In accordance with 10 CFR 71.43(b), as configured for transport, the CR3MP is sealed and would not be readily breakable by unauthorized persons. The CR3MP is welded closed using a minimum 3.75-in. thick weld. Entry into the package cannot occur without destructively breaching this weld. Thus, the requirement of 71.43(b) is satisfied.

2.4.3 Positive Closure

In accordance with 10 CFR 71.43(c), the package body and covers are the containment boundary and are joined at the interface seams by large full penetration welded joints. As such, the package cannot be opened unintentionally or by a pressure rise within the package. Thus, the requirements of 71.43(c) are satisfied.

2.4.4 Materials

The CR3MP meets the requirements of 10 CFR 71.43(d) as discussed in Section 2.2, *Materials*.

2.4.5 Valves

In accordance with 10 CFR 71.43(e), there are no packaging valves or other devices used in the CR3MP containment boundary and the pressure vent port plug is welded shut. Therefore, no such component needs protection and the requirements of 71.43(e) are satisfied.

2.4.6 Package Design and NCT Conditions

In accordance with 10 CFR 71.43(f), the CR3MP is designed to comply with NCT while preventing loss or dispersal of radioactive contents, not significantly increasing the external surface radiation level and not substantially reducing the effectiveness of the packaging. This is shown in Chapter 2.0, *Structural Evaluation,* Chapter 3.0, *Thermal Evaluation,* and Chapter 5.0, *Shielding Evaluation*, for the structural, thermal, and shielding requirements, respectively. Therefore, the requirements of 71.43(f) are satisfied for the CR3MP.

2.4.7 External Temperatures

In accordance with 10 CFR 71.43(g), the CR3MP is designed such that while exposed to a temperature of 100°F in the shade, that no accessible surface of the package will exceed 185°F when shipped as an exclusive use shipment. Since the CR3MP is a single-use package, there will only be a one-time, exclusive use shipment of the CR3MP. As shown in Table 3.1-1 from Section 3.1.3, *Summary Tables of Temperatures*, the maximum accessible surface temperature with no insolation is bounded by 85 °C, or 185 °F. This satisfies the limit of 71.43(g) for exclusive use shipments.

2.4.8 Venting

In accordance with 10 CFR 71.43(h), there is no pressure relief (i.e., venting) system features in the CR3MP during transport, therefore no continuous venting is intended to occur. The pressure vent port described in Section 1.2.1.1, *Containment Vessel*, is plugged and welded shut prior to transport. Thus, the requirements of 71.43(h) are satisfied.

2.5 Lifting and Tie-down Standards for All Packages

2.5.1 Lifting Devices

The CR3MP does not include any devices that are a structural part of the package that are present in the transport configuration. In addition, as indicated in Section 7.1.2, *Loading of Contents*, the threaded holes for lifting the top cover will be plugged in order to prevent any inadvertent lifting. Thus, 10 CFR 71.45(a) does not apply.

2.5.2 Tie-down Devices

As covered in Chapter 7.0, *Package Operations* during transport, the CR3MP is held down by means of passive, indirect tiedowns which rest on top of, and against the side of the CR3MP. The tiedowns include flexible lashings for use during road transport, and a rigid frame for use during barge transport, so that the package is vertically restrained in place when subjected to the transportation loads. There will also be bearing plate restraints and flexible lashings to react lateral loads on the CR3MP. In this configuration, these load securement components only contact against the CR3MP surfaces and do not directly connect to the CR3MP. In addition, as indicated in Section 7.1.2, *Loading of Contents*, the threaded holes for lifting the top cover will be plugged in order to render those holes inoperable for tiedown of the CR3MP during transport. Therefore, the CR3MP has no integral tie-down devices which are a structural part of the package. As a result, per 10 CFR 71.45(b)(1), the evaluation of tie-down devices is not required.

One tie-down method that may be used for barge transport is indicated in Figure 2.5-1, where the CR3MP is placed on a skid or beams and receives lateral support in multiple bearing plate locations. Then, as shown in Figure 2.5-1, the vertical tiedown frame for barge transport is constructed using four vertically oriented wide flange beams connected to X-shaped horizontal cross beams which rest on top of the CR3MP. Once in place over the CR3MP, the vertical tiedown frame is attached to the skid or conveyance, thus providing both lateral and vertical support for transportation inertial loading. The vertical tiedown frame is installed to the skid or conveyance with sufficient operational gap at the top interface locations, ensuring the frame can be securely attached to the skid or conveyance while applying no downward load to the CR3MP itself. As required, shims are used to reduce any excessive gaps, but in any case, the frame is not preloaded against the CR3MP. Similar tie-down methods may be used, depending upon the final selection of a carrier and available transport conveyance.

One tie-down method that may be used for road transport is shown in Figure 2.5-2, where the tiedown system for road transport includes a skid or beams, but with flexible lashings arranged in a crossing pattern. In this case, the flexible lashings bear against the CR3MP's top edges via corner pads. Flexible lashings may be used as necessary around the body of the CR3MP to restrain lateral loads. Similar tie-down methods may be used, depending upon the final selection of a carrier and available transport conveyance.

Besides transport inertial loads, the only loading between the tiedowns and the CR3MP that could occur would be the result of thermal expansion in the maximum heat conditions of 10 CFR 71.71(c)(1). However, the differential thermal expansion between the CR3MP and the rigid vertical tiedown frame used with the barge will be very small in magnitude. This is since the CR3MP is a relatively low-heat package and both the CR3MP and the frame will have similar temperatures. In addition, the CR3MP and frame are both made of steel with essentially identical thermal expansion coefficients. Furthermore, the frame will not be preloaded against the CR3MP, affording the possibility of the CR3MP to grow in length with respect to the frame without contact. Thus, the differential thermal expansion will be very small and of no adverse effect on the CR3MP design structural integrity during barge transport.

In the case of the road transport configuration, the CR3MP is preloaded to the skid or conveyance, but this is done using flexible tiedown elements that are much less stiff than the CR3MP. It follows that the flexible lashings may flex and stretch to the CR3MP accordingly. As a result, the tiedowns used during road transport have no adverse effect on the CR3MP design structural integrity.

For both modes of transport, the bearing plates and flexible lashings react lateral loads through usage of shims, ensuring a nominal clearance with the CR3MP. This makes certain the CR3MP can be placed securely on the skid or conveyance, and therefore be of no concern for thermal expansion. As a result, thermal expansion will create only an inconsequential load which does not adversely affect the CR3MP structural integrity in either road or barge transport configurations.

The NCT conditions delineated in 10 CFR 71.71(c)(2) (*Cold*), (c)(3) (*Reduced External Pressure*), and (c)(4) (*Decreased External Pressure*) will also be inconsequential on the CR3MP structural integrity with respect to either barge or road transport tiedown configurations.

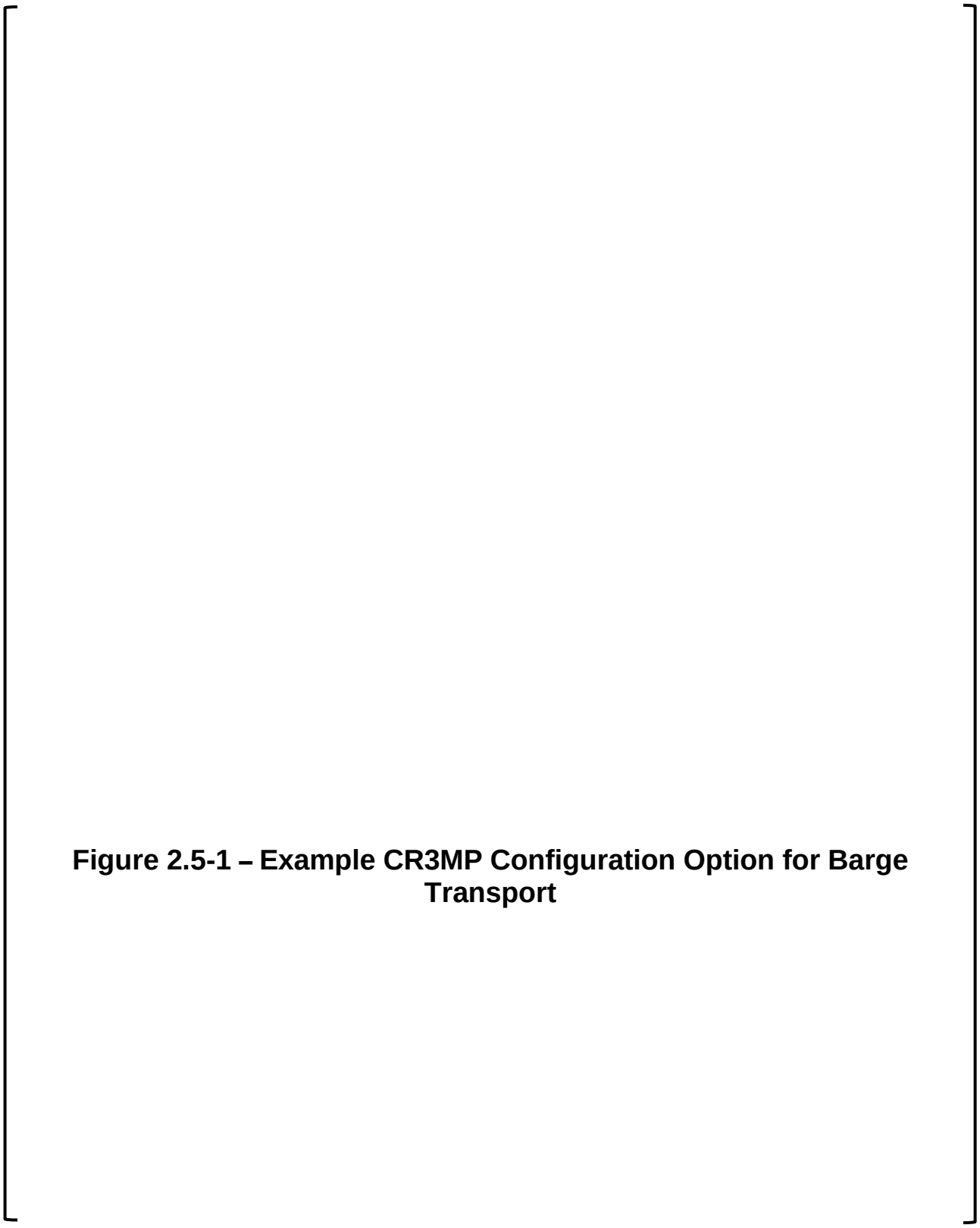

Figure 2.5-1 – Example CR3MP Configuration Option for Barge Transport

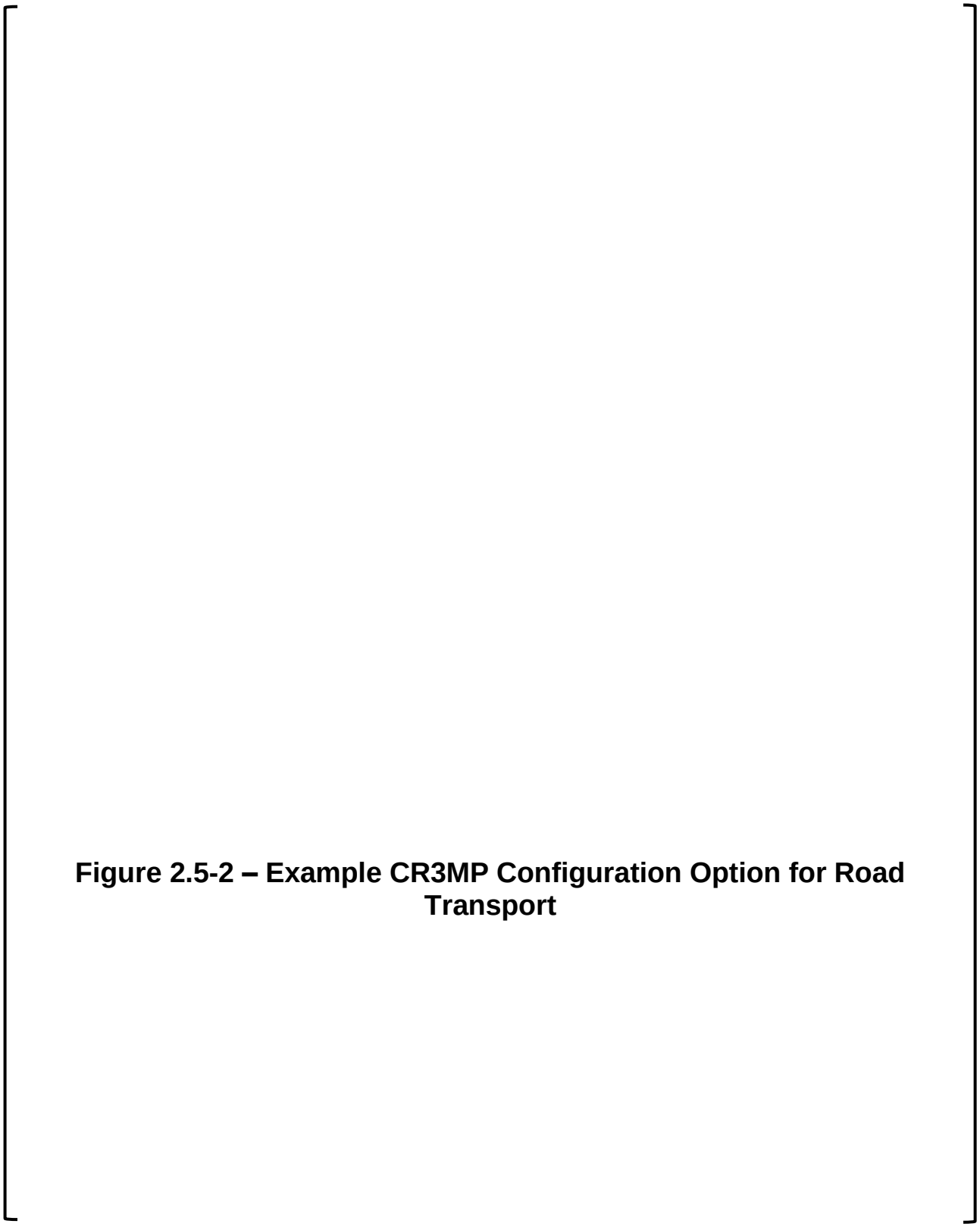

Figure 2.5-2 – Example CR3MP Configuration Option for Road Transport

2.6 Normal Conditions of Transport

As specified in 10 CFR 71.71 [1], the CR3MP meets the performance criteria specified in Subpart E of 10 CFR 71. This is demonstrated in the following subsections where each NCT condition is addressed and shown to meet the applicable design criteria. Load combinations used in this section are consistent with NRC Regulatory Guide 7.8 [3].

2.6.1 Heat

The NCT heat condition, as defined in 10 CFR 71.71(c)(1), is evaluated in Chapter 3.0, *Thermal Evaluation*. The bounding temperatures and pressures for use in structural analyses are summarized in the following subsections. Material properties and stress limits are taken from the design criteria shown in Table 2.1-2.

2.6.1.1 Summary of Pressures and Temperatures

The CR3MP containment components are bounded by a temperature of 51 °C or 123.8 °F in the 100 ºF ambient NCT condition, as presented in Table 3.1-1 of Chapter 3.0, *Thermal Evaluation*. Conservatively, a temperature of 150 °F will be used for NCT structural evaluations.

The initial pressure in the package at the time of welding shut the top cover is at Standard Temperature and Pressure (STP) conditions, (i.e., 14.7 psia). As discussed in Appendix 3.5.2, *Evaluation of Pressure in the CR3MP*, pressure may be generated in the CR3MP due to the release of moisture from the LDCC. Therefore, as determined in Section 3.3.2, *Maximum Normal Operating Pressure*, the MNOP is set at a value of 3.9 psig. The design pressure of the CR3MP is set at 25 psig.

2.6.1.2 Differential Thermal Expansion

As shown in Section 2.2, *Materials*, grout has a thermal expansion coefficient which is similar to that of carbon steel. The volume of grout that is significantly warmer than the steel packaging containment shell is limited to a small region at the central interior of the RPV. The expansion of this region will be absorbed by the cooler material outside of it and will not increase the stress of the packaging shell by expansion. The outer grout material near the shell body has essentially the same temperature and thermal expansion coefficient as the shell. Thus, differential thermal expansion is not of concern.

2.6.1.3 Stress Calculations

2.6.1.3.1 Stresses Due to Pressure Loading

The containment boundary will be evaluated for the internal pressure condition by combining the MNOP with the reduced external pressure condition of 3.5 psia per 10 CFR 71.71(c)(3). MNOP is 3.9 psig or 18.6 psia. For an external pressure of 3.5 psia, the differential pressure to be used in the following calculations is 18.6 – 3.5 = 15.1 psi. However, a conservative value of 26.2 psi will be used. This pressure is governing compared to the differential pressure formed using the internal design pressure of 25 psig.

Given that the CR3MP is a simple cylindrical shell with flat ends, the membrane stress in the cylindrical walls is:

$$\sigma_a = \frac{qr}{t} = 848\ psi$$

Where:

q = 26.2 psi

r = 97.15 inches, radius of closure, equal to half the Inside Diameter (ID) (or 194.3/2)

t = 3 inches, thickness of shell wall

The top and bottom covers are identical 6.0-in. thick plates. As shown in the SAR drawing, each cover tapers to a thickness of 3.75 inches for a radial distance of 5.75 inches at the outer edge. From Table 24, Case 10b of Roark [22], the bending stress at the center of the closure plate, assuming fixed edge support at the junction to the shell is:

$$\sigma_b = \frac{6M_c}{t^2} = \frac{6\left[\frac{qr^2(1+v)}{16}\right]}{t^2} = 3{,}349\ psi$$

Where:

v = 0.3, Poisson's ratio

t = 6 inches, thickness of the cover plates

From Table 24, Case 10b of [22], the stress at the outside edge of the cover (the weld), assuming a fixed edge, is:

$$\sigma_c = \frac{6M_c}{t^2} = \frac{6\left[\frac{qr^2}{8}\right]}{t^2} = 13{,}188\ psi$$

Where:

t = 3.75 inches, thickness of the cover plate welds.

2.6.1.3.2 Comparison with Allowable Stresses

From Table 2.1-2, at the bounding temperature of 150 ºF, the value of S_m for the package material is 23,300 psi.

The stress in the side wall, σ_a, is a membrane stress, P_m. From Table 2.1-2, the limit on membrane stress is S_m. The MS is:

$$MS_1 = \frac{23{,}300}{848} - 1 = +Large$$

The bending stress in the closure plates is calculated above to be σ_b = 3,349 psi, and is classified as membrane plus bending, or $P_m + P_b$. From Table 2.1-2, the limit on $P_m + P_b$ is $1.5S_m$, or 1.5 × 23,300 = 34,950 psi. The MS is:

$$MS_2 = \frac{34{,}950}{3{,}349} - 1 = +9.4$$

The bending stress in the closure plate welds is calculated above to be σ_c = 13,188 psi and is again classified as membrane plus bending, where the stress limit is 34,950 psi. The MS is:

$$MS_1 = \frac{34{,}950}{13{,}188} - 1 = +1.65$$

Thus, the NCT warm condition is of no concern.

2.6.2 Cold

For the cold condition of 10 CFR 71.71(c)(2), a -40 ºF steady state ambient temperature is used per NRC Regulatory Guide 7.8, with zero insolation and zero decay heat. This results in a uniform temperature of -40 ºF throughout the package. Since the steel containment shell and the grout have a similar coefficient of thermal expansion and the temperature of the materials is essentially the same, thus, no interference load will occur. Brittle fracture of the containment boundary is also of no concern because the CR3MP will be transported at a temperature above the LST, which has been set at 0 °F, as discussed in Section 2.1.2.1.1, *Brittle Fracture*.

2.6.3 Reduced External Pressure

The effect of reduced external pressure of 3.5 psia, per 10 CFR 71.71(c)(3), has been considered in the NCT structural analysis presented in Section 2.6.1, *Heat*. Based on the MNOP of 3.9 psig, the reduced external pressure condition would cause a pressure differential of 15.1 psi. However, conservatively using a pressure value of 26.2 psi, a bounding pressure stress was calculated. Given this pressure load, the worst-case bending stress in the closure plate welds show a positive margin. Therefore, the reduced external pressure case of 71.71(c)(3) is of no concern.

2.6.4 Increased External Pressure

The effect of an increased external pressure of 20 psia, per 10 CFR 71.71(c)(4), is acceptable for the CR3MP. Consistent with NRC Regulatory Guide 7.8, this loading corresponds to a minimum ambient temperature of -20 ºF, with no insolation, no decay heat, and minimum internal pressure.

With the CR3MP closed under ambient conditions, the internal pressure at a temperature of -20 ºF is:

$$p_i = p_{amb}\frac{(-20 + 460)}{(70 + 460)} = 12.2\ psia$$

Where p_{amb} is 14.7 psia. Therefore, the differential gas pressure from outside the shell side is p_{ds} = (20 – 12.2) = 7.8 psi. Since the package is filled with grout which has crush strength much greater than this pressure, the external pressure can be resisted by the grout alone without assistance from the steel shell. The top cover is not supported by grout. However, it has been evaluated for the much greater differential pressure of 26.2 psi in Section 2.6.1.3.1, *Stresses Due to Pressure Loading*. Thus, the increased external pressure load case of 71.71(c)(4) is of no concern.

2.6.5 Vibration

Per 10 CFR 71.71(c)(5), the vibration normally incident to transport will not have a deleterious effect on the CR3MP packaging or its contents. The massive components of the package have natural frequencies which are unlikely to receive any consequential amount of energy from transport vibration. The package is also filled with grout material which serves as a damping component. In addition, the overall number of loading cycles the CR3MP experiences is minor over a single use shipment. Therefore, fatigue of the CR3MP due to transportation vibration would not adversely affect compliance with the 10 CFR 71.51(a)(1) NCT requirements.

2.6.6 Water Spray

The material of construction (steel) used in the CR3MP is not affected by the water spray test identified in 10 CFR 71.71(c)(6).

2.6.7 Free Drop

10 CFR 71.71(c)(7) specifies a free drop from a height of one foot for a package weight more than 33,100 lb. The governing NCT free drop orientations are flat top-down end, side, and CG-over-corner with a follow-through tip-over on the CG-over-corner case. Details of the free drop analysis are provided in Appendix 2.12.2, *Free Drop Evaluation*.

First, an overall assessment of the free drop orientations is included and then a specific discussion of the individual orientations is provided in the sub-sections below. Based on experience, a package having a diameter-to-height ratio near to 1 (diameter and height nearly the same), as is the case for the CR3MP, will not have a significant slapdown response. Therefore, the worst-case orientation will be the one where the drop energy is concentrated on the least material volume (i.e., the CG-over-corner drop). This would be the drop case with the highest deformation. However, it is noted that a follow-through tip-over condition from the CG-over-corner end state may have more energy than the initial NCT end drop since the CG vertical height drop for the follow-through case is greater than that of the simple 1-ft NCT End Drop. Therefore, for completeness, a simulation of the follow-through tip-over analysis is run for comparison and evaluation with the other cases.

CR3MP acceleration results are compared for the NCT side, corner, end and tip-over drop orientations. Table 2.6-1 shows the results of the various cases. As the results show during the tip-over event, the additional energy produced the highest acceleration and total energy. Although the corner drop had higher deformation and higher resultant Effective Plastic Strain (EPS) build-up, the tip-over case includes the accumulated strain limit damage from the corner drop case, hence it provides the bounding margins. Since the CR3MP is symmetrical, a bottom-down end drop is not included, as the top-down case includes content shifting effects within the CR3MP 3-in. upper headspace. The side drop case is included for completeness. In all cases, when subjected to a 1-ft free drop onto an unyielding surface, the containment boundary of the CR3MP remains intact.

Table 2.6-1 – Assessment of Free Drop Orientations

Drop Case Description	Test #	Accel. (G's)	Maximum Elemental EPS (%)	Maximum Averaged through wall EPS (%)	Maximum Accumulated damage (%)	Damage Margin of Safety	Max. (1) Total Energy (in-lb$_f$)	Drop Orientation Assessment
1-foot, Top-Down End Drop	N1	104	3.36	1.27	1.9	+19.8	6.44e6	The large contact surface area of the top cover will result in little deformation with high accelerations. A high-speed stress wave will pass through the cylindrical body of the CR3MP. Includes added conservatism due to top cover loading from payload shifting to close the 3-in. upper headspace gap.
1-foot, Side Drop	N2	17.8	7.98	4.44	1.9	+19.8	5.60e6	The cylindrical shell of the CR3MP will be backed up by the relatively thick RPV wall. Minimal strains are present in both the lower regions of the top and bottom closure covers.
1-foot, CG-over-top corner	N3	9.4	21.0	6.91	17.9	+3.8	6.88e6	The concentrated load over the edge of the top cover results in the highest localized deformations. The secondary impact of the RPV/RVI imparts an additional region of stress on the inside of the shell and impacted portion of the top cover.
Tip-over from final state of test N3	N3_TO	225	21.1	6.91	21.1	+3.7	1.54e8(2)	Considers the deformed state resulting from N3 as the starting condition. Also, the case considers higher energy than the initial NCT end drop since the CG vertical height drop for the follow-through case is greater than that of the simple 1-ft NCT End Drop.
Slapdown to side	N/A	N/A	N/A	N/A	N/A	N/A	N/A	Not evaluated. This is like N3_TO but with lower initial CG height due to the aspect ratio of the CR3MP. This case will be bounded by the other drops for deformation and acceleration.

Notes 1. The energy values are taken from the plots in Appendix Section 2.12.2.7, *Model Energies*.
2: This value is conservatively higher than that determined in Appendix Section 2.12.2.5.4, as it conservatively uses an angular velocity of 3 rad/s.

2.6.7.1 Material Properties and Acceptance Criteria Used in Free Drop Analysis

A stress strain curve to full material failure for the governing heat of material used for the CR3MP containment boundary is developed in Appendix Section 2.12.2.4.2.4, *Packaging Steel*. This curve was used to represent the containment boundary (side 3-in thick shell and top and bottom 6-in cover plates) in all drop event impact computer simulations. It represents a conservative lower-bound result, and after the uniform true strain necking limit of 0.22, the curve is conservatively modeled as perfectly plastic.

The NCT acceptance criteria utilized in the drop impact evaluations allows for plastic deformation of the packaging while preventing release of the contents. The acceptance criteria, which is fully developed in Appendix Section 2.12.2.2.1, *Acceptance Criteria*, examines the stress state at limiting points in the containment components and compares the EPS with the limiting triaxial strain (Triaxiality Factor (TF) limit) as outlined in ASME BPVC, Section VIII, Division 2, Article 5.3.3 [20]. The allowable EPS limits at bounding points in the containment boundary is ascertained after running the LS-DYNA® simulation model, during post-processing.

By including the loading sequence, an accumulated strain limit damage calculation is made.

From Equation 5.11 of [20], the total strain limit damage is the sum of any forming strain and the sequence of drop event strains:

$$D_{\varepsilon} = D_{\varepsilon form} + \Sigma \Delta D_{\varepsilon,k} \leq 1.0 \qquad \text{Eq. 5.11}$$

Where $D_{\varepsilon form} = 0.029$ (See Appendix Section 2.12.2.2.1, *Acceptance Criteria*) is the forming damage due to forming of the shell and $\Sigma \Delta D_{\varepsilon,k}$ is the sum of impact event strain damage. Each element in the model is acceptable if the value is less than or equal to unity ($D_{\varepsilon} \leq 1$). Then, rearranging Eq. 5.11, the margin of safety with respect to accumulated strain limit damage can be written as follows:

$$MS = \frac{D_{\varepsilon}}{D_{\varepsilon form} + \Sigma \Delta D_{\varepsilon,k}} - 1 = \frac{1}{0.029 + \Sigma \Delta D_{\varepsilon,k}} - 1 > 0$$

Conservatively, the forming damage value is applied regardless of whether the location is in the formed shell, or the unformed top and bottom cover plates. If the margin of safety with respect to accumulated strain limit damage is above zero, fracture initiation of the containment boundary is precluded, and no elements are shown as eroded in the LS-DYNA® model. This is the case for all NCT evaluations; no fracture occurs, and the containment boundary remains fully intact.

2.6.7.2 NCT End Drop

The CR3MP end drop case was modeled with the top end cover facing down, since in that orientation, there is a 3-inch air gap between the RPV top surface and the top cover. From the time of release, external work is generated as the payload shifts, filling this gap. As shown in Table 2.6-1, when filtered at 1,000 Hz, the maximum impact acceleration on the package is 104 g.

As shown in Table 2.6-1, there is minimal plastic deformation, with the maximum accumulated strain limit damage in the center of the bottom cover at only 1.9% of the limit, or a margin of safety as follows:

$$MS = \frac{1}{.029 + .019} - 1 = 19.8$$

Therefore, the CR3MP containment boundary remains intact. Plots of strain and time histories of impact are provided in Appendix Section 2.12.2.5.1, *NCT End Drop*.

2.6.7.3 NCT Side Drop

The CR3MP side drop case was modeled with the shell cylindrical axis parallel to the ground, causing the radial surface of the shell to horizontally impact the drop pad. During the NCT side drop, some external work is observed due to gravity, boundary and symmetry loads on the model. As shown in Table 2.6-1, the maximum impact acceleration is 17.8 g. As shown in Table 2.6-1, there is minimal plastic deformation, with the maximum accumulated strain limit damage on the outer bottom cover edge at only 1.9% of the limit, or a margin of safety as follows:

$$MS = \frac{1}{.029 + .019} - 1 = 19.8$$

Therefore, the CR3MP containment boundary remains intact. Plots of strain and time histories of impact are provided in Appendix Section 2.12.2.5.2, *NCT Side Drop*.

2.6.7.4 NCT CG over Corner Drop

The CR3MP CG-over-corner drop case has the top end oriented downward with the cylindrical shell axis inclined at an angle of 47.8° from the horizontal surface of the drop pad. During the NCT corner drop, external work is generated as the content's mass shifts and slides from the time of release. The CR3MP hits the ground, peaking out with a force of 2.77×10^6 lb_f at .025ms, and then the RPV/RVI contents internally impacts with a second higher force of 4.0493×10^6 lb_f, peaking at .065ms. Therefore, as shown in Table 2.6-1, the maximum impact is 9.4 g. As shown in Table 2.6-1, the elemental EPS has a maximum value of 21.0% and is located near the outer edge of the top cover plate. Averaging the EPS through the cover thickness shows a maximum EPS of 6.91%. While there is plastic deformation, the maximum accumulated strain limit damage in the outside surface of the shell was only 17.9% of the limit, or a margin of safety as follows:

$$\mathrm{MS} = \frac{1}{.029 + .179} - 1 = 3.8$$

Therefore, the CR3MP containment boundary remains intact. Plots of strain and time histories of impact are provided in Appendix Section 2.12.2.5.3, *NCT Corner Drop*.

2.6.7.5 NCT CG over Corner Drop Tip-Over

While the end drop and side drop orientations result in stable final positions, the CG-over-corner drop orientation results in an unstable final position, and a final tip-over to a stable position is likely to follow the initial impact. Therefore, as detailed in Appendix Section 2.12.2.5.4, *NCT Corner Drop Tip-Over*, this follow-on drop load case is investigated for the NCT free drop event, because the fall of the CR3MP CG from the unstable position is larger than the initial one-foot drop height in the end drop. Of note, it is not necessary to consider it for the HAC free drop event because the initial drop height in that case is much larger than the final tip-over drop height.

The tip-over onto the end bounds any damage versus a tip-over onto the side, since the corner drop itself has the largest EPS appearing in the top cover, not the shell. Any further damage will be maximized in the top cover, not the shell, since the top cover containment boundary damage was highest (i.e., 17.9%) in Appendix Section 2.12.2.5.3, *NCT Corner Drop*. Therefore, a tip-over onto the top cover is selected. Also, an end orientation will physically manifest versus tipping onto the side. This is because both the CR3MP aspect ratio (diameter greater than that of its height) preferentially locates the CG in a position of instability, and because of the shifting of the contents which applies a force to the top cover.

Since allowing the tip-over to occur "naturally" as a continuation of the CG-over-corner free drop computer simulation would result in egregiously long LS-DYNA® run times, the CR3MP energy at the end of the CG-over-corner drop is applied to the model in the orientation that the CR3MP would have at the instant it hit the ground in the tip-over event. At the end of the CG-over-corner free drop impact event (i.e., when all downward vertical motion has ended), the CR3MP, still essentially in its CG-over-corner orientation, has a remaining kinetic energy of 6.98×10^5 in-lb$_f$ (See Figure 2.12.2-93) and the CG is approximately 118 inches above the impact surface.

The next event in this sequence will be the tip-over impact, in which the CR3MP is top-down on the impact surface, with the CG at a height of 89.5 inches (equal to half of the CR3MP cylindrical height, since the CG is assumed essentially at the geometric center). Thus, the energy available at the tip-over impact is the potential energy equivalent to a drop height of (118 - 89.5 inches) = 28.5 inches, and the residual kinetic energy of 6.98×10^5 in-lb$_f$. Therefore, the total energy available in the impact (E) is as follows:

$$E = E_p + E_k = mg\Delta h + E_k = 1.297 \times 10^7 in \cdot lb_f$$

In which case, the mass of the model is m = 1,114.5 lbf-s^2/in (See Table 2.12.2-3) and g = 386.4 in/s^2, and Δh = 28.5 inches. As a result, the tip-over event is modeled using the CR3MP in an axis-vertical, top-down orientation. In this orientation, and with the top cover parallel to the ground, an angular velocity (rotational energy) is inputted into the model, imparting load/energy into the CR3MP (impacting the bottom edge of the packaging shell). The origin of the rotational coordinate system is the lower right-hand corner of the deformed model. Having all the energy (E) convert to rotational kinetic energy and with the CR3MP mass-moment of inertia from the LS-DYNA® model being $I_{zz} = 6.614 \times 10^6$ lb$_f$-s^2-in, then the angular velocity applied to the model is as follows:

$$\omega = \sqrt{2E/I_{zz}} = 1.98\, rad/s$$

Conservatively, an angular velocity of 3 rad/s is used in the LS-DYNA® model.

As determined in Appendix Section 2.12.2.5.4, *NCT Corner Drop Tip-Over*, the maximum impact acceleration in the tip-over event is 225g. This is significantly higher than the initial CG-over-corner impact, which is since the top-down orientation is much stiffer than the CG-over-corner orientation. For this reason, most of the additional strain damage occurs outside the containment boundary, in the edge of the side shell. As shown in Appendix Section 2.12.2.5.4, *NCT Corner Drop Tip-Over*, a much smaller amount of accumulated strain (3.2%) occurs in the top cover. Conservatively adding this damage to the CG-over-corner drop accumulated damage (i.e., 17.9%) on the top cover, yields a total bounding damage of 21.1% of accumulated strain to the top cover, or a margin of safety of:

$$MS = \frac{1}{.029 + .211} - 1 = 3.7$$

Therefore, the CR3MP containment boundary remains intact. Plots of strain and time histories of impact are provided in Appendix Section 2.12.2.5.4, *NCT Corner Drop Tip-Over*.

2.6.8 Corner Drop

The CR3MP is not required to be evaluated for the 10 CFR 71.71(c)(8) corner drop condition, since it applies only to fiberboard, wood or fissile material packages of varying configurations. The material of construction of the CR3MP is steel and it is not a fissile package, therefore the CR3MP does not need to be evaluated for the NCT corner drop.

2.6.9 Compression

10 CFR 71.71(c)(9) specifies that for packages weighing up to 11,000 lb, a 24-hour compressive load be applied with the load being the larger load of either 5 times the package weight or the equivalent of 2 psi projected over the package area. The CR3MP weight exceeds the 11,000 lb limit, and therefore does not need to be evaluated for compression.

2.6.10 Penetration

In accordance with 10 CFR 71.71 (c)(10), the impact of a 1.25-in. diameter, hemispherical ended, 13-lb steel bar dropped vertically from a height of 40 inches would not have any deleterious effect on the safety features of the CR3MP. Dropping vertically, the bar would impact the 6-in. thick top closure plate or the 3.75-in. thick closure weld. The bar would possess an impact energy of only 520 in-lb and could not damage the package in any way. Therefore, consequential damage from the steel bar penetration test is of no concern.

2.7 Hypothetical Accident Conditions

When subjected to the HAC as specified in 10 CFR 71.73, the CR3MP meets the performance requirements specified in Subpart E of 10 CFR 71. This is demonstrated in the following subsections, where each accident condition is addressed, and the package shown to meet the applicable design criteria. The method of demonstration is by analysis. The loads specified in 10 CFR 71.73 are applied sequentially, per Regulatory Guide 7.8. Resulting stresses are maintained below the limits established by Regulatory Guide 7.6 or other limits on strain as established in the analysis sections herein. A summary of cumulative damage is provided in Section 2.7.8, *Summary of Damage*. The primary acceptance criterion for all HAC events is a release of no more than one A_2 of activity in one week, as established in Section 2.1.2, *Design Criteria*.

2.7.1 Free Drop

Subpart F of 10 CFR 71 requires that a 30-ft free drop be considered. The free drop is to occur onto a flat, essentially unyielding, horizontal surface, and the CR3MP is to strike the surface in an orientation for which maximum damage is reasonably expected. Three representative worst-case orientations are chosen: on the end, the side, and CG over corner. Because the package diameter and height do not differ significantly (diameter of 200.3-in. and height of 178.1-in.), secondary impacts such as slapdown are not considered. In order to include the damage which would occur from a prior NCT one-foot free drop, the drop height for all HAC drops is 31-ft. The evaluation was performed using LS-DYNA® software. A design pressure of 25 psi is applied to the internal surfaces of the package. The drop pad impact surface is unyielding. Material properties and acceptance criteria used in the HAC free drop evaluation are provided in Section 2.6.7.1, *Material Properties and Acceptance Criteria Used in Free Drop Analysis*. Other details of the HAC free drop analysis are provided in Appendix 2.12.2, *Free Drop Evaluation*.

In terms of the HAC containment boundary, evaluation for HAC outcomes does not rely on the CR3MP boundary remaining intact, only that the released quantity of contamination is based on 10 CFR 71.51(a)(2) limits [1]. Therefore, any breach of the CR3MP containment boundary due to the free drop must be quantified in terms of a volumetric rate of LDCC material lost from the CR3MP during the event. To quantify the potential loss of LDCC from within the CR3MP, an opening size, related to the fracture is required. The opening size is calculated in the following conservative fashion. If fracture occurs (i.e., if any elements erode in the simulation), then any other adjacent or nearby elements with an accumulated strain limit damage that is below a margin of safety of 3 will also be considered eroded. This is justified since such an opening assessment bounds the criteria of Subarticle 5.3.3.2, equation 5.11 of the ASME BPVC [20]. As a result, a fracture opening in the simulation model mesh is measured and then used in the containment evaluation shown in Section 4.3, *Containment under Hypothetical Accident Conditions*.

2.7.1.1 HAC End Drop

Like the NCT End Drop, the CR3MP end drop case was modeled with the top end facing down, since in that orientation, there is a 3-inch air gap between the RPV top surface and the top cover. Filtered at 1,000 Hz, as shown in Table 2.12.2-8, the maximum impact of the CR3MP is 394 g. The strain is uniform in a ring around the inside surface of the shell just above the top cover. While there is limited plastic deformation in both covers and shell, there is no erosion of elements and no significant accumulated damage at the end of the simulation (see Figure 2.12.2-69). The maximum element damage in the inner shell wall near the top cover plate accumulates only 4.5% of the limit, or a margin of safety as follows:

$$\text{MS} = \frac{1}{.029 + .045} - 1 = 12.5$$

Therefore, the CR3MP containment boundary remains intact. Plots of strain and time histories of impact are provided in Appendix Section 2.12.2.6.1, *HAC End Drop*.

2.7.1.2 HAC Side Drop

The CR3MP side drop case was modeled with the shell cylindrical axis parallel to the ground, causing the radial edge of the shell to horizontally impact the drop pad. As shown in Table 2.12.2-8, the maximum impact is 104 g. While there is limited plastic deformation in both covers, there is no erosion of elements and no significant accumulated damage at the end of the simulation (see Figure 2.12.2-79). The maximum element damage in the bottom cover accumulates only 11.2% of the limit, or a margin of safety as follows:

$$\text{MS} = \frac{1}{.029 + .112} - 1 = 6.1$$

Therefore, the CR3MP containment boundary remains intact. Plots of strain and time histories of impact are provided in Appendix 2.12.2.6.2, *HAC Side Drop*.

2.7.1.3 HAC CG over Corner Drop

The CR3MP CG-over-corner drop case was modeled with the top end down and the shell cylindrical axis inclined at an angle of 47.8° from the horizontal surface of the drop pad. Plots of strain and time histories of impact are provided in Appendix Section 2.12.2.6.3, *HAC Corner Drop*. As shown in Table 2.12.2-8, the maximum impact is 49 g. As shown in Figure 2.12.2-83, damage accumulation was sufficient to erode only two elements in the CR3MP shell, along the inner edge of the top cover-shell interface. These two elements eroded from the model are in the zone where the RPV is expected to impact the inside of the shell wall. While this erosion means only a small crack is projected to initiate on the inside wall, the potential for wall failure is conservatively assumed to be much greater.

Therefore, to be cautious and to provide a conservative assessment of the volume of the opening, it is assumed that any accumulated strain limit damage that is below a margin of safety of 3 will have eroded through the wall thickness, creating a fracture seam in the mesh element adjacent and extending along the pathway region of excessive strain. Based on the margin of safety equation in Section 2.6.7.1, *Material Properties and Acceptance Criteria Used in Free Drop Analysis*, this is equivalent to an elemental EPS as follows:

$$MS = \frac{D_\varepsilon}{D_{\varepsilon form} + \Sigma \Delta D_{\varepsilon,k}} - 1 = 3 = \frac{1}{.029 + \Sigma \Delta D_{\varepsilon,k}} \therefore \Sigma \Delta D_{\varepsilon,k} = .221 \; or \; 22.1\%$$

Accordingly, erosion through the wall is assumed to occur in elements having an accumulated strain limit damage of 22.1% or greater. This results in a total half-symmetry opening value extending 44.81 inches long by 4.13 inches wide along the shell-cover joint seam (See Figure 2.12.2-88). There are no other areas in the containment boundary that exceed an accumulated strain limit damage margin of safety of 3. Based on this opening and due to the CR3MP geometry and symmetry, the total area of opening is determined to be 373 in^2. As a result of this opening area, the amount of possible content release is evaluated in Section 4.3, *Containment under Hypothetical Accident Conditions*.

2.7.2 Crush

The 10 CFR 71.73(c)(2) crush test is required only when the package has a mass under 1,100 lb. Since the weight of the CR3MP exceeds 1,100 lb, the crush test specified in 71.73(c)(2) does not apply.

2.7.3 Puncture

The CR3MP is evaluated for puncture resistance under HAC as defined in 10 CFR 71.73(c)(3). The puncture event is defined as a free drop from a height of 40 inches onto a vertical, cylindrical mild steel bar, 6 inches in diameter, in an orientation and in a location for which maximum damage is expected. Puncture performance of the CR3MP is evaluated on two surfaces: puncture on the flat ends, and puncture on the cylindrical side shell.

2.7.3.1 Puncture on the Ends

The puncture resistance of the end covers of the CR3MP, both of which have the same material and thickness, is evaluated using Nelms' Equation [23]. From Table 2.2-1, for the NCT warm case bounding temperature of 150 ºF, the ultimate strength of the package steel material (S_u) is 70,000 psi. The bounding weight of the CR3MP (W) is 860,000 lb. The required thickness (t) to resist puncture then becomes:

$$t = \left(\frac{W}{S_u}\right)^{0.71} = 5.94 \; inches$$

The thickness of the closure plate is 6.0 inches. The MS on the package closure plate thickness is:

$$MS = \frac{6.00}{5.94} - 1 = +0.01$$

Of note, this calculation conservatively neglects the load limit of a mild steel puncture bar. Assuming a bar made of ASTM A36 material, with properties as provided in Appendix Section 2.12.2.4.2.1, *RPV Shell*, , having a yield strength at room temperature of 36 ksi, and a tensile strength of 58 ksi, the "flow stress" of the puncture bar is the average of yield and tensile strengths, or 47 ksi. Since the bar has a 6-in. OD and has an area of 28.3 in^2, the maximum load that could be sustained by the bar is based on the flow stress of the bar material and is equal to $28.3 \times 47{,}000 = 1.33 \times 10^6$ lb. The minimum load to shear a 6-in. diameter hole through a 6-in.

thick cover plate (F_τ), conservatively assuming a shear length of only 50% of the thickness, or 3 inches, is:

$$F_\tau = 6 \times \pi \times 3 \times 0.6 \times 70{,}000 = 2.38 \times 10^6\ lb$$

In this equation, the ultimate shear strength of the plate is considered to be 0.6 times the tensile strength of 70 ksi for the ASTM A516 Grade 70 steel [4]. Thus, the maximum load which can be sustained by the mild steel puncture bar, 1.33×10^6 lb, is only about 56% of the load needed to fully shear through the 6-in. closure plate of 2.38×10^6 lb, implying that the bar would fail in compression before the plate sheared through. Therefore, the MS is considerably larger than +0.01, and puncture of the CR3MP top and bottom cover plates is of no concern.

2.7.3.2 Puncture on the Package Body Shell

From the foregoing, it is evident that the 3-in. thick body shell may experience perforation from the puncture bar, both from the perspective of Nelms' equation and from the fact that the maximum puncture bar load of 1.33×10^6 lb is greater than the load to fully shear a 3-in. thick section of ASTM A516 Grade 70 steel (again assuming 50% shear, or 1.5 inches), equal to half of 2.38×10^6 lb, or 1.19×10^6 lb. Thus, it may be reasonably assumed that a puncture drop on the cylindrical side shell could result in the configuration shown in Figure 2.7-1. Conservatively, intervening grout material between the shell and the RPV will be neglected.

The consequences of a puncture impact on the side shell of the CR3MP will be inconsequential due to the resistance to puncture from the thick RPV wall, which is located just behind the packaging shell. The RPV wall (t) is [ ] thick with an OD of [ ] Table 30, Case 7a of Roark [22] provides a formula for the deflection under a concentrated load on a circular shell. [

] The deflection under the load (d) (i.e., the local radial deformation of the RPV shell) due to the puncture bar load then becomes:

$$d = 6.5\frac{P}{Et}\left(\frac{R}{t}\right)^{3/2}\left(\frac{L}{R}\right)^{-3/4} = 0.70\ inches$$

Where:

$P = 1.33 \times 10^6$ lb, the maximum sustainable load of the puncture bar

$E = 29.0 \times 10^6$ psi, the modulus of elasticity for carbon steel (taken from Table 2.2-1 at 150 °F)

t = [ ] the RPV wall thickness

R and L are defined above.

Thus, the distance (G) shown in Figure 2.7-1 is 0.70 inches. This is a very conservative value since it neglects any inward deformation of the package shell that will occur due to puncture bar loading and any thickness of grout compressed between the side shell and the RPV. The same formula as used above could be applied to the package shell, resulting in a significant local dent in the package shell that would reduce the magnitude of G and possibly allow the package shell to be supported by the RPV and prevent complete perforation of the shell. However, the actual deformation of the package shell prior to its perforation is difficult to evaluate due to the resistance of the grout, and this effect is conservatively neglected, as depicted in Figure 2.7-1.

The upper-bound width of the opening into the package, (G), is just under ¾-in., and very little grout could escape through such an opening. In addition, the grout in the side annulus is poured in place after the placement of the grouted RPV, and therefore is not contaminated. Consequently, no activity from within the package would be released in such a puncture event.

If the puncture bar were applied to the free drop damage resulting from the CG-over-corner impact evaluated in Section 2.7.1.3, *HAC CG over Corner Drop* , it could penetrate the damaged area where contaminated grout may be present. However, as calculated in Section 4.3, *Containment under Hypothetical Accident Conditions*, the open area due to the weld damage is conservatively bounded by 370.2 in^2, and the added opening due to the puncture event would be unlikely to significantly exceed the area of the puncture bar itself, equal to 28.2 in^2.

As a result, the potential additional opening due to puncture is small relative to the free drop damage opening. In addition, while the release of contaminated grout in the free drop event is conservatively calculated using the full free drop impact velocity of the package combined with a rebound time period, the puncture event has a much lower impact velocity and essentially no rebound. Consequently, any further release of contaminated grout from the puncture event on the worst-case free drop damage is considered negligible. Therefore, puncture of the CR3MP is of no concern.

2.7.4 Thermal

The CR3MP is designed to withstand the HAC 30-minute fire specified in 10 CFR 71.73(c)(4). The thermal evaluation is presented in Section 3.4, *Thermal Evaluation under Hypothetical Accident Conditions*.

2.7.4.1 Summary of Pressures and Temperatures

As shown in Table 3.1-3, the maximum internal pressure of the CR3MP as a result of the HAC fire event is bounded by a value of 5.0 psig. From Section 3.4.3, *Maximum Temperatures and Pressure*, the maximum temperature of the weld between the end covers and the body shell as a result of the HAC fire event is 490 °C or 914 °F.

2.7.4.2 Differential Thermal Expansion

As shown in Section 2.2, *Materials*, LDCC has a thermal expansion coefficient which is like that of carbon steel. In the HAC fire event, the shell is hotter than the LDCC. The maximum temperature of the packaging from Table 3.4-1 is 568 °C (1054.4 °F). As shown in the legend of Figure 3.4-3, the bright green color top-end limit shows a high of 469.9 °C, whereas the minimum of that range is 388.66 °C. Excluding the small "notched" region of LDCC that could be exposed to the fire due to a free drop fracture, only a very small sliver of the LDCC outer radial volume approaches the low-end temperature of 388.66 °C. Therefore, to be conservative, the maximum bulk temperature of the annular LDCC may be assumed 470 °C (878 °F). Thus, differential thermal expansion is of no concern.

2.7.4.3 Stress Calculations

Pressure stress in the CR3MP was calculated in Section 2.6.1.3.1, *Stresses Due to Pressure Loading*. The governing stress was found to be located at the outside edge of the package cover, assuming a fixed edge condition. For an internal pressure of 3.9 psig (MNOP) and an external pressure of 3.5 psia, a differential pressure of 15.1 psi was formed. Using a conservative pressure of 26.2 psi, the maximum stress (σ_c) was calculated to be 13,188 psi. Since the maximum internal pressure stated in Section 2.7.4.1, *Summary of Pressures and Temperatures* is lower than 26.2 psi, it is conservative to use the same stress, $\sigma_{c\text{-}HAC}$ = 13,188 psi for the HAC fire case.

From Table 2.1-2, for a primary membrane plus bending stress under HAC, the allowable stress is the lesser of $3.6S_m$ or S_u. At the peak weld temperature of 914 °F provided in Section 2.7.4.1, *Summary of Pressures and Temperatures*, the yield stress of ASTM A516 material (S_y) is 23,800 psi by interpolation from ASME BPVC, Section II, Part D, Table Y-1 [17]. S_m is 2/3 of this value, or S_m = 15,900 psi. Thus, $3.6S_m$ = 57,240 psi. Again at 914 °F, S_u = 50,510 psi by interpolation from ASME BPVC, Section II, Part D, Table U [17]. Thus, the lesser value of 50,510 psi is governing.

The MS then becomes:

$$MS_1 = \frac{50{,}510}{13{,}188} - 1 = +2.83$$

Of note, this result is conservative because it assumes that the peak temperature of the containment occurs at the same time as the peak internal pressure, whereas these two peaks will not coincide. Thus, pressure stress is of no concern for the HAC fire event.

2.7.5 Immersion – Fissile

An immersion test for fissile material packages is required by 10 CFR 71.73(c)(5). Since the CR3MP does not transport fissile materials, this requirement does not apply.

2.7.6 Immersion – All Packages

An immersion test for all packages is required by 10 CFR 71.73(c)(6), in which a separate, undamaged specimen must be subjected to an equivalent pressure of 21.7 psig. Since the CR3MP is filled with grout which has a crush strength which is much greater than this pressure, the external pressure can be resisted by the grout alone without assistance from the steel shell. Thus, the immersion load case of 71.73(c)(6) is of no concern.

2.7.7 Deep Water Immersion Test

For Type B packages containing an activity of more than 10^5 A_2, 10 CFR 71.61 requires that an undamaged containment system withstand an external water pressure of 290 psi for a period of not less than one hour without collapse, buckling, or inleakage of water. As stated in Section 1.2.2.3, *Radioactive Contents Description*, the bounding activity in the CR3MP is 3,000 A_2. Therefore, this requirement does not apply.

2.7.8 Summary of Damage

The CR3MP is analytically subjected to the applicable sequence of HAC events from 10 CFR 71, which include free drop, puncture, and thermal. Free drop of the package is considered using three representative worst-case orientations: end, side, and CG over corner. Computer simulation using LS-DYNA® software indicates that openings into the containment boundary can occur in the CG-over-corner drop orientation. A conservative estimate of the size of the openings is recorded, and the containment evaluation documented in Section 4.3, *Containment under Hypothetical Accident Conditions* shows that the containment criterion of Section 2.1.2, *Design Criteria*, is met.

Puncture is evaluated using Nelms' equation and shows no penetration of the top or bottom covers. Penetration of the package shell is possible. However, a manual analysis of the effect of puncture bar loading on the RPV wall shows that the RPV wall deformation will be minimal and the contaminated grout inside the RPV will not be disturbed. Thus, penetration of the side shell of the package will expose only uncontaminated grout, and due to the small size of the opening, very little will be lost. Puncture of the damaged package post-CG-over-corner free drop is also considered, and it is concluded that such a puncture will have an inconsequential influence on the activity release calculations of Section 4.3, *Containment under Hypothetical Accident Conditions*.

Consideration is also given to the effect of internal pressure due to the generation of water vapor from the grout in the fire event. The review assumes that no breach of the containment boundary has occurred before the regulatory fire event occurs. The resulting maximum stress is shown to be below allowable limits.

The evaluations of HAC in Section 2.7, *Hypothetical Accident Conditions*, along with the containment evaluation shown in Section 4.3, *Containment under Hypothetical Accident Conditions*, shows that the design criteria of Section 2.1.2, *Design Criteria*, have been met by the CR3MP.

Figure 2.7-1 – HAC Side Wall Puncture Configuration

2.8 Accident Conditions for Air Transport of Plutonium

This section does not apply, since plutonium is not transported in the CR3MP.

2.9 Accident Conditions for Fissile Material Packages for Air Transport

This section does not apply, since fissile material is not transported in the CR3MP.

2.10 Special Form

This section does not apply, since special form materials are not authorized contents of the CR3MP.

2.11 Fuel Rods

This section does not apply, since fuel rods are not authorized contents of the CR3MP.

2.12 Appendices

2.12.1 References

1. Title 10, Code of Federal Regulations, Part 71 (10 CFR 71), *Packaging and Transportation of Radioactive Material*, 01–01–20 Edition.
2. U. S. Nuclear Regulatory Commission, Regulatory Guide 7.6, *Design Criteria for the Structural Analysis of Shipping Cask Containment Vessels*, Revision 1, March 1978.
3. U. S. Nuclear Regulatory Commission, Regulatory Guide 7.8, *Load Combinations for the Structural Analysis of Shipping Casks for Radioactive Material*, Revision 1, March 1989.
4. ASTM A516 – 2017, *Standard Specification for Pressure Vessel Plates, Carbon Steel, for Moderate- and Lower-Temperature Service*, ASTM International, November 2017.
5. American Society of Mechanical Engineers (ASME) Boiler and Pressure Vessel Code, *Section II, Materials, Part A, Ferrous Material Specifications (SA-451 to End), SA516/SA-516M, Specification for Pressure Vessel Plates, Carbon Steel, for Moderate- and Lower-Temperature Service*, 2017 Edition.
6. American Society of Mechanical Engineers (ASME) Boiler and Pressure Vessel Code, *Section III, Rules for Construction of Nuclear Facility Components, Division 1 – Subsection NB, Class 1 Components*, 2017 Edition.
7. American Society of Mechanical Engineers (ASME) Boiler and Pressure Vessel Code, *Section III, Rules for Construction of Nuclear Facility Components, Division 1 – Subsection ND, Class 3 Components*, 2017 Edition.
8. ASTM E208 – 2020, *Standard Test Method for Conducting Drop-Weight Test to Determine Nil-Ductility Transition Temperature of Ferritic Steels*, ASTM International, July 2020.
9. U. S. Nuclear Regulatory Commission, Regulatory Guide 7.11, *Fracture Toughness Criteria of Base Material for Ferritic Steel Shipping Cask Containment Vessels with a Maximum Wall Thickness of 4 Inches (0.1 m)*, June 1991, NRC Accession Number ML003739413.
10. L. E. Fischer, W. Lai, *Fabrication Criteria for Shipping Containers*, NUREG/CR–3854, UCRL–53544, U.S. Nuclear Regulatory Commission, March 1985.
11. M. W. Schwartz, L. E. Fischer, *Recommendations for Protecting Against Failure by Brittle Fracture/Category II and III Ferritic Steel Shipping Containers with Wall Thickness Greater than Four Inches*, NUREG/CR-6491, UCRL-ID-124583, U.S. Nuclear Regulatory Commission, August 1996.
12. R. E. Monroe, H. H. Woo, and R. G. Sears, *Recommended Welding Criteria for Use in the Fabrication of Shipping Containers for Radioactive Materials*, NUREG/CR–3019, UCRL–53044, U.S. Nuclear Regulatory Commission, March 1984.
13. ASTM C150/C150M – 2020, *Standard Specification for Portland Cement*, ASTM International, April 2020.
14. ASTM C869/C869M – 2016, *Standard Specification for Foaming Agents Used in Making Preformed Foam for Cellular Concrete*, ASTM International, August 2016.
15. ACI 523.1R – 2006, *Guide for Cast-in-Place Low-Density Cellular Concrete*, American Concrete Institute, August 2006.

16. ACI 523.3R – 2014, *Guide for Cellular Concretes above 50 lb/ft^3 (800 kg/m^3)*, American Concrete Institute, April 2014.
17. American Society of Mechanical Engineers (ASME) Boiler and Pressure Vessel Code, *Section II, Materials, Part D, Properties*, 2017 Edition.
18. ASTM A36 – 2019, *Standard Specification for Carbon Structural Steel*, ASTM International, July 2019.
19. American Society of Mechanical Engineers (ASME) Boiler and Pressure Vessel Code, Section IX, *Qualification Standard for Welding and Brazing Procedures, Welders, Brazers, and Welding and Brazing Operators*, Latest Edition.
20. American Society of Mechanical Engineers (ASME) Boiler and Pressure Vessel Code, *Section VIII, Rules for Construction of Pressure Vessels, Division 2, Alternate Rules*, 2017 Edition.
21. ASTM C495/C495M – 2019, *Standard Test Method for Compressive Strength of Lightweight Insulating Concrete*, ASTM International, December 2019.
22. *Roark's Formulas for Stress and Strain, Sixth Edition*, McGraw–Hill, New York, 1989.
23. A. Nelms, *Structural Analysis of Shipping Casks, Effect of Jacket Physical Properties and Curvature on Puncture Resistance*, ORNL–TM–1312, Vol. 3, Oak Ridge National Laboratory, 1968.
24. ASME V&V 20-2009, "Standard for Verification and Validation in Computational Fluid Dynamics and Heat Transfer," ASME 2009
25. Livermore Software Technology Corporation, *LS-DYNA® Keyword User's Manual/Volume II/Material Models*, Version R7.0, February 2013.
26. Livermore Software Technology Corporation (LSTC), *LS-DYNA® Keyword User's Manual, Volume III, Multi-Physics Solvers*, Version R7.0, February 2013.
27. Livermore Software Technology Corporation (LSTC), *LS-DYNA® Theory Manual*, Revision 5061, March 2014.
28. American Society of Mechanical Engineers (ASME) Boiler and Pressure Vessel Code, *Section V, Nondestructive Examination*, 2017 Edition.
29. Xue, Liang, *Damage Accumulation and Fracture Initiation In Uncracked Ductile Solids Subject to Triaxial Loading*, International Journal of Solids and Structures, 44 (2007) 5163-5181.
30. Binod Tiwari et al, *Review of State of the Practice Use of Lightweight Cellular Concrete (LCC) Materials in Geotechnical Applications*, California Nevada Cement Association, July 2020.
31. Binod Tiwari et al, *Mechanical Properties of Lightweight Cellular Concrete for Geotechnical Applications*, Journal of Materials in Civil Engineering, Vol. 29, Issue7, July 2017.
32. ASTM A370 – 2021, *Standard Test Methods and Definitions for Mechanical Testing of Steel Products*, ASTM International, December 2021.

Proprietary Information on Pages 2.12-4 through 2.12-89 withheld pursuant to 10 CFR 2.390

3.0 THERMAL EVALUATION

The following analysis demonstrates that the CR3MP complies with the thermal requirements of 10 CFR 71 [1] for exclusive use transport of the unique, one-time payload.

3.1 Description of Thermal Design

3.1.1 Design Features

The CR3MP is a thick-walled steel shell constructed of ASTM A516 Grade 70 carbon steel. The package internal cavity has a 194.3-inch inner diameter and a 166.13-inch height. Both the top and bottom covers are 6-in. thick, while the shell wall is 3-in. thick. The exterior top and side package surfaces are painted white.

The CR3MP payload is comprised of the sectioned RPV along with the RVI components. Within the RPV shell, the RVI components are surrounded by cellular concrete fill material (i.e., grout). The activated RVI components are constructed of carbon steel and stainless steel, with the majority of decay heat coming from Co-60. The RVI components are rigidly constrained as one body within the RPV by the LDCC grout. The LDCC has a density range of 30 to 60 pcf.

The RPV payload is approximately 6-in. smaller in diameter than the packaging internal cavity. Therefore, this radial annulus formed between the RPV outer shell and the CR3MP inner shell wall will be filled with the aforementioned LDCC grout, while the upper 3-in. gap above the RPV payload and bottom of the top cover is nominally free of grout.

3.1.2 Content's Decay Heat

Based on a NAA of the RVI components within the payload, the maximum decay heat of the CR3MP payload is calculated in Section 5.2, *Source Specification*, as 358.1 watts. However, a bounding value of 500 watts is set to characterize the payload decay heat. All decay heat is conservatively modeled as a volumetric heat source within the payload steel.

3.1.3 Summary Tables of Temperatures

The CR3MP is shipped vertically-oriented under exclusive use requirements. For exclusive use under NCT and HAC, the following load conditions are analyzed:

- *NCT Hot with Insolation*: Per 10 CFR 71.71(c)(1) [1], the package is evaluated with an ambient air temperature of 38 °C (100 °F), maximum decay heat, and maximum insolation to determine maximum component temperatures during NCT.
- *NCT Hot without Insolation*: Per 10 CFR 71.43(g) [1], the package is evaluated with an ambient air temperature of 38 °C (100 °F), maximum decay heat, and in shade to verify no accessible surface of the package exceeds 85 °C (185 °F).
- *NCT Cold*: Per 10 CFR 71.71(c)(2) [1], the package is evaluated with an ambient air temperature of -40 °C (-40 °F), minimum decay heat, and in shade to determine minimum component temperatures during NCT.

- *HAC Fire Transient*: Per 10 CFR 71.73(c)(4) [1], the package is evaluated engulfed in flame (or equivalent condition) for a period of 30 minutes to determine maximum component temperatures during HAC. The fire load must simulate an average flame temperature of at least 800 °C (1475 °F) with an average flame emissivity coefficient of 0.9. The package surface absorptivity coefficient should be based on expected package conditions, but may not be less than 0.8. The most limiting NCT conditions (*NCT Hot*) are maintained before and after the fire event.

Temperatures for the CR3MP are computed using ANSYS® 19.2 (Mechanical via Workbench). CR3MP component temperatures resulting from the worst-case conditions specified by 10 CFR 71 are summarized in Table 3.1-1 and Table 3.1-2. All temperatures are below applicable limits. Note, LDCC bulk temperature (rather than peak) is limited based on pressure calculations and thus no explicit maximum temperature limit is applied.

Detailed summaries of the analyzed NCT and HAC cases, including values of case-specific variables and heat transfer mechanisms, are documented in Appendix 3.5.5, *Summary of Analyzed Thermal Evaluation Cases*.

Table 3.1-1 – Summary of CR3MP NCT Temperatures

Component	Maximum Temperature (°C)	Maximum Limit (°C)	Minimum Temperature (°C)	Minimum Limit (°C)
CR3MP Shell	51	371	-40	< -40
Payload Steel	160	371	-40	< -40
LDCC	159	-	-40	< -40
CR3MP Surface (in shade)	40	85	-	-

Table 3.1-2 – Summary of CR3MP HAC Temperatures

Component	Maximum Temperature (°C)	Maximum Limit (°C)
CR3MP Shell	568	1495
Payload Steel	284	1400
LDCC	795	-

3.1.4 Summary Tables of Maximum Pressures

MNOP, NCT pressure, and HAC pressure are evaluated in Appendix 3.5.2, *Evaluation of Pressure in the CR3MP* with a summary of the maximum pressures shown in Table 3.1-3

Table 3.1-3 – Summary of Maximum Pressures for the CR3MP

Condition	CR3MP Cavity Pressure, psi gage
NCT Hot and HAC Post Fire	3.9
HAC Fire Transient	5.0

3.2 Material Properties and Component Specifications

3.2.1 Material Properties

The material properties for the CR3MP shell carbon steel and payload stainless steel are taken from Tables TCD and PRD in [2]. The payload is a mixture of carbon steel and stainless steel but is modeled solely as stainless steel. Stainless steel has lower thermal conductivity than carbon steel, and thus its use in payload modeling results in conservatively high temperatures. The density of carbon steel is set to 7750 kg/m^3, while the density of stainless steel is set to 8030 kg/m^3. Specific heat, C_p, is calculated from the thermal conductivity, thermal diffusivity, and density values (k, α, and ρ respectively) in [2] using the following relation:

$$C_p = \frac{k}{\rho\alpha}$$

The material properties for carbon steel and stainless steel are shown in Table 3.2-1 and Table 3.2-2, respectively.

The exterior top and side surfaces of the CR3MP shell will be painted with white paint. Per Table 4.2 of [3], the solar absorptivity of white paint ranges from 0.18 to 0.34 while the emissivity ranges from 0.88 to 0.92. To maximize heat flow into the package and minimize heat flow out, the solar absorptivity and emissivity values are assumed to be 0.34 and 0.88 respectively for NCT. For HAC, the solar absorptivity and emissivity values rise to 0.8 and 0.9 as required by [1].

The CR3MP shell inner surfaces will not be painted. The emissivity of rough steel is assumed to be 0.95 (Table 13 of [9]), while the emissivity of concrete can be assumed to be 0.90 (Section 6.2.3 of [12]). For radiation across the internal air gap, the CR3MP shell inner surface is modeled with an emissivity of 0.95 while the payload surface is modeled with an emissivity of 0.90.

The LDCC has a minimum as-cast density of 30 pcf (481 kg/m^3). Limited data for thermal conductivity and specific heat of grout is available in [4] and [5]. For thermal conductivity, values are reported as a function of oven-dry density rather than as-cast density. Equation 6.1.2.3b in [5] provides a means to estimate oven-dry density, D, from as-cast density, γ_f:

$$D = \left[\gamma_f - 122\right] \frac{\text{kg}}{\text{m}^3}$$

Based on Figure 3.4 in [4], thermal conductivity as a function of oven-dry density follows exponential behavior. Thus, the thermal conductivity of the LDCC is calculated from an exponential curve fitted to the available data points. This curve fitting is shown in Figure 3.2-1. Minimum LDCC density is utilized resulting in conservatively low thermal conductivity. The resulting material properties for LDCC are shown in Table 3.2-3. The specific heat of LDCC is set to 980 J/kg·K per [5][1]. All modeling uses as-cast density rather than oven-dry density.

[1] The specific heat of 0.98 J/kg·K stated in [5] is incorrect and does not match the corresponding value stated in U.S. customary units (0.23 BTU/lb·°F). A literature review (see Table 1 in [6]) confirms this correction.

LDCC thermal properties are not adjusted to account for changes in temperature and thus are modeled as singular values. Per Table 2 and Figure 85 in [7], lightweight concretes with densities and thermal conductivities similar to the LDCC have relatively constant thermal conductivities across a wide range of temperatures (0 °C to 1000 °C). Figures 94 through 97 in [7] show concrete specific heat increases with increases in temperature. Since higher specific heat values oppose increases in temperature, it is conservative to not account for this behavior.

The thermal properties of air are used directly within ANSYS® as well as for calculation of convective heat transfer coefficients. Air properties are taken from Table A.6 in [8] and are shown in Table 3.2-4.

Table 3.2-1 – Carbon Steel Material Properties

Temperature (°C)	Thermal Conductivity (W/m·K)	Specific Heat (J/kg·K)
20	60.4	431
50	59.8	453
75	58.9	467
100	58.0	480
125	57.0	490
150	55.9	500
175	54.7	508
200	53.6	516
225	52.5	525
250	51.4	534
275	50.3	543
300	49.2	553
325	48.1	564
350	47.0	575
375	45.9	586
400	44.9	600
425	43.8	614
450	42.7	628
475	41.6	644
500	40.5	660
525	39.3	675
550	38.2	694
575	37.0	712
600	35.8	732
625	34.7	755
650	33.5	780
675	32.3	816
700	31.2	877
725	30.1	1011
750	29.1	1552

Table 3.2-2 – Stainless Steel Material Properties

Temperature (°C)	Thermal Conductivity (W/m·K)	Specific Heat (J/kg·K)
20	14.8	473
50	15.3	484
75	15.8	493
100	16.2	499
125	16.6	507
150	17.0	511
175	17.5	520
200	17.9	526
225	18.3	530
250	18.6	532
275	19.0	537
300	19.4	542
325	19.8	546
350	20.1	548
375	20.5	551
400	20.8	552
425	21.2	557
450	21.5	558
475	21.9	562
500	22.2	563
525	22.6	566
550	22.9	568
575	23.3	571
600	23.6	573
625	24.0	576
650	24.3	578
675	24.7	580
700	25.0	582
725	25.4	586
750	25.7	587

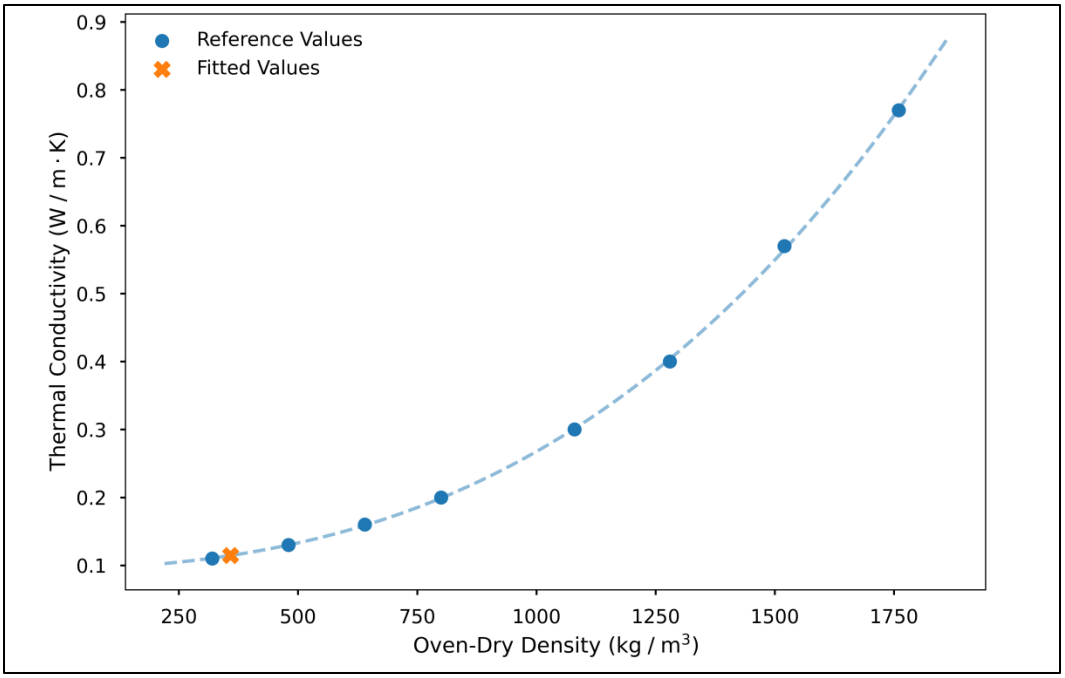

Figure 3.2-1 – LDCC Thermal Conductivity versus Oven-Dry Density

Table 3.2-3 – LDCC Material Properties

As-Cast Density (kg/m^3)	Oven-Dry Density (kg/m^3)	Thermal Conductivity (W/m·K)	Specific Heat (J/kg·K)
481	359	0.11	980

Table 3.2-4 – Air Material Properties

Temperature (°C)	Density (kg/m^3)	Specific Heat (J/kg·K)	Kinematic Viscosity (m^2/s)
-73	1.769	1007	7.537E-06
-23	1.413	1006	1.135E-05
-13	1.359	1006	1.218E-05
-3	1.308	1006	1.304E-05
7	1.261	1006	1.392E-05
17	1.218	1006	1.482E-05
27	1.177	1006	1.575E-05
37	1.139	1007	1.670E-05
47	1.103	1007	1.766E-05
57	1.070	1008	1.865E-05
67	1.038	1009	1.966E-05
77	1.009	1009	2.069E-05
127	0.882	1014	2.613E-05
177	0.784	1021	3.204E-05
227	0.706	1030	3.839E-05
277	0.642	1040	4.515E-05
327	0.588	1051	5.232E-05
377	0.543	1063	5.987E-05
427	0.504	1075	6.780E-05
477	0.471	1087	7.608E-05
527	0.441	1099	8.472E-05
577	0.415	1110	9.371E-05
627	0.392	1121	1.030E-04
677	0.372	1131	1.127E-04
727	0.353	1141	1.227E-04
827	0.321	1159	1.436E-04

Table 3.2-4 – Air Material Properties (continued)

Temperature (°C)	Thermal Conductivity (W/m·K)	Thermal Diffusivity (m^2/s)	Prandtl Number
-73	0.0185	1.04E-05	0.726
-23	0.0226	1.59E-05	0.715
-13	0.0233	1.71E-05	0.713
-3	0.0241	1.83E-05	0.711
7	0.0249	1.96E-05	0.710
17	0.0256	2.09E-05	0.708
27	0.0264	2.23E-05	0.707
37	0.0271	2.37E-05	0.706
47	0.0279	2.51E-05	0.705
57	0.0286	2.65E-05	0.704
67	0.0293	2.80E-05	0.703
77	0.0300	2.95E-05	0.702
127	0.0335	3.74E-05	0.699
177	0.0368	4.59E-05	0.698
227	0.0399	5.50E-05	0.698
277	0.0430	6.45E-05	0.700
327	0.0460	7.44E-05	0.703
377	0.0489	8.48E-05	0.706
427	0.0518	9.55E-05	0.710
477	0.0545	1.07E-04	0.714
527	0.0572	1.18E-04	0.717
577	0.0599	1.30E-04	0.721
627	0.0625	1.42E-04	0.724
677	0.0651	1.55E-04	0.727
727	0.0677	1.68E-04	0.730
827	0.0727	1.96E-04	0.734

3.2.2 Component Specifications

For NCT, the maximum allowable temperature for the carbon steel CR3MP shell is based on the maximum temperature limits in Table 2A of [2] (SA 516 Gr. 70, applicability limit for Part III). The maximum allowable temperature for NCT is 371 °C (700 °F). For HAC, the maximum allowable temperature for the carbon steel CR3MP shell is based on the melting temperature of carbon steel. Per Table 4 of [9], carbon steel begins melting at 1495 °C (2723 °F).

For steel within the payload, credit is taken for components remaining in the loading configuration throughout transport. Thus, similar to the CR3MP shell steel, the NCT maximum allowable temperature is based on Table 2A of [2] (SA-240 Gr. 304 for stainless steel) and the HAC maximum allowable temperature is based on the melting temperature in Table 4 of [9]. Since both carbon steel and stainless steel exist in the payload, the lower of the two limits is applied for both NCT and HAC. The maximum allowable temperatures for the payload steel are 371 °C (700°F) and 1400 °C (2552 °F) for NCT and HAC, respectively.

No explicit temperature limits, for either NCT or HAC, are applied to the LDCC. The primary concern for high LDCC temperatures is the saturation conditions of the liquid/gaseous water mixture for generating internal pressure within the CR3MP. Thus, acceptance of the NCT and HAC LDCC temperatures is based on the pressure calculations shown in Appendix 3.5.2, *Evaluation of Pressure in the CR3MP*.

The minimum allowable temperature for all CR3MP components is -40 °C (-40 °F). Steel components will not be negatively affected as the strength characteristics improve as component temperatures decrease [10]. Cellular concrete "*has excellent resistance to freezing and thawing due to its high cement content and extended internal void structure*", with strength even improving after freezing and thawing [5]. Thus, the LDCC will not be compromised by reduced temperatures.

3.3 Thermal Evaluation under Normal Conditions of Transport

Temperatures for the CR3MP are computed using ANSYS® 19.2 (Mechanical via Workbench). Two steady-state thermal runs are performed to evaluate the maximum NCT temperatures with and without solar insolation. No thermal run is performed to evaluate minimum temperatures. The CR3MP is simulated using a 2D, axisymmetric (i.e., cylindrical symmetry) model. The LDCC is modeled as two distinct regions: one for the internal, central region LDCC which surrounds the RVI and the second region for the annular grout layer between the outside of the RPV shell wall and the inside of the CR3MP shell wall. The payload steel is split into two regions: the RPV shell wall and a centrally-located slug containing the remaining volume of payload steel. Modeling the RVI as a centrally-located slug and not extending the steel to the bottom and top of the RPV was a conservative simplifying assumption. The LDCC is more insulating than steel (i.e., lower conductivity); therefore, the payload peak temperature is maximized internally. Except for the air gap at the top of the payload, regions are modeled with shared nodes and thus there is no additional thermal resistance to heat transfer between materials. Due to the large size of the package and grouted payload, gaps are expected to be small and have an insignificant effect on heat transfer relative to the bulk materials. The air gap does not use shared nodes to allow modeling of radiation heat transfer across the gap.

All decay heat is conservatively concentrated in the payload steel slug since the RPV contains only a small fraction of the total decay heat. Insolation is modeled on the top and side surfaces, as the CR3MP will be shipped in a vertical orientation. Since the CR3MP is thermally massive, component temperatures will be effectively decoupled from diurnal changes in insolation loading. Thus, steady-state modeling with constant insolation loads, equal to the 10 CFR 71.71(c) [1] 12-hour total insolation loads averaged over 24 hours, can be used to evaluate maximum component temperatures under NCT. The modeled insolation loads, $\dot{q}_{model}$, are calculated as a function of the regulation-specified 12-hour total insolation loads, $q_{specified}$, and the solar absorptivity, a:

$$\dot{q}_{model} = a * \frac{q_{specified}}{24\ hrs}$$

For NCT, the insolation loads for the top ("flat surface transported horizontally") and side ("curved surface") surfaces are 131.72 W/m^2 and 65.86 W/m^2, respectively.

Radiation and convection to 38 °C ambient is modeled at the top and side surfaces, while the bottom surface is modeled with no heat transfer mechanisms (i.e., perfectly insulated). Calculation of convective heat transfer coefficients for use in ANSYS® is discussed in Appendix 3.5.3, *Natural Convection Heat Transfer*.

A mesh refinement study has been performed to confirm that the mesh is sufficiently detailed and results to do not change significantly with increases in the number of nodes and elements. The mesh is defined to have quadrilateral elements of approximately 0.025 m side lengths. The resulting mesh has 56,367 nodes and 18,468 elements. The results of this study are summarized in Appendix 3.5.4.1, *Mesh Sensitivity Study*.

The thermal model is shown in Figure 3.3-1. Model dimensions are shown in Table 3.3-1. Modeling is done with nominal dimensions as tolerances are very small relative to their corresponding dimensions.

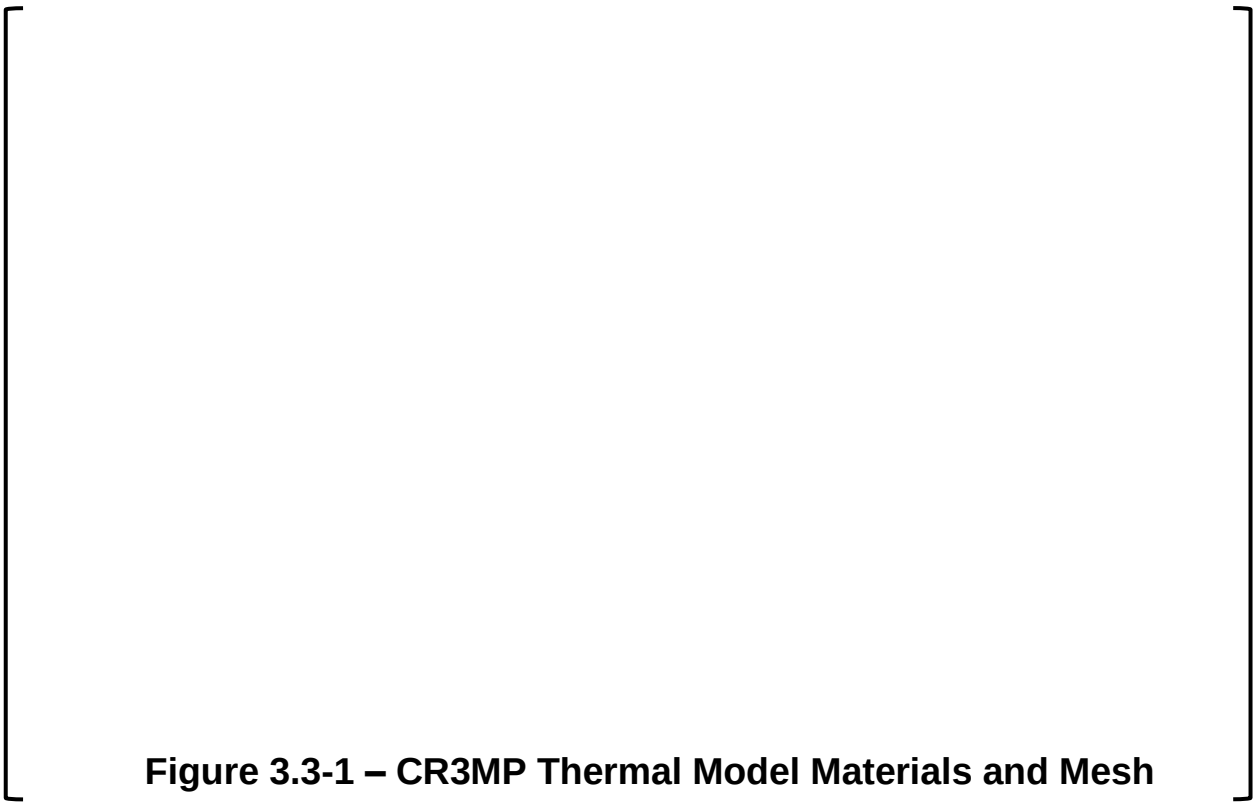

Figure 3.3-1 – CR3MP Thermal Model Materials and Mesh

Table 3.3-1 – Key CR3MP Thermal Model Dimensions

3.3.1 Heat and Cold

NCT maximum temperatures are summarized in Table 3.3-2. The maximum distribution throughout the package is shown in Figure 3.3-2. All components are below their allowable temperature limits. In addition, to support the evaluation in Appendix 3.5.2, *Evaluation of Pressure in the CR3MP*, from the ANSYS® model, the LDCC node-averaged temperature is 87 °C during the NCT Hot case.

No modeling of minimum temperatures is performed. For the minimum temperature condition (no decay heat and -40 °C ambient air), as shown in Table 3.1-1, all components will eventually reach -40 °C steady-state. Per Section 3.2.2, *Component Specifications*, this temperature is acceptable for all components.

3.3.2 Maximum Normal Operating Pressure

A MNOP of 3.9 psig is calculated in Appendix 3.5.2, *Evaluation of Pressure in the CR3MP*. Since the saturation temperature remains below 100 °C, this pressure results solely from the buildup of radiolysis gases. Indeed, as stated in Section 3.3.1, *Heat and Cold*, the LDCC node-averaged temperature is 87 °C during the NCT Hot case.

Table 3.3-2 – CR3MP NCT Temperatures

Component	Maximum Temperature (°C)	Allowable Temperature (°C)
CR3MP Shell	51	371
Payload Steel	160	371
LDCC	159	-
Packaging Surface (in shade)	40	85

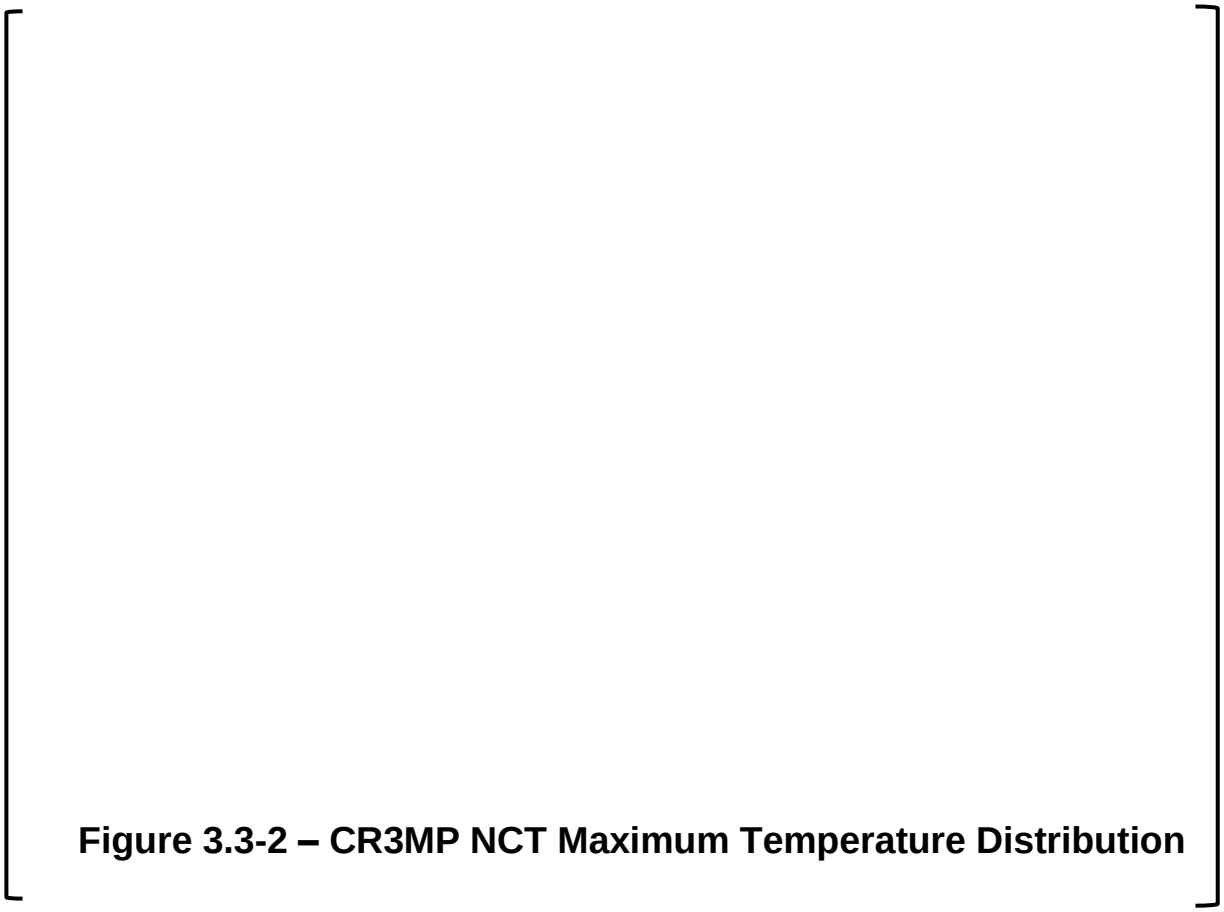

Figure 3.3-2 – CR3MP NCT Maximum Temperature Distribution

3.4 Thermal Evaluation under Hypothetical Accident Conditions

The NCT thermal model described in Section 3.3, *Thermal Evaluation under Normal Conditions of Transport* is reused for the HAC analysis. Geometry and general model design are unchanged. Specific parameters are adjusted as discussed below to model the HAC fire event.

3.4.1 Initial Conditions

The initial conditions assumed for the package prior to the HAC fire transient are as follows:

- Package temperatures are initialized based on NCT maximum temperature conditions. These maximums are calculated at steady-state with 38 °C ambient air and insolation loads based on undamaged package surfaces.
- For pre- and post-fire steady-state analysis, package orientation is vertical as this orientation results in lower heat removal to ambient and higher insolation loads. During the fire event, package orientation is horizontal so all sides are exposed to the fire and heat flow into the package is maximized.
- The surface absorptivity of all external surfaces is increased to 0.8 in order to account for possible oxidation and/or soot accumulation.

3.4.2 Fire Test Conditions

The HAC fire transient is evaluated as follows:

- At initiation of the fire (t = 0), any heat removal due to convection to ambient as well as insolation loads are suspended. The ambient air temperature is increased to 800 °C, resulting in a heat flux into the package. A surface emissivity of 0.9 conservatively bounds the 10 CFR 71 [1] fire conditions.
- As part of the HAC, it is assumed a crack may form at the lower corner of the CR3MP shell. As such, the fire radiation condition is also applied to an exposed 3-in. segment of internal LDCC at the lower corner to simulate direct exposure to the fire. This crack is shown in Figure 3.4-1.
- At termination of the fire (t = 30 minutes), the ambient air temperature is reduced to 38 °C. For the post-fire transient analysis, convective heat removal is not restored. Increased insolation loads (due to increased post-fire solar absorptivity) are applied. The insolation loads for the top and side surfaces are 309.93 W/m^2 and 154.96 W/m^2, respectively.
- To allow for any transient temperature responses to subside, the transient is evaluated for a period of 1 day.
- A post-fire steady-state model ($t \rightarrow \infty$) is evaluated using the post-fire conditions described above to determine the steady-state maximum temperatures. Convective heat removal is applied for this portion of the analysis.

The 10 CFR 71 [1] prescribed fire condition results in the following radiation heat flux, $\dot{q}_{fire}^{radiation}$:

$$\dot{q}_{fire}^{radiation} = a\sigma\left(\varepsilon_{fire}T_{fire}^4 - T_s^4\right)$$

Where:

- a : surface absorptivity
- σ : Stefan-Boltzmann constant
- ε_{fire} : fire emissivity
- T_{fire}, T_s: fire and surface temperatures (absolute)

To ensure that modeling of the fire is representative of an engulfing fire with moving hot air, the total fire heat flux must also include a convection component:

$$\dot{q}_{fire}^{total} = \dot{q}_{fire}^{radiation} + \dot{q}_{fire}^{convection}$$

Per [11]:

> *"For purposes of analysis, the hypothetical accident thermal conditions are specified by the surface heat flux values. Peak regulatory heat fluxes for low surface temperatures typically range from 55 to 65 kW/m^2. Convective heat transfer from air is estimated from convective heat transfer correlations, and contributes of 15 to 20 % of the total heat flux. The value of 15 to 20 % value is consistent with experimental estimates."*

Convection is conservatively set to 20% of the total heat flux:

$$\dot{q}_{fire}^{total} = \dot{q}_{fire}^{radiation} + \left(0.2 \cdot \dot{q}_{fire}^{total}\right)$$

Simplifying the previous equation shows that convection can be accounted for by applying a scalar factor to the regulatory radiation heat flux:

$$0.8 \cdot \dot{q}_{fire}^{total} = \dot{q}_{fire}^{radiation}$$

$$\Rightarrow \dot{q}_{fire}^{total} = \left(\frac{1}{0.8}\right) \cdot \dot{q}_{fire}^{radiation}$$

Based on a surface absorptivity of 0.8, a fire emissivity of 0.9, and a fire temperature of 800 °C (1073 K), the total fire heat flux is simplified to the following:

$$\begin{aligned}\dot{q}_{fire}^{total} &= \left(\frac{1}{0.8}\right) \cdot a\sigma\left(\varepsilon_{fire}T_{fire}^4 - T_s^4\right) \\ &= \left(\frac{1}{0.8}\right) \cdot (0.8) \cdot \sigma \cdot [(0.9) \cdot (1073\ \text{K})^4 - T_s^4] \\ &= \sigma \cdot [(0.9) \cdot (1073\ K)^4 - T_s^4]\end{aligned}$$

Within the ANSYS model, the total fire heat flux is conservatively replicated by applying an ambient radiation condition to the package surface with a surface emissivity of 0.9:

$$\begin{aligned}\dot{q}_{fire}^{model} &= \varepsilon_{surface}\sigma\left(T_{fire}^4 - T_s^4\right) \\ &= (0.9) \cdot \sigma \cdot [(1073\ \text{K})^4 - T_s^4]\end{aligned}$$

As shown in Figure 3.4-2 the modeled radiation condition conservatively bounds the derived regulatory total fire heat flux. Furthermore, it can be seen that the modeled heat flux is consistent with [11] as it results in a heat flux of approximately 65 kW/m^2 at low temperatures.

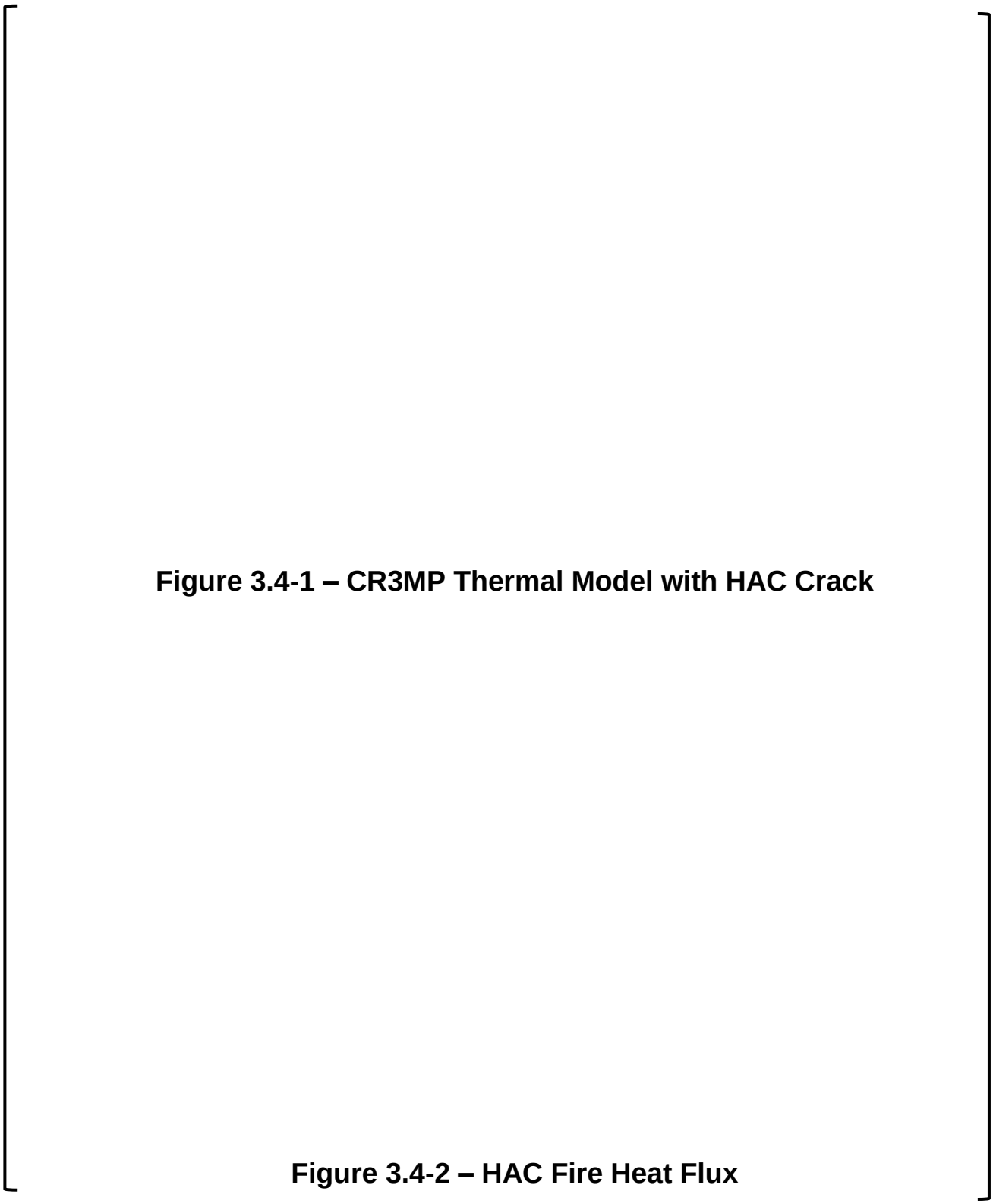

Figure 3.4-1 – CR3MP Thermal Model with HAC Crack

Figure 3.4-2 – HAC Fire Heat Flux

3.4.3 Maximum Temperatures and Pressure

HAC maximum temperatures are summarized in Table 3.4-1. The maximum temperatures achieved throughout the CR3MP (for each node at any time step) are shown in Figure 3.4-3, while the post-fire steady-state temperature distribution is shown in Figure 3.4-4. Fire transient maximums are achieved at or shortly after termination of the fire (30 minutes $\leq t \leq$ 60 minutes). Plots of component temperatures as a function of time during the fire transient are shown in Figure 3.4-5. All components are below their temperature limits.

A time step sensitivity study, performed to ensure that the conclusions of the thermal analysis are not impacted by further refinement of the model time steps, is documented in Appendix 3.5.4.2, *Time Step Sensitivity Study*.

The maximum temperature of the weld region connecting the end closure plate to the side shell, not including the region of the opening crack, is 490 °C.

Maximum pressure is calculated in Appendix 3.5.2, *Evaluation of Pressure in the CR3MP*. The maximum HAC pressure is 5.0 psig. This pressure results from saturated water vapor as well as buildup of radiolysis gases. The HAC pressure calculation conservatively assumes that the damage to the containment boundary discussed in Section 3.4.2, *Fire Test Conditions*, has not prevented the retention of pressure. From the ANSYS® model, the LDCC node-averaged temperature peaks at 102 °C during the fire transient and drops to 96 °C once the CR3MP reaches post-fire steady-state.

Table 3.4-1 – CR3MP HAC Temperatures

Component	Fire Transient Maximum Temperature (°C)	Post-Fire Steady-State Maximum Temperature (°C)	Allowable Temperature (°C)
CR3MP Shell	568	64	1495
Payload Steel	284	169	1400
LDCC	795	169	-

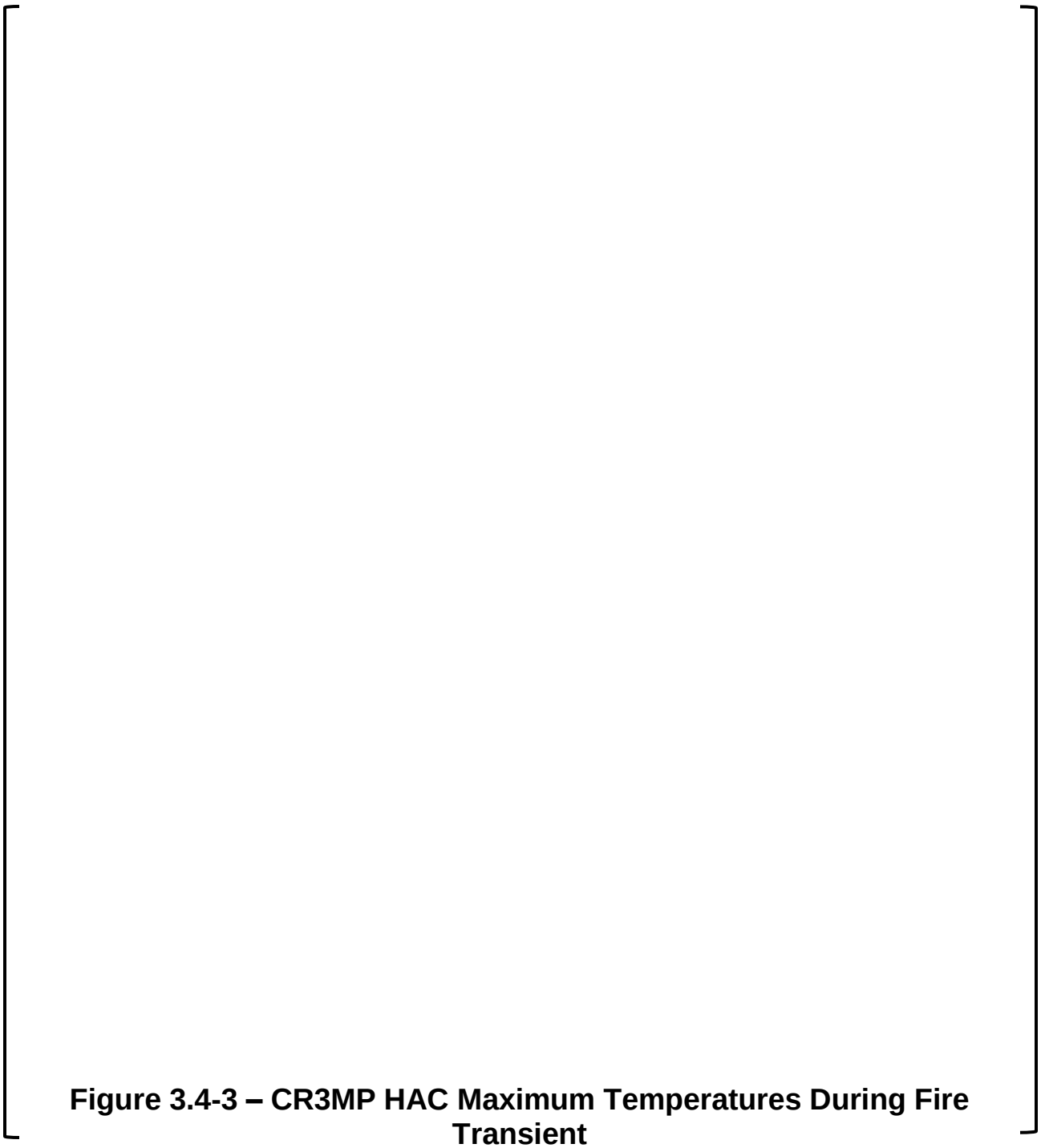

Figure 3.4-3 – CR3MP HAC Maximum Temperatures During Fire Transient

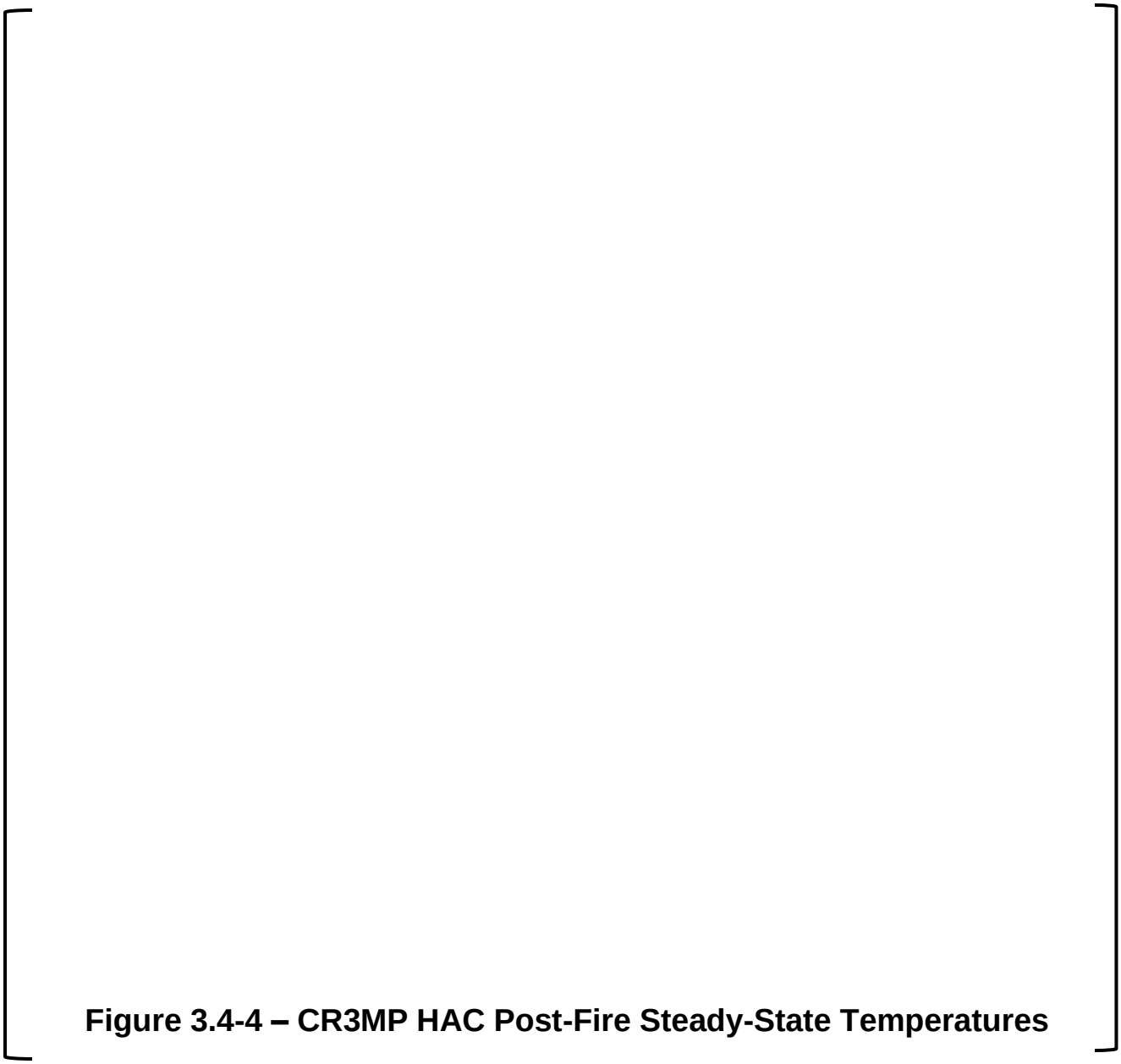

Figure 3.4-4 – CR3MP HAC Post-Fire Steady-State Temperatures

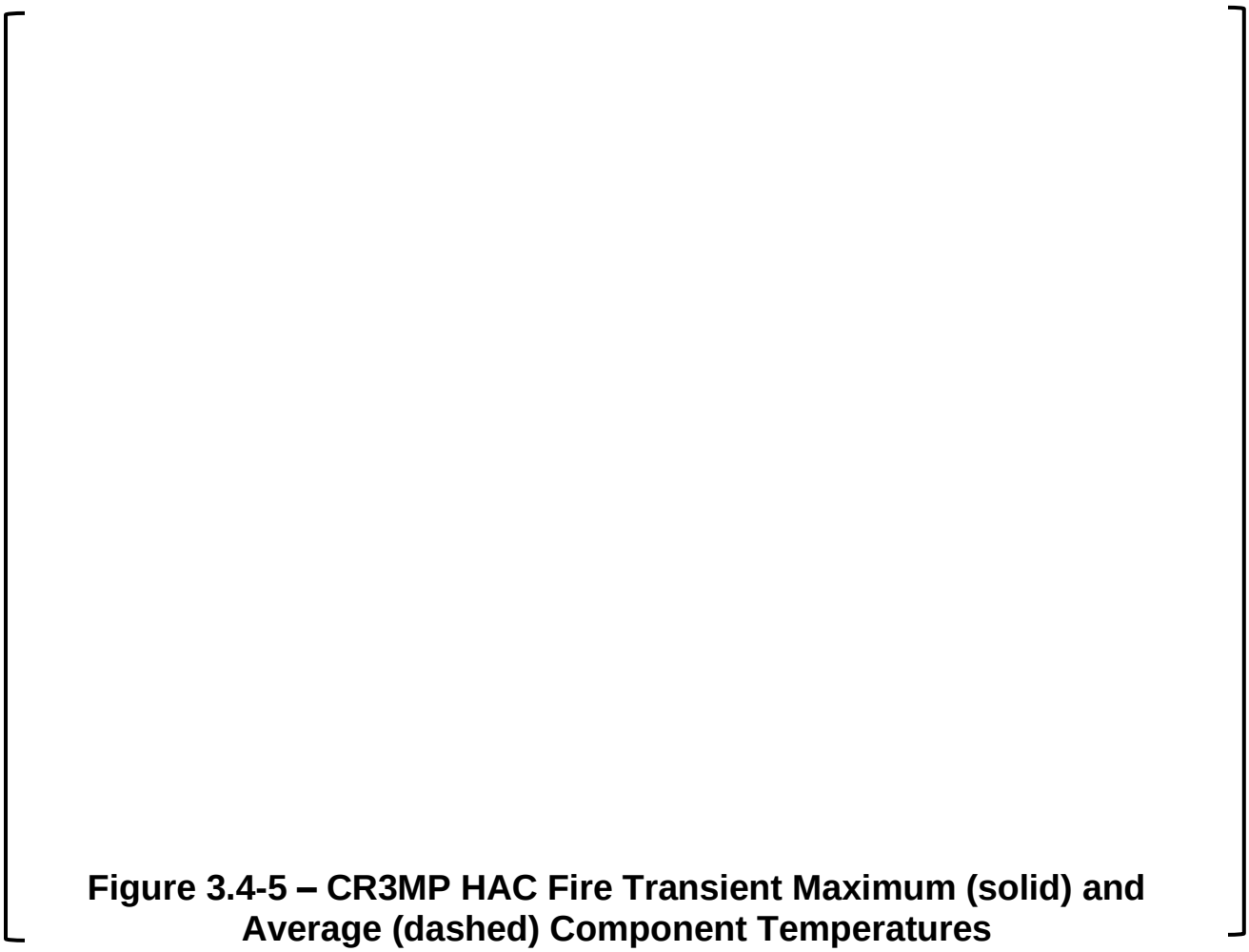

Figure 3.4-5 – CR3MP HAC Fire Transient Maximum (solid) and Average (dashed) Component Temperatures

3.4.4 Maximum Thermal Stresses

The maximum thermal stresses are addressed in Section 2.7.4, *Thermal*.

3.4.5 Accident Conditions for Fissile Material Packages for Air Transport

This section is not applicable as the CR3MP does not contain fissile material and will not be transported by air.

3.5 Appendices

3.5.1 References

1. Title 10 – Energy, Code of Federal Regulations, Part 71 (10 CFR 71), *Packaging and Transportation of Radioactive Material*, 01-01-20 Edition.
2. American Society of Mechanical Engineers Standard Boiler and Pressure Vessel Code, *Section II, Materials Part D: Properties (Metric)*, 2017 Edition.
3. NASA/TP-2005-212762, *Spacecraft Thermal Control Coatings References*, NASA/Goddard Space Flight Center, December 2005.
4. American Concrete Institute Report, ACI 523.1R-06, *Guide for Cast-in-Place Low-Density Cellular Concrete*, American Concrete Institute, August 2006.
5. American Concrete Institute Report, ACI 523.3R-14, *Guide for Cellular Concretes above 50 lb/ft^3 (800 kg/m^3)*, American Concrete Institute, April 2014.
6. Roberz, F., R.C.G.M Loonen, P. Hoes, and J.L.M. Hensen, *Ultra-lightweight concrete: Energy and comfort performance evaluation in relation to buildings with low and high thermal mass*, Energy and Buildings Volume 138, March 2017.
7. NUREG/CR-6900, *The Effect of Elevated Temperature on Concrete Materials and Structures - A Literature Review*, March 2006, NRC Accession Number ML060970563.
8. Lienhard IV, John H. and Lienhard V, John H., *A Heat Transfer Textbook*, 5th edition, Phlogiston Press, 2020.
9. Valencia, Juan J. and Quested, Peter N., *ASM Handbook, Volume 15: Casting, Thermophysical Properties*, ASM Handbook Committee, p468-481, 2008.
10. McClintock, R. Michael and Hugh P. Gibbons, *Mechanical Properties of Structural Material at Low Temperatures: A Compilation from the Literature*, U.S. Department of Commerce, National Bureau of Standards Monograph 13, June 1960.
11. ASTM E2230 – 2013, *Standard Practice for Thermal Qualification of Type B Packages for Radioactive Material*, ASTM International, April 2013.
12. American Concrete Institute Report, ACI/TMS 122R-14, *Guide to Thermal Properties of Concrete and Masonry Systems*, December 2014.
13. W. Zhao, Q. Su, W. Wang, L. Niu, & T. Liu, *Experimental Study on the Effect of Water of the Properties of Cast In Situ Foamed Concrete*, Advances in Materials Science and Engineering, Volume 2018, DOI: 10.1155/2018/7130465
14. Md Azree Othuman, Mydin, Y.C. Wang, *Mechanical Properties of Foamed Concrete Exposed to High Temperatures*, Construction and Building Materials, Volume 26, Issue 1, 2012, Pages 638-654.
15. E. W. Lemmon, I. H. Bell, M. L. Huber, & M. O. McLinden, *Thermophysical Properties of Fluid Systems*, NIST Chemistry WebBook (NIST Standard Reference Database Number 69), National Institute of Standards, DOI: 10.18434/T4D303.
16. NUREG-2152, *Computational Fluid Dynamics Best Practice Guidelines for Dry Cask Applications*, March 2013

3.5.2 Evaluation of Pressure in the CR3MP

When cement and water are mixed together with the foam during casting of the wet LDCC, most of the water will be used during the chemical bonding of the Portland cement to the water, forming air bubbles during the process. Depending on the time period of curing, the density of the LDCC, and the curing temperature, the amount of free, evaporable water in the porous structure may vary. However, most of the hydration process is completed for 800 kg/m^3 (50 pcf) foam concrete (i.e., LDCC) by approximately 90 days [13]. The internal LDCC is expected to have 6 months to cure whereas the annular LDCC will have around 30 days to cure. Also, the internal LDCC region may cure at a faster rate due to the payload decay heat. Experimental data has shown that the free water content of low-density foam concrete (similar to LDCC) is approximately 1 – 2 % by weight (section 3.1 of [14]).

As a result of the uncertainty in the exact amount of unbound water, the final LDCC moisture state at CR3MP closure may vary and consist of mostly bound, but some unbound water. To mitigate the development of any gas buildup between package closure and shipment, a vent port on the CR3MP cover will be left open until just prior to transport and then closed (see Appendix 1.3.2, *Packaging General Arrangement Drawings*). However, to be conservative during transport, it is assumed there is enough unbound water available for heating such that there could be an increase in pressure.

As the LDCC is heated, free moisture will migrate from regions of high temperature to cooler regions due to pressure-induced flow. Due to the high porosity of LDCC, water movement is significant during heating. Void space (e.g., porosity) in the LDCC regions will increase as the LDCC is heated. As pockets within the LDCC heat up, localized pockets will connect due to microcracking produced by the expansion of the cement paste (section 3.2 of [14]). Therefore, assuming an excess of available evaporable water, the overall system can be reasonably treated as a saturated mixture of liquid and gaseous water.

Given sufficient permeation time through the LDCC porous structure, the maximum pressure on the CR3MP shell containment boundary will be based on the saturation conditions of the entire LDCC vapor mixture [15] at a given temperature. Since the vapor is at saturation, additional moisture generated by cement dehydration processes will not further increase pressure. As stated in Section 3.3.1, *Heat and Cold*, and Section 3.4.3, *Maximum Temperatures and Pressure*, the average LDCC temperature is less than 100 °C for both the NCT Hot and HAC post-fire steady-state cases. This means the water vapor will not exert a pressure greater than the initial atmospheric pressure. As stated in Section 3.4.3, *Maximum Temperatures and Pressure*, for the HAC fire transient, the maximum average LDCC temperature is 102 °C which corresponds to a saturation pressure of 1.1 psig [15].

Independently, it is conservatively assumed that all gases generated by radiolysis will further increase the system pressure. Based on the results of the radiolysis analysis as evaluated in Appendix 5.5.4, *Step-by-Step Radiolysis Evaluation*, 222.6 moles of radiolysis products will be added to the credited initial gas quantity of 829.7 moles. Therefore, the steady-state gage pressure, $P_{package}$, can be calculated from the relative increase in gas quantity, n, and the initial atmospheric pressure, P_{atm}:

$$\begin{aligned} P_{package} &= \left(\frac{n_{initial} + n_{radiolysis}}{n_{initial}} - 1\right) P_{atm} \\ &= \left(\frac{222.6 \text{ mol} + 829.7 \text{ mol}}{829.7 \text{ mol}} - 1\right) (14.7 \text{ psia}) \\ &= 3.9 \text{ psig} \end{aligned}$$

Thus, the maximum pressure during NCT (i.e., maximum normal operating pressure) will be 3.9 psig solely due to radiolysis gases while the maximum pressure during HAC will be (3.9 psig + 1.1 psig = 5.0 psig) due to saturated water vapor in addition to radiolysis gases.

Proprietary Information on Page 3.5-5 withheld pursuant to 10 CFR 2.390

Convective heat transfer coefficients for the side and top surfaces are shown in Figure 3.5-2.

Figure 3.5-1 – Rayleigh Numbers for CR3MP Surfaces

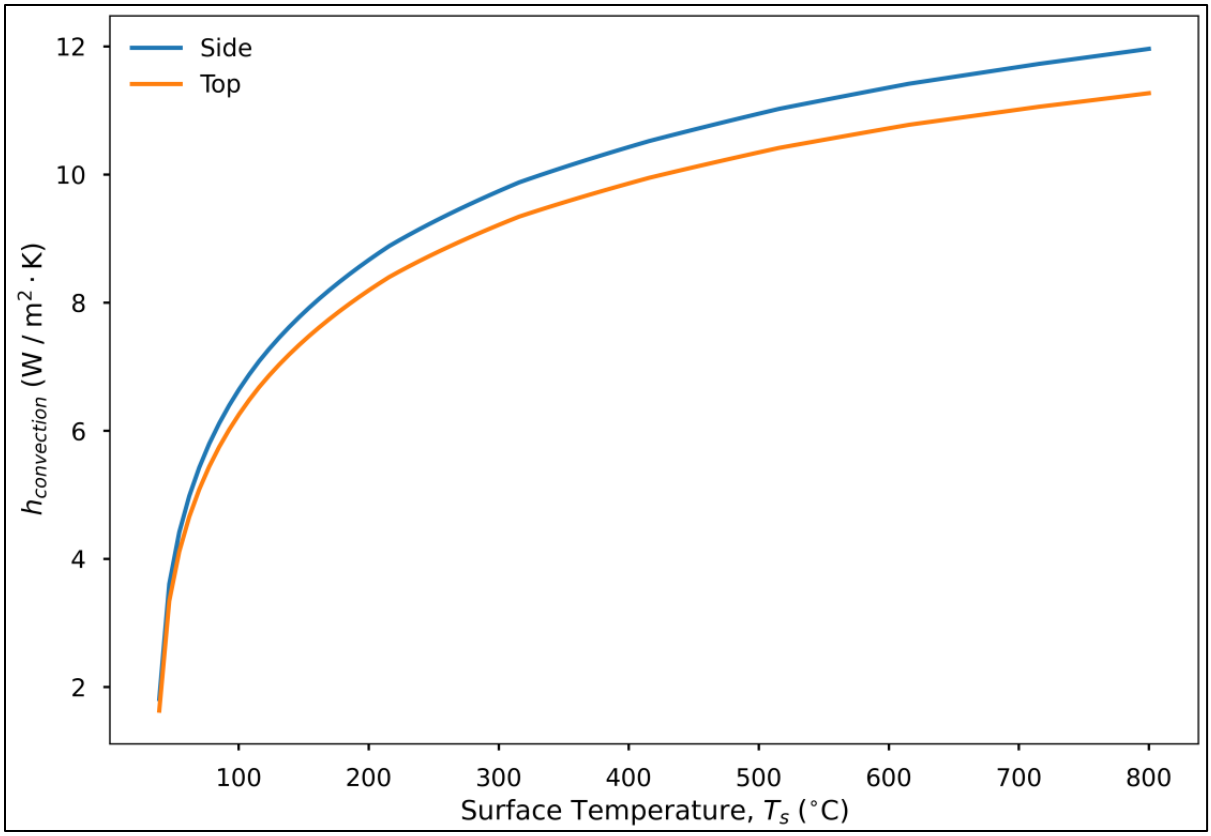

Figure 3.5-2 – Natural Convection Heat Transfer Coefficients for CR3MP Surfaces

3.5.4 Thermal Model Sensitivity Studies

The sensitivity studies are performed consistent with the general guidance contained in [16].

Table 3.5-1 – Evaluated Mesh Sizes

Table 3.5-2 – CR3MP Component Maximum Temperatures (°C)

Proprietary Information on Pages 3.5-9 through 3.5-13 withheld pursuant to 10 CFR 2.390

3.5.5 Summary of Analyzed Thermal Evaluation Cases

For each steady-state case, the final solution for temperatures should result in balanced heat flow into and out of the CR3MP. The heat flow residual, *r*, is calculated as the difference between the heat flows into ($\dot{Q}_{in}$) and out of ($\dot{Q}_{out}$) the CR3MP:

$$r = \dot{Q}_{in} - \dot{Q}_{out}$$

The residual indicates how much the final ANSYS solution deviates from the exact solution.

Proprietary Information on Pages 3.5-15 through 3.5-16 withheld pursuant to 10 CFR 2.390

4.0 CONTAINMENT

4.1 Description of the Containment System

4.1.1 Containment Boundary

The CR3MP provides a single level of containment for the payload defined in Section 1.2.2, *Contents*. A leak-tight containment boundary is obtained by means of thick, volumetrically inspected closure welds. The containment boundary of the CR3MP consists of the bottom closure plate cover, the cylindrical shell, and the top closure plate cover, along with the optional pressure vent plug port and its closure groove weld. All containment boundary components are made from ASTM A516/ASME SA516, Grade70 carbon steel. A full description of the packaging is given in Chapter 1.0, *General Information*.

4.1.2 Containment Penetrations, Closures, and Seals

There are no valves, ports, bolted closures, or seals in the containment boundary. The package is permanently welded closed after placement of the payload and annular packaging grout.

4.1.3 Welds

The weld material meets the requirements of ASME BPVC, Subsection ND, Subarticle ND-2400 [1]. All welds used in the containment boundary are full penetration and volumetrically inspected to ensure structural and containment integrity. However, the pressure vent port plug is surface and sub-surface inspected only. The weld inspections that are performed are discussed in Section 2.3.2, *Examination*.

4.2 Containment under Normal Conditions of Transport

The containment criterion for NCT is stated in Section 2.1.2, *Design Criteria*, and is based on 10 CFR 71.51(a)(1) [2] which states that there is to be no loss or dispersal of radioactive contents exceeding 10^{-6} A_2 per hour. The results of the NCT structural and thermal evaluations presented in Sections 2.6, *Normal Conditions of Transport*, and 3.3, *Thermal Evaluation under Normal Conditions of Transport*, respectively, demonstrate that there is no release of radioactive materials under any of the NCT tests described in 10 CFR 71.71. While some damage occurs to the closure weld in the NCT one foot, CG-over-corner free drop, the weld remains intact, thus maintaining containment (see section 2.6.7.4, *NCT CG over Corner Drop*).

4.2.1 Hydrogen Concentration in the Package

Hydrogen gas may be generated by irradiation of the grout located both within the RPV and in the annulus between the RPV and the package wall. As stated in Section 4.4.2.3 of NUREG-2216 [3], "*For normal conditions of transport, the application should demonstrate that the 5 percent concentration value, or lower if warranted by the flammable gas, is not generated during a period of 1 year*." For the CR3MP, the principal flammable gas is hydrogen. As calculated in Section 5.4.4, *Radiolytic Gas Generation*, for a realistically conservative decay heat of 358.1 watts, the hydrogen concentration in void spaces within the package reaches a value of 5% by volume in 429 days. Since this is greater than one year, hydrogen concentration within the package is not of concern.

4.3 Containment under Hypothetical Accident Conditions

The containment criterion for HAC is stated in Section 2.1.2, *Design Criteria*, and is based on 10 CFR 71.51(a)(2) [2]: there shall be no escape of krypton-85 exceeding 10 A_2 in one week, and no escape of other radioactive contents exceeding one A_2 in one week. Under HAC, the immersion and thermal evaluations performed in Sections 2.7, *Hypothetical Accident Conditions*, and 3.4, *Thermal Evaluation under Hypothetical Accident Conditions*, respectively, show no release of radioactive material. Under the HAC free drop and puncture events, some release of radioactive material may occur, however, as demonstrated in this section, the containment criterion of 10 CFR 71.51 is met by the CR3MP. The following evaluation provides a conservative estimate of the maximum amount of radioactivity that could be released under HAC by the free drop and puncture events.

Regarding the puncture test condition, Section 2.7.3.2, *Puncture on the Package Body Shell*, contains a discussion of the effect of the HAC puncture event on potential release of contamination. As concluded from that discussion, no significant release of contaminated grout is to be expected from the puncture event.

Regarding the free drop test condition, as stated in Section 1.2.2, *Contents*, the total dispersible activity within the package is bounded by a quantity of 24.8 Ci. This represents the radioactive contamination distributed over all of the RPV inside surfaces, including the RPV inner walls and RVI surfaces of the Class B and C components. Of the major constituents of surface contamination (C-14, Fe-55, Co-60, Ni-63, and Cs-137), the bounding A_2 value is for Co-60. Therefore, the contamination will be conservatively assumed to be all Co-60, which per Table A-1 of 10 CFR 71 [2], Co-60 has an A_2 value of 0.40 TBq or 10.8 Ci. Thus, the dispersible contamination is equivalent to a quantity of $24.8/10.8 = 2.3A_2$.

[

]

Proprietary Information on Page 4.3-2 withheld pursuant to 10 CFR 2.390

As a result of this conservative evaluation, the containment criterion for HAC is met.

4.4 Leakage Rate Tests for Type B Packages

The CR3MP is closed using a thick, 3.75-inch weld which is volumetrically inspected. This weld and its Non-Destructive Examination (NDE) (see Section 4.1.3, *Welds*) complete the leak-tight boundary of the package. No leakage rate tests are performed.

4.5 Appendix

4.5.1 References

1. American Society of Mechanical Engineers (ASME) Boiler and Pressure Vessel Code, Section III, *Rules for Construction of Nuclear Facility Components*, *Division 1 – Subsection ND, Class 3 Components*, 2017 Edition.
2. Title 10, Code of Federal Regulations, Part 71 (10 CFR 71), *Packaging and Transportation of Radioactive Material*, 01–01–20 Edition.
3. U.S. Nuclear Regulatory Commission, NUREG-2216, *Standard Review Plan for Spent Fuel Transportation*, August 2020, NRC Accession Number ML20234A651.

5.0 SHIELDING EVALUATION

The following analysis demonstrates that the CR3MP complies with the dose rate requirements of 10 CFR 71 [1] for exclusive use transport of the unique, one-time payload.

5.1 Description of Shielding Design

5.1.1 Design Features

The CR3MP is a relatively thick-walled, sealed cylinder constructed of ASTM A516 Grade 70 carbon steel. The package internal cavity has a 194.3-in. nominal diameter and a 166.13-in. nominal height. The top and bottom axial package walls are 6-in. thick, while the side package wall is 3-in. thick.

The CR3MP payload is comprised of activated RPV and RVI surrounded by cellular concrete fill material (i.e. grout). [

] The activated payload components are constructed of carbon steel and stainless steel, with the majority of radiation coming from Co-60. LDCC grout fills the interior of the RPV, surrounding the RVI.

The CR3MP payload is slightly smaller than the package internal cavity. All free volume outside the RPV will be filled with an additional volume of LDCC grout. There will be a 3-in. nominal air gap between the payload and the package top cover.

[

Figure 5.1-1 – CR3 RPV/RVI (Decommissioning Configuration, Middle Segment)

5.1.2 Summary of Maximum Radiation Levels

The package is shipped vertically-oriented under exclusive use requirements. The requirements for exclusive use under NCT and HAC, per 10 CFR 71.47(b) and 10 CFR 71.51(a)(2) [1], respectively, are summarized and applied as follows:

Limits for NCT

- 200 mrem/hr on the external surface of the package
- 200 mrem/hr at the projected outer surfaces of the transport vehicle
- 10 mrem/hr at any point 2 meters from the projected side surfaces of the transport vehicle (Note: per 10 CFR 71.47(b)(3) excludes the top and underside of the vehicle in Table 5.1-1)
- 2 mrem/hr in any normally occupied space

Limits for HAC

- 1000 mrem/hr at any point 1 meter from the outer surface of the package

The external surfaces of the package are conservatively used as the projected outer surfaces of the transport vehicle. Any normally occupied space is assumed to be at least 25 feet from the centerline of the package.

Summaries of the maximum dose rates are shown in Table 5.1-1 and Table 5.1-2 for NCT and HAC, respectively. Based on these results, it can be concluded that the CR3MP complies with the external radiation requirements of 10 CFR 71 for exclusive use transport.

Table 5.1-1 – Summary of Maximum NCT Dose Rates (mrem/hr)

Radiation	***Package Surface***			***2 Meters from Package Surface***			***Occupied Location***
	Top	**Side**	**Bottom**	**Top**	**Side**	**Bottom**	**25 ft from Package center**
Total (Gamma Only)	7.17	6.43	1.67	-	1.90	-	0.55
10 CFR 71.47 (b) Limit	200	200	200	10	10	10	2

Table 5.1-2 – Summary of Maximum HAC Dose Rates (mrem/hr)

Radiation	***1 Meter from Package Surface***		
	Top	**Side**	**Bottom**
Total (Gamma Only)	2.53	3.78	1.17
10 CFR 71.51 (a)(2) Limit	1000	1000	1000

5.2 Source Specification

The geometry and source distribution of the payload is based on RPV/RVI models and mapped activation data calculated by the CR3 Original Equipment Manufacturer (OEM). [

] Only gamma sources are present among the isotopes (no neutron sources). Ni-63 and Fe-55 are relatively weak radiation sources relative to Co-60, and thus key parameters such as total decay heat, total gamma energy release rate, and total A_2 quantity are dominated by Co-60 [ ].

The CR3MP activation source term is modeled as solely Co-60. The total activation activity is set to a bounding value of 30,000 Ci. A similarly bounding value of 3,000 A_2 is set for the A_2 quantity. These values are significantly higher (≥ 55% increases) than the values calculated by the NAA and are intended to bound any uncertainties. The relative spatial distribution calculated by the NAA is used for distributing the activation source. The spatial distribution of the Co-60 source term as calculated in the NAA is shown in Figure 5.2-1.

The surface contamination of CR3 components is estimated to be [ ] based on empirical samples. The total contamination source strength is 24.8 Ci. The surface contamination is composed primarily of Co-60 (58%), Ni-63 (30%), Cs-137 (5%), and Fe-55 (5%). Like the activation source term, the contamination source term is conservatively modeled as only Co-60.

]

Unlike the shielding source term and A_2 value, the payload decay heat is calculated based on a payload of [ ] Co-60 with additional decay to the earliest ship date of March 31st, 2023. To account for the uncertainty in OEM flux calculations, the decay heat is increased by a [ ] factor. Additionally, to account for decay heat from isotopes other than Co-60 as well as contamination, the decay heat is further increased by [ ] The resulting bounding payload decay heat is 358.1 watts.

5.2.1 Gamma Source

The Co-60 gamma spectrum is shown in Table 5.2-1. The Co-60 gamma spectrum is taken from ORIGEN discrete gamma data included within SCALE 6.2.4 [2]. ORIGEN decay data is based on ENDF/B-VII.1 evaluations. The total activation gamma source strength, $S_{activation}$, is calculated as a function of the average gammas per Co-60 decay, $\Sigma P(\gamma)$, and the total activation Co-60 activity, $A_{activation}$. Since a quarter-symmetry shielding model is utilized, the model source term is reduced by a factor of 4.

$$S_{activation} = \frac{1}{4} * \Sigma P(\gamma) * A_{activation}$$
$$= \frac{1}{4} * \left(1.9986 \ \frac{\gamma}{decay}\right) * \left(30{,}000 \ Ci * \frac{3.7 * 10^{10} \ \frac{decay}{sec}}{Ci}\right)$$
$$= 5.546 * 10^{14} \frac{\gamma}{sec}$$

The total contamination gamma source strength is calculated similar to the activation source.

$$S_{contamination} = \frac{1}{4} * \Sigma P(\gamma) * A_{contamination}$$
$$= \frac{1}{4} * \left(1.9986 \ \frac{\gamma}{decay}\right) * \left(24.8 \ Ci * \frac{3.7 * 10^{10} \ \frac{decay}{sec}}{Ci}\right)$$
$$= 4.585 * 10^{11} \frac{\gamma}{sec}$$

Table 5.2-1 – Co-60 Discrete Gamma Spectrum

Gamma Energy (MeV)	Probability of Gamma per Isotope Decay
7.5100E-04	1.6946E-06
8.5234E-04	8.0550E-07
8.7689E-04	1.3826E-08
8.8364E-04	5.6638E-07
7.4178E-03	3.1894E-05
7.4358E-03	6.2286E-05
8.2223E-03	3.9005E-06
8.2246E-03	7.6481E-06
8.2879E-03	3.3435E-09
8.2881E-03	4.8594E-09
3.4714E-01	7.5000E-05
8.2610E-01	7.6000E-05
1.1732E+00	9.9850E-01
1.3325E+00	9.9983E-01
2.1586E+00	1.2000E-05
2.5057E+00	2.0000E-08

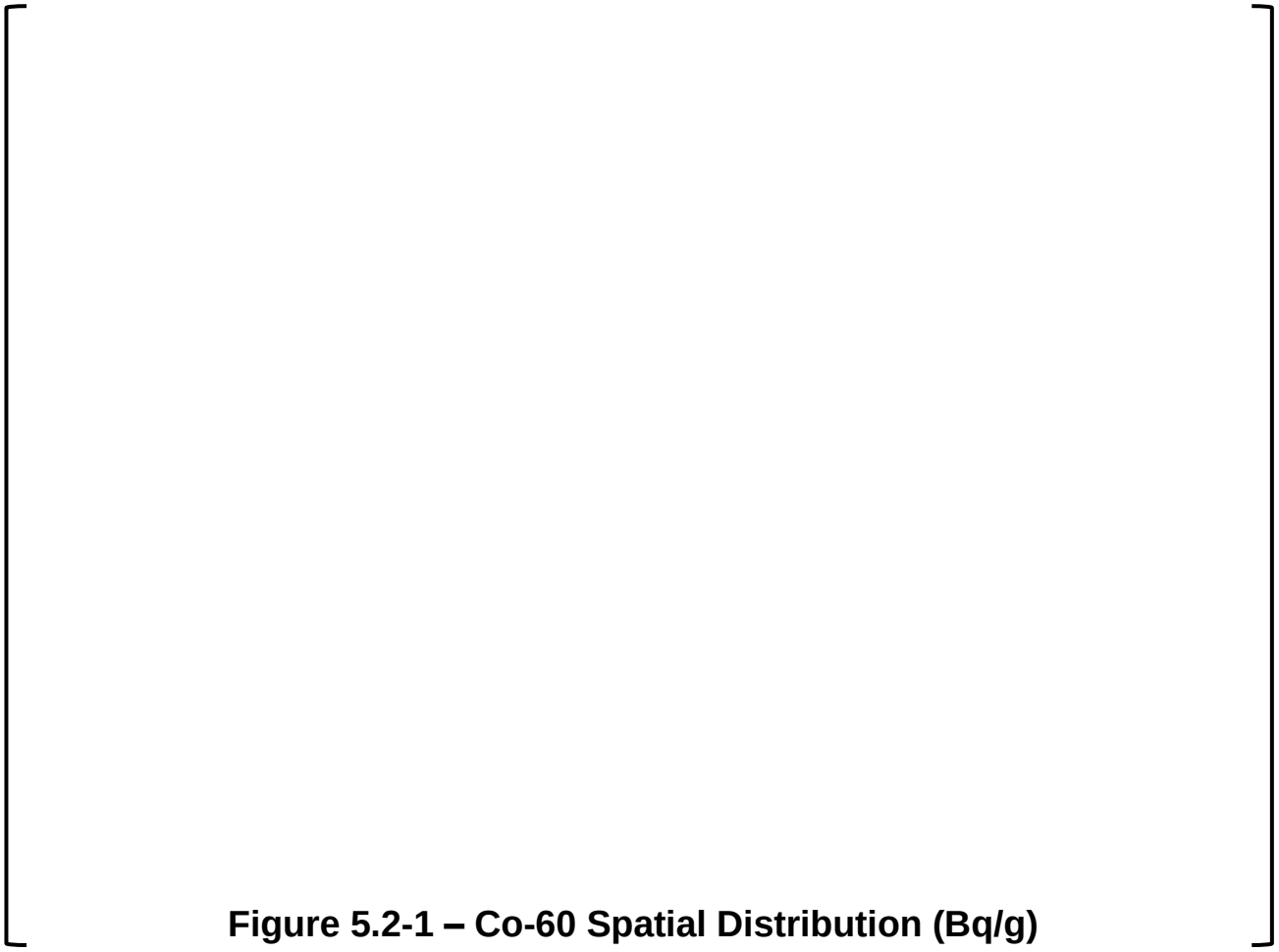

Figure 5.2-1 – Co-60 Spatial Distribution (Bq/g)

5.2.2 Neutron Source

No neutron sources are utilized.

5.3 Shielding Model

5.3.1 Configuration of Source and Shielding

All relevant design features of the CR3MP are modeled in Monte Carlo N-Particle® (MCNP) Version 6.2 [3]. The key dimensions of the modeled CR3MP are summarized in Table 5.3-1. The RPV and RVI components are modeled algorithmically, based on OEM 3D models, using hexahedron voxels. The remaining volume in the payload is conservatively filled with LDCC based on planned fill dimensions. As a result, the payload dimensions are inexact but otherwise reasonably representative of the source and material distributions.

The MCNP model is shown in Figure 5.3-1, Figure 5.3-2, and Figure 5.3-3. For all figures the color scheme is as follows: payload steel in purple, package steel in blue, LDCC in green, and void in white.

Table 5.3-1 – Key CR3MP Dimensions

Proprietary Information on Pages 5.3-2 through 5.3-3 withheld pursuant to 10 CFR 2.390

5.3.2 Material Properties

The CR3MP is constructed of carbon steel, while the payload consists of carbon steel and stainless steel RVI components surrounded by grout.

Carbon steel is modeled per [5] (material 294, "Steel, Carbon") and shown in Table 5.3-2. The payload steel is conservatively modeled as solely carbon steel. The package carbon steel uses a reference density of 7.82 g/cm^3, while the payload carbon steel uses a reduced density of 6.92 g/cm^3 to offset the increase in component volume due to the conversion to voxels. This reduced density, $\rho_{payload\ steel}$, is a function of the payload component masses, m_i, and the component voxel volumes, V_i^{voxel}:

$$\rho_{payload\ steel} = \frac{\sum m_i}{\sum V_i^{voxel}}$$

The payload LDCC is modeled as Portland concrete per [5] (material 98, "Concrete, Portland"). The grout density is the set to a minimum wet-cast density of 0.48 g/cm^3 (30 pcf). The grout composition is shown in Table 5.3-3.

Table 5.3-2 – Carbon Steel Composition

Element	ZAID	Weight Fraction
C	6000	0.005000
Fe	26000	0.995000

Table 5.3-3 – Portland Concrete (Grout) Composition

Element	ZAID	Weight Fraction
H	1000	0.010000
C	6000	0.001000
O	8000	0.529107
Na	11000	0.016000
Mg	12000	0.002000
Al	13000	0.033872
Si	14000	0.337021
K	19000	0.013000
Ca	20000	0.044000
Fe	26000	0.014000

5.4 Shielding Evaluation

5.4.1 Methods

5.4.1.1 Conversion of OEM Models to MCNP

[

]

5.4.1.2 MCNP Shielding Model

Dose rates from the CR3MP are computed using MCNP6.2 [3] using default cross-sections (ENDF/B-VI.8 for photons [7]). All modeling is done in three dimensions. A quarter-symmetry package shielding model is utilized. The packaging and payload are symmetric across the x- and y- axes (radial axes), and thus a quarter-symmetry model utilizing reflective x- and y- axes is acceptable. The CR3MP payload is modeled as reduced density carbon steel and LDCC, while the packaging is modeled as standard density carbon steel. A 3-in. air gap exists between the top of the payload and the package top cover, which is modeled as void. Any volume outside the CR3MP is also modeled as void.

Separate runs are performed to model the activation and contamination sources. [

] Each source is composed of individual voxel probabilities describing the portion of the total source strength located within the associated voxel. Source particle starting position is sampled uniformly within associated voxel volumes.

For NCT, the payload and packaging are modeled without damage. For HAC, the welds may fail in limited areas and allow for some release of grout. The damage to the CR3MP is insignificant with respect to shielding and thus no CR3MP damage is modeled. The loss of grout may be significant and is conservatively modeled by removing all grout outside the RPV outer radius, bounding the grout loss during HAC.

Dose rates are computed using segmented mesh tallies. Mesh tallies compute fluxes in thin, non-physical volumes (using track-length estimates) before converting to dose rates using the flux-to-dose rate conversion factors in Section 5.4.2, *Flux-to-Dose Rate Conversion*. Tallies are subdivided to capture variations in dose rates and properly identify localized maximums.

5.4.2 Flux-to-Dose Rate Conversion

American National Standards Institute ANSI/ANS-6.1.1-1977 photon flux-to-dose rate conversion factors [8] are used in this analysis. The reference conversion factors have been multiplied by a factor of 1,000 to generate dose rates in units of mrem/hr rather than rem/hr. The conversion factors are provided in Table 5.4-1.

Table 5.4-1 – Photon Flux-to-Dose Rate Conversion Factors

Energy, E (MeV)	DF(E) (mrem/hr)/(γ/cm^2-s)	Energy, E (MeV)	DF(E) (mrem/hr)/(γ/cm^2-s)
0.01	3.96E-03	1.40	2.51E-03
0.03	5.82E-04	1.80	2.99E-03
0.05	2.90E-04	2.20	3.42E-03
0.07	2.58E-04	2.60	3.82E-03
0.10	2.83E-04	2.80	4.01E-03
0.15	3.79E-04	3.25	4.41E-03
0.20	5.01E-04	3.75	4.83E-03
0.25	6.31E-04	4.25	5.23E-03
0.30	7.59E-04	4.75	5.60E-03
0.35	8.78E-04	5.00	5.80E-03
0.40	9.85E-04	5.25	6.01E-03
0.45	1.08E-03	5.75	6.37E-03
0.50	1.17E-03	6.25	6.74E-03
0.55	1.27E-03	6.75	7.11E-03
0.60	1.36E-03	7.50	7.66E-03
0.65	1.44E-03	9.00	8.77E-03
0.70	1.52E-03	11.00	1.03E-02
0.80	1.68E-03	13.00	1.18E-02
1.00	1.98E-03	15.00	1.33E-02

5.4.3 External Radiation Levels

[

]

For NCT, CR3MP surface dose rates are calculated using three tallies at the top, bottom, and side surfaces while 2-meter dose rates are calculated using a single tally located 2 meters from the side surface. The occupied location dose rate is calculated with a side tally located 25 feet from the CR3MP centerline. For HAC, 1 meter dose rates are calculated using three tallies located 1 meter from the top, bottom, and side surfaces.

The maximum dose rates for each location along with associated relative errors are shown in Table 5.4-2. Relative errors for all maximum dose rates are less than or equal to 10% (except for the NCT package bottom surface), satisfying guidance in [3]. In the case of the NCT package bottom surface, dose rates are significantly below applicable limits and thus the associated high relative errors are acceptable.

Table 5.4-2 – Tally Maximum Dose Rates (mrem/hr)

Location	Activation		Contamination		Total	
	Result	Error	Result	Error	Result	Error
NCT, Package Surface, Side	6.42	0.4%	0.01	4%	6.43	0.4%
NCT, Package Surface, Top	6.60	0.2%	0.57	1%	7.17	0.2%
NCT, Package Surface, Bottom	1.16	19%	0.51	3%	1.67	13%
NCT, Package 2 meter, Side	1.89	0.3%	0.01	5%	1.90	0.3%
NCT, Occupied Location	0.54	0.1%	0.01	3%	0.55	0.1%
HAC, Package 1 meter, Side	3.77	1%	0.01	3%	3.78	1%
HAC, Package 1 meter, Top	1.94	2%	0.60	0.5%	2.53	2%
HAC, Package 1 meter, Bottom	0.77	9%	0.40	1%	1.17	6%

Note: Total dose rates may not be equal to the exact sum of activation and contamination dose rates due to rounding.

5.4.4 Radiolytic Gas Generation

The generation of gases due to radiolysis in the payload grout may result in an increase in package pressure. Additionally, generation of hydrogen gas specifically may result in a combustible internal gas mixture. To support the evaluation of CR3MP pressure and gas mixture, the maximum quantities of total gas and hydrogen gas that may be generated due to radiolysis are calculated. Similarly, to support the evaluation of gas flammability, the maximum quantity of hydrogen generated due to radiolysis is also calculated.

An explicit, step-by-step evaluation of all parameters discussed below is documented in Appendix 5.5.4, *Step-by-Step Radiolysis Evaluation*.

Proprietary Information on Page 5.4-4 withheld pursuant to 10 CFR 2.390

The payload grout will include a foaming agent. The foaming agent may be highly hydrogenous. G-values for the foaming agent (solely CMX foam concentrate) are calculated in Appendix 5.5.3, *G-value Calculation*. Per NUREG-6673 [9], the effective G-value of a composite material is the summation of the energy absorbed in each component material, F_i, multiplied by the component material G-value, G_i. The effective G-value of the payload grout is calculated by approximating the energy absorbed in component material based on corresponding weight fractions within the grout, w_i:

$$G_{effective} = \sum F_i G_i \approx \sum w_i G_i$$

The effective G-values used to represent LDCC incorporate the higher G-values of the foaming agent. Per Table 5.5-3, the foam concentrate-to-grout weight ratio will not exceed 0.096%.

The type of radiation is modeled as solely Co-60 gamma radiation. 99.5% for the CR3MP payload decay heat is due to Co-60. For Co-60, 96.3% of the decay heat released is gamma radiation while the remainder is beta radiation (no alpha radiation). No significant amount of alpha radiation from other isotopes would be expected since the payload does not contain nuclear fuel waste (i.e., no common alpha emitters such as actinides). Beta radiation can be conservatively treated as gamma radiation since beta radiation deposits a much larger proportion of its energy in the steel source material rather than the grout. Based on data in [12] and [13], the range of Co-60 beta particles in steel is over 100 times lower than the mean free path of Co-60 gamma particles.

The energy emitted by the source, $E_{emitted}$, is calculated from the integral of the decay heat, P. For a single isotope source with a decay constant λ evaluated over time period t, the energy emitted is as follows:

$$E_{emitted}(t) = \int_0^t P_0 e^{-\lambda x} dx = \frac{P_0 e^{-\lambda x}}{-\lambda}\Big|_0^t = \frac{P_0}{-\lambda}\left(e^{-\lambda t} - 1\right)$$

The fraction of energy absorbed in the grout is calculated using the existing MCNP shielding model. The shielding model used to calculate external dose rates is modified to generate a conservative energy deposition fraction. This is done by maximizing the LDCC density (i.e., 60 pcf). The model is evaluated using the activation source term since this is the source of the majority of energy released (activation source term is roughly 1,000 times larger than contamination). Energy deposition is calculated for each material present in the model (payload steel, package steel, and LDCC). The model is run until highly converged, with all MCNP energy deposition relative errors less than 1%. The radiolysis MCNP model is shown in Figure 5.4-1. The color scheme is the same as previous figures (i.e., Figure 5.3-1, Figure 5.3-2, and Figure 5.3-3).

Co-60 decay is evaluated using a decay constant of 4.167×10^{-9} s^{-1} per Appendix 5.2.E of [2]. Based on the MCNP energy deposition model, 11.6% of emitted radiation energy will be deposited in grout.

Proprietary Information on Pages 5.4-6 through 5.4-9 withheld pursuant to 10 CFR 2.390

5.5 Appendices

5.5.1 References

1. Title 10, "Energy", Code of Federal Regulations, Part 71 (10 CFR 71), *Packaging and Transportation of Radioactive Material*, 01–01–20 Edition.
2. W. A. Wieselquist, R. A. Lefebvre, and M. A. Jessee, Eds., *SCALE Code System*, ORNL/TM-2005/39, Version 6.2.4, Oak Ridge National Laboratory , Oak Ridge, Tennessee, April 2020.
3. LA-UR-17-29981, *MCNP® User's Manual: Code Version 6.2*, Los Alamos National Laboratory, October 2017.
4. LA-UR-03-1987, *MCNP – A General Monte Carlo N-Particle Transport Code, Version 5, Volume 1: Overview and Theory*, Los Alamos National Laboratory, April 2003.
5. PNNL-15870, *Compendium of Material Composition Data for Radiation Transport Modeling*, Pacific Northwest National Laboratory, Revision 1, March 2011.
6. Schroeder, Will; Martin, Ken; Lorensen, Bill (2006), *The Visualization Toolkit* (4th ed.), Kitware, ISBN 978-1-930934-19-1 (see vtk.org for additional information).
7. LA-UR-17-20709, *Listing of Available ACE Data Tables*, Los Alamos National Laboratory, October 2017.
8. ANSI/ANS-6.1.1-1977, *American National Standard Neutron and Gamma-Ray Flux-to-Dose-Rate Factors*, March 1977.
9. Lawrence Livermore National Laboratory, *Hydrogen Generation in TRU Waste Transportation Packages*, NUREG/CR-6673, UCRL-ID-13852, U.S. Nuclear Regulatory Commission, May 2000, NRC Accession Number ML003723404.
10. EPRI NP-5977, *Radwaste Radiolytic Gas Generation Literature Review*, Electric Power Research Institute, September 1988
11. BNL-NUREG-50957, *Properties of Radioactive Wastes and Waste Containers*, Brookhaven National Laboratory, August 1979
12. NIST Standard Reference Database 8, *XCOM: Photon Cross Sections Database*, National Institute of Standards and Technology, DOI: 10.18434/T48G6X
13. NIST Standard Reference Database 124, *Stopping-Power & Range Tables for Electrons, Protons, and Helium Ions*, National Institute of Standards and Technology, DOI: 10.18434/T4NC7P
14. S. Kim, J. Chen, T. Cheng, et al., *PubChem in 2021: new data content and improved web interfaces*, Nucleic Acids Research Volume 49 Issue D1, DOI:10.1093/nar/gkaa971
15. Taylor, S. and G. Halsted., *Guide to Lightweight Cellular Concrete for Geotechnical Applications*, Portland Cement Association, Washington, DC, and National Concrete Pavement Technology Center at Iowa State University, Ames, IA, January 2021.

Proprietary Information on Pages 5.5-3 through 5.5-14 withheld pursuant to 10 CFR 2.390

6.0 CRITICALITY EVALUATION

As shown in Table 1.2-1, the CR3MP contains less than 2g of fissile material. Thus, per the provisions of 10 CFR 71.15(a) [1], the CR3MP is exempt from classification as a fissile material package. Therefore, a criticality evaluation is not required.

6.1 References

1. Title 10 – Energy, Code of Federal Regulations, Part 71 (10 CFR 71), *Packaging and Transportation of Radioactive Material*, 01–01–20 Edition.

7.0 PACKAGE OPERATIONS

In accordance with NRC Regulatory Guide 7.9, this chapter describes the operating procedures to be used for loading and transport of the CR3MP in order to ensure safe operations in compliance with the regulations and the package evaluation in this SAR. The CR3MP is a 10 CFR Part 71, exclusive use Type B package used for a onetime shipment and disposal of a portion of the CR3 RPV at a licensed low level radioactive waste disposal facility. Since the package is permanently sealed and will be buried with its contents, the "*Preparation of Empty Package for Transport*" as defined in Regulatory Guide 7.9 does not apply. For the same reason, package opening instructions as stated in 10 CFR 71.89 are not applicable. In addition, operational controls and precautions as described in 10 CFR 71.35(c) for fissile material packages does not apply since the package is fissile exempt.

All the required operations discussed in this chapter will be performed in accordance with written procedures approved under the licensee's QA Program.

7.1 Procedures for Loading the Package

This section delineates the procedures for loading the payload into the CR3MP. The CR3MP is loaded and closed in accordance with detailed written procedures, the contents are authorized in the package approval, and the package is in unimpaired physical condition. [ ] The steps provided in the below subsections may be performed out-of-order such that the most appropriate sequence is achieved.

7.1.1 Preparation for Loading

[ ] The RPV is drained of water and filled with LDCC. The LDCC is allowed to cure [ ] The CR3MP [ ] is secured [ ] The empty [ ]

7.1.2 Loading of Contents

Visual inspections of packaging components delineated in the following steps may be performed at any time during the loading sequence. [ ]

1. If operational controls require it, verify that the open CR3MP interior contains no foreign material capable of interfering with the proper placement of the RPV.
2. The middle RPV segment is lifted from the reactor cavity, into the waiting CR3MP.

3. The annulus between the segmented RPV contents and the inner shell wall of the CR3MP is filled with LDCC.
4. The CR3MP top cover is placed on the package body.
5. The CR3MP top cover is welded onto the package body and NDEs are completed on the closure weld in accordance with the SAR drawings in Appendix 1.3.2, *Packaging General Arrangement Drawings*.
6. The pressure vent port plug is installed, welded shut and inspected per the SAR drawing.
7. Paint any unpainted CR3MP external surfaces white.
8. Plug the threaded top cover lifting holes.

7.1.3 Preparation of the CR3MP for Transport

The following conditions are required to prepare for and complete the CR3MP transport:

- Complete all necessary shipping papers in accordance with Subpart C of 49 CFR 172 [3]. The CR3MP shall comply with applicable DOT requirements, including for marking, labeling and placarding of the package and conveyance. In this regard, the CR3MP shall follow the requirements of 10 CFR §71.85(c) [1] and Subpart D of 49 CFR 172 [3]. Package labeling shall be in accordance with Subpart E of 49 CFR 172. Package placarding shall be in accordance with Subpart F of 49 CFR 172.
- If there is a credible scenario for the ambient temperature to reach 0°F, then provide a continuous ambient temperature monitoring sensor as part of the transport. If at any point during the transport, the ambient temperature reaches a range between 0°F and 5°F, the transport shall be halted until the ambient temperature sensor measures a value above this temperature requirement.
- As detailed in Section 4.2.1, *Hydrogen Concentration in the Package*, in order to keep the hydrogen concentration to 5% or less by volume, the shipment window after package closure shall be set to a maximum of 1 year.
- The CR3MP contamination limits shall not exceed the limits set forth in Table 9 of 49 CFR 173.443 [2].

The following basic steps are performed to transport the package:

1. Perform a radiation survey of all accessible surfaces of the CR3MP. For transport requirements, and as specified in 49 CFR §173.441 [2], the dose rate must be less than 200 mrem/hr on the surface and less than 10 mrem/hr at a distance of 2 meters from the surface.

Proprietary Information on Page 7.1-4 withheld pursuant to 10 CFR 2.390

7.2 Package Unloading

This section delineates the procedures for unloading the CR3MP through removal of package from transporter.

7.2.1 Receipt of Package from Carrier

[ ]

3. The CR3MP is moved into its final disposal location.
4. The CR3MP is disposed of in accordance with disposal site requirements.

7.2.2 Removal of Contents

This subsection is not applicable. The package with contents will be disposed of as a one-time use package and the CR3MP will not be opened at the disposal site.

7.3 Preparation of Empty Package for Transport

This subsection is not applicable since no transport of the empty package occurs.

7.4 Other Operations

There are no other special operational control provisions necessary for operation of the CR3MP.

7.5 Appendix

7.5.1 References

1. Title 10, Code of Federal Regulations, Part 71 (10 CFR 71), *Packaging and Transportation of Radioactive Material*, 01–01–20 Edition.
2. Title 49, Code of Federal Regulations, Part 173 (49 CFR 173), *Shippers–General Requirements for Shipments and Packagings*, 10–01–20 Edition
3. Title 49, Code of Federal Regulations, Part 172 (49 CFR 172), *Hazardous Materials Tables and Hazardous Communications Regulations*, 10–01–20 Edition.

8.0 ACCEPTANCE TESTS AND MAINTENANCE PROGRAM

This section describes the acceptance tests and the maintenance program that shall be used on the CR3MP to ensure compliance with its design requirements, and the requirements of Subpart G of 10 CFR 71 [1].

8.1 Acceptance Tests

Per the requirements of 10 CFR §71.85, this section discusses the inspections and tests to be performed prior to first use of the CR3MP for transportation activities. Acceptance criteria for all inspections and tests are found either on the drawings in Appendix 1.3.2, *Packaging General Arrangement Drawings*, or in the sections that follow. All the tests and inspections on the CR3MP described in this chapter are conducted and documented in accordance with written procedures approved under an NRC approved QA program.

8.1.1 Visual Inspection and Measurements

The CR3MP packaging is visually inspected and measured to ensure that all of the requirements delineated on the SAR drawing in Appendix 1.3.2, *Packaging General Arrangement Drawings* are satisfied. This includes but is not limited to such items as materials, physical arrangement of components, quantities, dimensions, welds, and measurements. All controlling dimensions and associated tolerances specified on the SAR drawing are confirmed by measurement using calibrated and controlled Measuring and Test Equipment (M&TE).

[ ]

8.1.2 Weld Examinations

The locations, types, and sizes of all welds are identified and recorded to ensure compliance with the SAR drawing in Appendix 1.3.2, *Packaging General Arrangement Drawings*. All welds are Visually Examined (VT) in accordance with the SAR drawing.

All containment boundary welds are in accordance with Subarticle ND-5300 of the ASME BPVC [2]. The Category A and B cover and shell welds are specified to have a full RT examination along with MT or PT examinations on both the inner and outer surfaces. In lieu of the RT requirement of Subsubarticle ND-5230, and in accordance with Paragraph ND-5279, NDE of the Category C closure joints (both top and bottom covers) includes a full volumetric UT of the final weld joint. In addition, either a MT or PT examination is also performed on the Category C closure joint welds on both the inner/outer finished surfaces of the bottom cover and root/final pass of the top cover outer finished surface. The pressure vent port groove weld described in Section 1.2.1.1, *Containment Vessel*, shall be PT or MT inspected on the final surface in accordance with ASME BPVC, Subarticle ND-5300 [2], and ASME BPVC Section V [5], Article 6 (PT) or Article 7 (MT), as applicable.

8.1.3 Structural and Pressure Tests

8.1.3.1 Lifting Device Load Testing

The CR3MP does not have any integral lifting devices and thus does not contain any lifting devices that require load testing.

8.1.3.2 Containment Boundary Pressure Testing

10 CFR 71.85(b) stipulates testing the containment system at an internal pressure at least 50 percent higher than the MNOP, if the MNOP exceeds 5 psi. As stated in Section 3.3.2, *Maximum Normal Operating Pressure*, the MNOP is less than 5 psi. Therefore, the containment system does not require a pressure test.

8.1.4 Leakage Tests

The containment boundary consists of a welded cylindrical steel shell plus top and bottom plates welded to the shell. The welds which are used to fabricate the shell and the top and bottom covers along with the closure joint welds between the shell and covers undergo examinations as stated in Sections 8.1.1, *Visual Inspection and Measurements* and 8.1.2, *Weld Examinations* in order to ensure that the welds are sound and continuous. In addition, there are no mechanical closures, gaskets, valves or other similar types of penetrations into the containment boundary, although the threaded pressure vent port is plugged, welded closed and examined for weld integrity. The package contains solid radioactive material with only a very small percentage of radioactive material as surface contamination in the RPV, which will be fixed in place by LDCC within the RPV. There is no gaseous or liquid radioactive material in the package. As concluded in Section 4.2, *Containment under Normal Conditions of Transport*, the package integrity under NCT provides assurance that the radioactive materials will remain contained in the package and that there is no release of radioactive materials under any of the NCT tests described in 10 CFR 71.71. The discussion in Section 4.3, *Containment under Hypothetical Accident Conditions*, shows that in the event of a partial loss of containment under HAC, the released radioactivity levels are within the limits of 10 CFR 71. As a result, leakage rate tests are not applicable to the CR3MP.

8.1.5 Component and Material Tests

8.1.5.1 Steel Shell, Covers and Welds

The containment shell and top and bottom covers consist of a welded steel enclosure used for the transportation and disposal of the RPV. Plate material is to be provided with certified mechanical and chemical test reports in compliance with the SAR drawing in Appendix 1.3.2, *Packaging General Arrangement Drawings*. In addition, material tests of the base metal and weld filler metal are completed in compliance with the SAR drawing.

8.1.5.2 Low Density Cellular Concrete

Both the LDCC within the RPV and that between the CR3MP interior shell and the outside of the RPV shall have both density and compressive strength confirmed. A minimum of two sample cylinders are to be molded for each LDCC placement using ASTM C495 [3] for guidance. The wet-cast density is measured and recorded using guidance from ASTM C796/C796M [4] at the point of placement. The mix is adjusted as required in order to obtain the specified wet-cast density of 30-60 pcf. The minimum compressive strength of the LDCC shall be 100 psi at 28 days when tested in accordance with ASTM C495 [3]. Consistent with Section 5.4.4, *Radiolytic Gas Generation*, a QA controlled operating procedure shall be established to control both the LDCC wet-cast density and the slurry density, in order to ensure a minimum LDCC air fraction (f_{air}) of 40% is obtained.

8.1.6 Shielding Tests

As discussed below, shielding tests prior to final acceptance for shipment are not required for the CR3MP. CR3MP fabrication is performed in accordance with the OFS QA Program, which provides assurance that the as-built package is constructed in compliance with the design requirements described in this SAR. The controlled processes for loading the package described in Section 7.1, *Procedures for Loading the Package*, the weld examinations described in Sections 8.1.1, *Visual Inspection and Measurements* and 8.1.2, *Weld Examinations*, and the pre-shipment dose rate surveys discussed in Section 7.1.3, *Preparation of the CR3MP for Transport*, confirm the adequacy of the shielding as required by the package design.

Moreover, *Chapter 5.0, Shielding Evaluation*, provides calculated dose rates that are based upon a bounding estimate of the contents and the package built to the certified design using certified materials. Notably, the calculated dose rates are bounded by the regulatory limits defined in 10 CFR 71.47 [1].

8.1.7 Thermal Tests

Tests to demonstrate the heat transfer capability of the CR3MP are not required because the thermal evaluations presented in Chapter 3.0, *Thermal Evaluation*, are based on conservative heat transfer properties and methodologies. In addition, the CR3MP design does not incorporate active heat transfer features nor are passive heat transfer mechanisms particularly sensitive to normal variations in the materials of construction or fabrication methods. As such, the CR3MP is capable of withstanding temperatures within its design envelope, therefore thermal testing is not applicable. See Chapter 3.0, *Thermal Evaluation* for further discussions.

8.1.8 Miscellaneous Tests

No additional tests are necessary to be performed prior to use of the CR3MP.

8.2 Maintenance Program

No maintenance program is applicable to the CR3MP since the CR3MP is a single-shipment package used for transportation and disposal of the CR3 RPV and RVI.

8.2.1 Structural and Pressure Tests

Not applicable. A maintenance program and associated tests are not required for this package.

8.2.2 Leakage Tests

Not applicable. A maintenance program and associated tests are not required for this package.

8.2.3 Component and Material Tests

Not applicable. A maintenance program and associated tests are not required for this package.

8.2.4 Thermal Tests

Not applicable. A maintenance program and associated tests are not required for this package.

8.2.5 Miscellaneous Tests

Not applicable. A maintenance program and associated tests are not required for this package.

8.3 Appendix

8.3.1 References

1. Title 10 – Energy, Code of Federal Regulations, Part 71 (10 CFR 71), *Packaging and Transportation of Radioactive Material*, 01–01–20 Edition.
2. American Society of Mechanical Engineers (ASME) Boiler and Pressure Vessel Code, *Section III, Rules for Construction of Nuclear Facility Components, Division 1 – Subsection ND, Class 3 Components*, 2017 Edition.
3. ASTM C495/C495M – 12, *Standard Test Method for Compressive Strength of Lightweight Insulating Concrete*, American Society for Testing and Materials (ASTM), 2012.
4. ASTM C796/C796M – 19, *Standard Test Method for Foaming Agents for Use in Producing Cellular Concrete Using Preformed Foam*, American Society for Testing and Materials (ASTM), 2019.
5. American Society of Mechanical Engineers (ASME) Boiler and Pressure Vessel Code, *Section V, Nondestructive Examination*, 2017 Edition.